2001

Nonlinear adaptive optimal control of HVAC systems

Tuba Tigrek
University of Iowa

Recommended Citation

Tigrek, Tuba. "Nonlinear adaptive optimal control of HVAC systems." MS (Master of Science) thesis, University of Iowa, 2001.
https://doi.org/10.17077/etd.5elav8dm

www.manaraa.com

NONLINEAR ADAPTIVE OPTIMAL CONTROL

OF

HVAC SYSTEMS

by

Tuba Tigrek

A thesis submitted in partial fulfillment of the
requirements for the Master of Science degree
in Electrical and Computer Engineering
in the Graduate College of
The University of Iowa

December 2001

Thesis supervisor: Professor Soura Dasgupta

Graduate College
The University of Iowa
Iowa City, Iowa

CERTIFICATE OF APPROVAL

_____

MASTER'S THESIS

_____

This is to certify that the Master's thesis of

Tuba Tigrek

has been approved by the Examining Committee
for the thesis requirement for the Master of Science
degree in Electrical and Computer Engineering
at the December 2001 graduation.

Thesis committee: _____
                   Thesis supervisor

                   _____
                   Member

                   _____
                   Member

In the name of God, the Merciful, the Compassionate

We did indeed offer the Trust
to the heavens and the earth and the mountains;
but they refused to undertake it, being afraid thereof;
but man undertook it;
he was indeed tyrant and ignorant.

The Holy Koran, The Final Testament, 33:72

ACKNOWLEDGEMENTS

ABSTRACT

This study considers a nonlinear adaptive controller for a Heating, Ventilation and Air-Conditioning (HVAC) system. The controller is designed to optimize a cost function that trades energy cost off against a cost associated with the loss of thermal and environmental comfort. The cost function that is used is non-quadratic in the airflow-rate, making its derivation and implementation at variance with traditional Linear Quadratic Regulator (LQR) based techniques.

Imbedded in the adaptive controller is an adaptive identification algorithm that treats the system parameters as unknown variables. Two distinct strategies are investigated for identification; gradient descent and recursive least squares (RLS). A cost comparison is made between adaptive and nonadaptive operation for several different cases.

TABLE OF CONTENTS

LIST OF TABLES

LIST OF FIGURES

LIST OF NOMENCLATURE

Acronyms

HVAC	heating, ventilating, and air conditioning
ISE	integral squared error
LQR	linear quadratic regulator
MRAS	model reference adaptive system
RLS	recursive least squares

Symbols

A	linearized system state coefficient matrix
B	linearized system costate coefficient matrix
C	linearized subsystem state coefficient matrix
C_p	constant pressure specific heat, [kJ/kg-^{o}C]
E	graient descent error
f	volumetric flow rate, [m^3/s]
H	Hamiltonian function
J	cost function
J_e	minimum steady state cost function
k	$\rho \times C_p$, [J/m^3-^{o}C]
$\mathcal{L}$	Laplace transform
p	Lagrange multiplier, costate vector
P	solution to the differential matrix Riccati equation

q_h	heat exchanger input,[W]	
q_z	thermal load on zone, [W]	
t	time, [s], [min] or [hr]	
T	temperature, [°C]	
u	control variable	
V	volume, [m^3]	
x	state vector	
$\bar{x}$	modified state vector	

Greek Symbols

α	cost weighting factor
δ	variation
Δ	difference
ϵ	least squares error
θ	parameter vector
$\hat{\theta}$	estimated parameter vector
λ	update gain
Λ	update gain matrix
ρ	density, [kg/m^3]

Superscripts

$*$	steady state

Subscripts

a	ambient air
am	ambient air minimum
f	final
h	heat

p	pressure
r, ref	reference
z	zone

CHAPTER 1

INTRODUCTION

A major contributor to energy consumption in both the US and abroad is environmental conditioning of commercial buildings. In the US it accounts for over a third of the net national consumption [1]. Overseas this figure is even higher [2]. It is clear that given this high proportion of energy consumption cost attributable to heating and cooling of commercial buildings, even moderate increase in its efficiency can be expected to result in major energy savings. Consequently, in recent years there has been renewed interest in the design of heating, ventilating and air-conditioning (HVAC) systems that are more energy efficient and do not sacrifice thermal and environmental comfort.

This thesis focuses on the formulation and evaluation of an adaptive nonlinear optimal feedback control scheme that achieves such a balance. Simply put, the optimal control methodology requires two steps. First, one must formulate a cost function that in this case must include both the energy cost and a cost associated with overall level of comfort. Such a function must penalize at the same time excessive energy consumption and large deviations from user selected conditions that ensure prescribed levels of comfort. The second step would be the formulation of a feedback control law that minimizes the selected cost, thereby balancing the competing needs of energy efficiency and the maintenance of a comfortable environment.

The bulk of the previous work in this area has focused on the use of linear optimal control schemes, specifically the Linear Quadratic Regulator (LQR). The most important assumptions underlying LQR control are that the system to be controlled is linear and that the cost function to be optimized is quadratic in the system state and the input [3]. For non-linear systems, LQR theory can be applied, to yield a suboptimal controller that assumes a linearized plant. Specifically, one must select a nominal trajectory for the state and the optimizing input and assume that neither the state nor the input ever departs significantly from this nominal. Under these conditions the nonlinear system can be reasonably approximated by a linear system obtained by linearization around the nominal trajectory. The suboptimal controller is then designed via traditional LQR theory by treating the linear approximation as the actual system. Such an approach has been used by Zaheeruddin et. al. [4] in devising a suboptimal contoller for space heaters. Two drawbacks of this method are that (i) many of the system parameters may be imprecisely known or may even vary with time; and (ii) the cost function to be optimized may be non-quadratic. Such is indeed the case for HVAC systems. Not only is the HVAC system highly nonlinear, but the corresponding cost function that trades off energy cost against comfort cost is non-quadratic, with the term arising from the cost of fan operation being cubic in the air flow rate [5]. What is more, some of the key system parameters, such as external temperature and thermal load vary over time, and are difficult to accurately measure. Some of these difficulties are ameliorated by Roth et al. [6]. In their scheme, Roth et al. [6] adopt an adaptive approach. In essence this calls for an estimation process that starts with initial estimates of the unknown parameters. These estimates are continuously updated as more and more input-output information becomes available. At each instant of time,

the controller parameters are chosen on the assumption that the current parameter estimates represent true values of the quantities they respectively approximate. The controller parameters are then updated with the parameter estimates offered by the estimation process. In the sequel, the parameter estimation part of an adaptive controller will be referred to as the adaptive identification algorithm.

Roth et al. [6] design such an adaptive controller where the underlying controller parameters are selected on the basis of LQR design. To accommodate the needs of LQR design they (i) linearize the plant and (ii) select a quadratic cost function by dropping the component attributable to the cubic term associated with the cost of operating the fan. An exact optimal controller is provided by House et al. [5]. This controller assumes perfect forecast of ambient temperature and thermal load and is not amenable to on-line implementation.

A recent report [7], had reported a new optimal control strategy that had the following features. It assumed the non-quadratic cost function that included the fan operation cost. Furthermore, while some approximations were used in its formulation, unlike LQR control, it resulted in a non-linear controller. Nonetheless, this scheme did assume perfect knowledge of the HVAC system parameters. This thesis, however, discusses a control scheme that relaxes the assumption of perfectly known system parameter estimates. To allow for these uncertainties, the previously formulated nonlinear optimal control scheme is combined with an adaptive approach. Thus, an adaptive identification algorithm that continuously updates estimates of the system parameters is employed. The controller parameters are updated in accordance with these estimates.

This thesis is structured as follows. Since [7] had given only the conceptual essentials of the non-adaptive optimal control scheme, Chapter 2 gives full details of

this scheme and its derivation. Chapter 3 presents the first approach to a nonlinear adaptive control scheme which uses gradient descent as an identifier. Chapter 4 provides simulations for the Chapter 3. Chapter 5 presents the second approach to a nonlinear adaptive control scheme using recursive least squares as an identifier and gives simulations. Chapter 6 is the conclusion.

CHAPTER 2

AN OPTIMAL CONTROLLER

This Chapter presents a feedback scheme for the Optimal Control of a Heating, Ventilating and Air-conditioning (HVAC) System. The goal is to reduce the cost of system operation while retaining acceptable conditions of thermal and environmental comfort. The scheme presented here assumes perfect knowledge of the system parameters . In later chapters this scheme is modified into an adaptive version which no longer requires this knowledge. The outline of this chapter is as follows. Section 2.1 presents the HVAC system, the cost function to be optimized, and some other preliminary information. Section 2.2 derives and presents the promised Optimal Control scheme. Section 2.3 proves the local stability of the system and Section 2.4 is the conclusion.

2.1 Preliminaries

The HVAC system model is given by

$$T_1(t) = T_3(t) + \left(T_a - T_3(t)\right)\frac{f_a}{f(t)} \tag{2.1}$$

$$\rho C_p V_h \dot{T}_2(t) = f(t)\rho C_p \left(T_1(t) - T_2(t)\right) + q_h(t) \tag{2.2}$$

$$\rho C_p V_z \dot{T}_3(t) = f(t)\rho C_p \left(T_2(t) - T_3(t)\right) + q_z \tag{2.3}$$

where $(\dot{\ }) \equiv d/dt$, $T_1(t)$ and $T_2(t)$ are, respectively, the air temperatures prior to and immediately following the heat exchanger, $T_3(t)$ is the temperature of the thermal zone, T_a is the temperature of the outside air, ρ is the air density, C_p is the
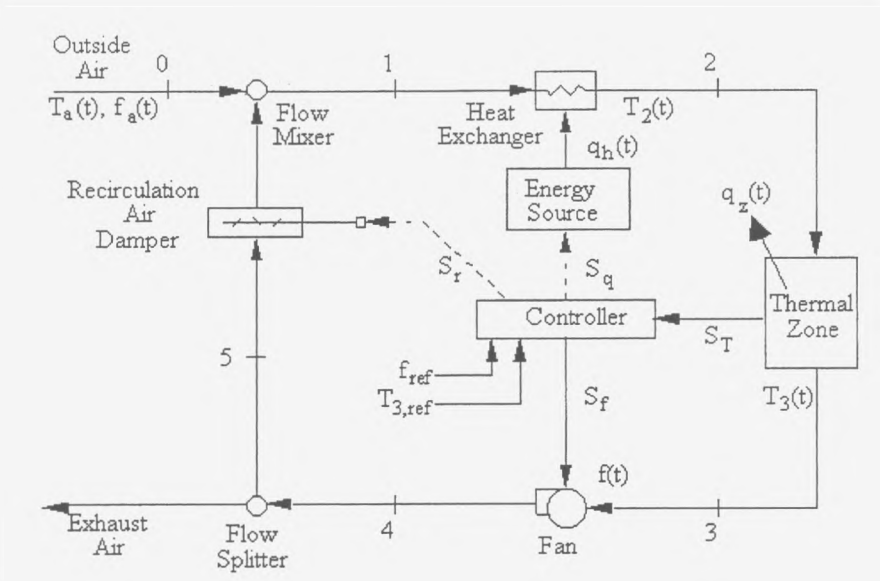
Figure 2.1: The HVAC System

constant pressure specific heat of air, V_h is the effective volume of the heat exchanger, V_z is the effective thermal space volume, f_a is the flow rate at which the external air enters the system, $q_h(t)$ is the heat input to the heat exchanger, $f(t)$ is the volumetric airflow rate and q_z is the thermal load. The HVAC system is depicted in Figure 2.1.

In the sequel, the external air flow rate is kept at its minimum allowable value

$$f_a = f_{am}.$$

The overall goal is to devise a feedback law that uses the temperatures $T_2(t)$ and $T_3(t)$ to modulate the two quantities $q_h(t)$ and $f(t)$ so as to minimize the performance index

$$J = \int_0^\infty \left[\alpha_2 (T_3(t) - T_{3,ref})^2 + \alpha_3 q_h^2(t) + \alpha_4 (f(t) - f_{ref})^2 + \alpha_5 f^3(t) \right] dt \qquad (2.4)$$

where the α_i's are cost weighting factors and the subscript "*ref*" refers to the value

Table 1: Physical Parameters

Parameter	Value
ρ	1.19 kg/m^3
C_p	1005 J/kg-°C
V_h	25.5 m^3
V_z	255 m^3
T_a	30°C
q_z	1900 Watts
α_2	4.86×10^{-3} \$/min-°C^2
α_3	5.39×10^{-10} \$/min-W^2
α_4	5.20×10^{-5} \$-min/m^6
α_5	1.22×10^{-6} \$-min^2/m^9
f_{am}	0.05 m^3/sec

corresponding to the maximum level of comfort. Further, $T_2(t)$ and $T_3(t)$ constitute the system states and $q_h(t)$ and $f(t)$ the control inputs. Accordingly, one defines the state vector

$$x(t) = [x_1(t) \ x_2(t)]' = [T_2(t) \ T_3(t)]' \tag{2.5}$$

and the input vector

$$u(t) = [u_1(t) \ u_2(t)]' = [q_h(t) \ f(t)]' \tag{2.6}$$

where *prime* denotes the transpose. The physical parameters in the foregoing are given in Table 1. The minimization must be performed subject to the additional constraint that

$$f(t) \geq f_{am} .$$

The first and the third terms in the cost function of (2.4) are comfort costs due to temperature mismatch and the level of draft, respectively, while the second and the

fourth are energy costs deriving from heat exchange and fan operation, respectively. The optimization of this cost function thus affects a trade off between comfort level and the resulting operating cost of the HVAC system.

It is noteworthy that the cost function to be minimized here is *non-quadratic*. By way of comparison one can cite the Optimal Control law embedded in the Adaptive Optimal Control algorithm of [6]. Appealing as it does to Linear Quadratic Regulator (LQR) theory, [6] drops the non-quadratic term $\alpha_5 f^3(t)$ in (2.4) and derives a linear controller obtained on the basis of a linearized version of the model equations (2.1), (2.2) and (2.3). The controller of [6] thus seeks to minimize the modified cost function:

$$J_m = \int_0^\infty \left[\alpha_2 \left(T_3(t) - T_{3,ref} \right)^2 + \alpha_3 q_h(t)^2 + \alpha_4 (f(t) - f_{ref})^2 \right] \mathrm{d}t$$

where here onwards

$$T_r = T_{3,ref}$$

and

$$f_r = f_{ref} .$$

By contrast the work reported here does not ignore the $\alpha_5 f^3(t)$ term, and formulates instead a nonlinear control law described in Section 2.2.

2.2 The Controller

First note that, for the optimization problem to be well posed, there must exist control input and state values for which the system equations (2.1), (2.2) and (2.3) are at steady state and, moreover, the integrand of the cost function to be minimized is zero. Otherwise the cost function would be infinite over the infinite

horizon of its operation and consequently the optimization problem would not have a solution. It is readily verified that the integrand in (2.4) cannot in general be zero. To circumvent this difficulty one may pose the alternative problem of minimizing:

$$J_x = \int_0^\infty \left[\alpha_2 (T_3(t) - T_r)^2 + \alpha_3 q_h^2(t) + \alpha_4 (f(t) - f_r)^2 + \alpha_5 f^3(t) - J_e \right] dt \qquad (2.7)$$

where J_e is a constant representing the minimum steady state value that the integrand in (2.4) can assume; i.e.

$$J_e = \min \left(\alpha_2 (T_3(t) - T_r)^2 + \alpha_3 q_h^2(t) + \alpha_4 (f(t) - f_r)^2 + \alpha_5 f^3(t) \right) \qquad (2.8)$$

subject to

$$\dot{T}_2(t) = 0, \qquad \dot{T}_3(t) = 0 \qquad (2.9)$$

and

$$f(t) \geq f_{am}. \qquad (2.10)$$

Indeed, while technically one can have a lower value of the integrand in (2.7) by setting

$$T_3(t) = T_r,$$

$$q_h(t) = 0$$

and

$$f(t) = \max \left\{ f_{am}, \frac{-\alpha_4 + \sqrt{\alpha_4^2 + 6\alpha_4 \alpha_5 f_r}}{3\alpha_5} \right\},$$

at these values the derivative of $T_3(t)$ is not zero. Consequently, these values themselves can only be momentarily maintained.

The problem of minimizing (2.8) subject to (2.9) and (2.10) is readily solvable and the constant determined. Further, as J_e is a constant, the control law that

minimizes (2.7) also minimizes (2.4). Henceforth J_x , (2.7), is referred to as the *excess cost*.

Proceeding in a standard fashion that is explained in Appendix A, and using the notations (2.5) and (2.6), we work with the finite horizon cost function

$$
\begin{aligned}
J_e(t_f) &= \int_0^{t_f} F(x, u, t)\mathrm{d}t \\
&= \int_0^{t_f} \left[\alpha_2(x_2(t) - T_r)^2 + \alpha_3 u_1^2(t) + \alpha_4(u_2(t) - f_r)^2 + \alpha_5 u_2^3(t) - J_e\right]\mathrm{d}t ,
\end{aligned}
$$

(2.11)

to formulate the two dimensional costate vector $p(t) = [p_1(t) \ p_2(t)]'$ and the Hamiltonian as given by (A.5)

$$
\begin{aligned}
H &= F(x, u, t) + p'(t)g(x, u, t) \\
&= \alpha_2(x_2(t) - T_{3,ref})^2 + \alpha_3 u_1^2(t) + \alpha_4(u_2(t) - f_r)^2 + \alpha_5 u_2^3(t) - J_e + \\
&\quad p_1(t)\dot{x}_1(t) + p_2(t)\dot{x}_2(t)
\end{aligned}
$$

(2.12)

and obtain the control law from

$$
[\dot{p}_1(t) \ \dot{p}_2(t)] = -\frac{\partial H}{\partial x} ,
$$

(2.13)

$$
p(t_f) = 0 ,
$$

(2.14)

and

$$
\left(\frac{\partial H}{\partial u_i}\right)_{u=u^*} = 0, \quad i = 1, 2
$$

(2.15)

which are the applications of (A.7), (A.8) and (A.9) to the HVAC System.

First observe that (2.1), (2.2) and (2.3) can be rewritten as

$$
\dot{x}_1(t) = \frac{1}{V_h}\left[u_2(t)(x_2(t) - x_1(t)) + f_a(T_a - x_2(t)) + \frac{u_1(t)}{k}\right]
$$

(2.16)

and

$$\dot{x}_2(t) = \frac{u_2(t)}{V_z}\left(x_1(t) - x_2(t)\right) + \frac{q_z}{kV_z} \tag{2.17}$$

where

$$k = \rho C_p \,,$$

resulting in $g(x, u, t) = [\dot{x}_1(t), \dot{x}_2(t)]'$ of (2.12). Moreover (2.13) becomes

$$\dot{p}_1(t) = u_2(t)\left(\frac{p_1(t)}{V_h} - \frac{p_2(t)}{V_z}\right) \tag{2.18}$$

and

$$\dot{p}_2(t) = -2\alpha_2\left(x_2(t) - T_r\right) + u_2(t)\left(\frac{p_2(t)}{V_z} - \frac{p_1(t)}{V_h}\right) + f_a\frac{p_1(t)}{V_h}\,. \tag{2.19}$$

Then (2.15) gives

$$\frac{\partial H}{\partial u_1} = 2\alpha_3 u_1(t) + \frac{p_1(t)}{kV_h} = 0$$

and

$$\begin{aligned}
\frac{\partial H}{\partial u_2} &= 2\alpha_4[u_2(t) - f_r] + 3\alpha_5 u_2^2(t) + \\
&\qquad \frac{p_1(t)}{V_h}[x_2(t) - x_1(t)] + \frac{p_2(t)}{V_z}[x_1(t) - x_2(t)] \\
&= 0\,,
\end{aligned}$$

which result in

$$u_1(t) = \frac{-p_1(t)}{2\alpha_3 kV_h} \tag{2.20}$$

and

$$u_2(t) = \max\left\{f_{am}, \frac{-\alpha_4 + \sqrt{\alpha_4^2 + 3\alpha_5\left[2\alpha_4 f_r - (x_2(t) - x_1(t))\left(\frac{p_1(t)}{V_h} - \frac{p_2(t)}{V_z}\right)\right]}}{3\alpha_5}\right\}\,. \tag{2.21}$$

It is found that in (2.21) the second term on the right hand side always dominates. Thus we can effectively replace (2.21) by

$$u_2(t) = \frac{-\alpha_4 + \sqrt{\alpha_4^2 + 3\alpha_5 \left[2\alpha_4 f_r - (x_2(t) - x_1(t)) \left(\frac{p_1(t)}{V_h} - \frac{p_2(t)}{V_z} \right) \right]}}{3\alpha_5}. \qquad (2.22)$$

Observe, the determination of $u_1(t)$ and $u_2(t)$ requires the knowledge of both $p(t)$ and $x(t)$. As the former is the solution of a differential equation for which a boundary, (2.14), as opposed to an initial condition, is provided, the above control law is unimplementable online and in fact may not even have a closed form solution.

To remove this difficulty, we introduce an approximation. The following approximation turns out to be nothing but the same linearization process that is explained in Appendix B. With this approximation, we basically expand the nonlinear state equations (2.16), (2.17), (2.18), and (2.19) into a Taylor series about a nominal operating point (x^*, u^*, p^*) with *star* denoting the steady-state value.

Define p^*, x^* to be such that with $p = p^*$ and $x = x^*$ the integrand in (2.7) is zero under (2.20) and (2.22). Observe, if at some t^*, $p(t^*) = p^*$ and $x(t^*) = x^*$, then for all $t \geq t^*$, under (2.20) and (2.22), $p(t) = p^*$ and $x(t) = x^*$ and moreover, the integrand in (2.7) is zero. Further with $\Delta p(t) = p(t) - p^*$ and $\Delta x(t) = x(t) - x^*$, if for some t^*, $\Delta p(t^*)$ and $\Delta x(t^*)$ is sufficiently small, then to a first order approximation (2.16)-(2.19) can be replaced by

$$\begin{bmatrix} \Delta \dot{x}(t) \\ \Delta \dot{p}(t) \end{bmatrix} = \begin{bmatrix} A & -B \\ -C & -A' \end{bmatrix} \begin{bmatrix} \Delta x(t) \\ \Delta p(t) \end{bmatrix} \qquad (2.23)$$

where B is positive definite symmetric and C is positive semidefinite symmetric. This approximation becomes better as t_f tends to infinity. Also as t_f tends to infinity, [6], the solution to (2.23) can be written as

$$\Delta p(t) = P \Delta x(t)$$

where P is the unique (under mild assumptions) positive definite symmetric solution to the Riccati equation

$$A'P + PA + C - PBP = 0. \tag{2.24}$$

Once A, B and C are obtained, (2.24) is easily solved. The control law we propose then is (2.20), (2.22) and

$$p(t) = P\left(x(t) - x^*\right) + p^* \tag{2.25}$$

with P the positive definite solution of (2.24). If $t_f = \infty$, and $\Delta p(0)$ and $\Delta x(0)$ are "small", this law is to a first approximation the desired optimal controller for all finite t. Local stability of this particular solution will be shown in Section 2.3. Observe, despite the linearization in the design process, one has a nonlinear controller.

Following is the required x^*, p^*, A, B and C which are obtained in Section B.1 as (B.17), (B.23), (B.24) and (B.25);

$$x_1^* = \frac{3\,\alpha_5\,q_z}{k\,(\alpha_4 - S)} + x_2^*, \tag{2.26}$$

$$x_2^* = \frac{T_r\,\alpha_2 + k\,f_a\,(q_z + k\,f_a\,T_a)\,\alpha_3}{\alpha_2 + k^2\,f_a^2\,\alpha_3}, \tag{2.27}$$

$$p_1^* = \frac{2\,k\,(q_z + k\,f_a\,(T_a - T_r))\,V_h\,\alpha_2\,\alpha_3}{\alpha_2 + k^2\,f_a^2\,\alpha_3}, \tag{2.28}$$

$$p_2^* = \frac{V_z}{V_h}p_1^*, \tag{2.29}$$

$$A = \frac{\alpha_4 - S}{3\alpha_5}\begin{bmatrix} 1/V_h & -1/V_h \\ -1/V_z & 1/V_z \end{bmatrix} - f_a\begin{bmatrix} 0 & 1/V_h \\ 0 & 0 \end{bmatrix}, \tag{2.30}$$

$$B = \frac{9q_z^2\alpha_5^2}{2k^2S(S-\alpha_4)^2}\begin{bmatrix} 1/V_h^2 & -1/(V_hV_z) \\ -1/(V_hV_z) & 1/V_z^2 \end{bmatrix} + \frac{1}{2\alpha_3k^2}\begin{bmatrix} 1/V_h^2 & 0 \\ 0 & 0 \end{bmatrix},$$

(2.31)

$$C = \begin{bmatrix} 0 & 0 \\ 0 & 2\alpha_2 \end{bmatrix}.$$

(2.32)

where

$$S = \sqrt{\alpha_4^2 + 6\,\alpha_4\,\alpha_5\,f_r}\,.$$

(2.33)

Notice aforementioned positive definite symmetric characteristics of B and positive semidefinite symmetric characteristics of C.

The overall optimal controller is, then, as in (2.20) and (2.22), with $p(t)$ computed by (2.25), (2.26)-(2.29), and P, the unique positive definite symmetric solution of (2.24), with A, B and C as in (2.30)-(2.32). Observe when the system parameters are constant and known, P, x^* and p^* can be computed offline and only (2.20), (2.22) and (2.25) need to be computed online.

2.3 Local Stability

In this section, we determine local stability of linearized HVAC system given by (2.23) as

$$\begin{bmatrix} \Delta\dot{x}(t) \\ \Delta\dot{p}(t) \end{bmatrix} = \begin{bmatrix} A & -B \\ -C & -A' \end{bmatrix}\begin{bmatrix} \Delta x(t) \\ \Delta p(t) \end{bmatrix}$$

where

$$A = \frac{\alpha_4 - S}{3\alpha_5}\begin{bmatrix} 1/V_h & -1/V_h \\ -1/V_z & 1/V_z \end{bmatrix} - f_a\begin{bmatrix} 0 & 1/V_h \\ 0 & 0 \end{bmatrix},$$

$$B = \frac{9q_z^2\alpha_5^2}{2k^2S(S-\alpha_4)^2}\begin{bmatrix} 1/V_h^2 & -1/(V_hV_z) \\ -1/(V_hV_z) & 1/V_z^2 \end{bmatrix} + \frac{1}{2\alpha_3k^2}\begin{bmatrix} 1/V_h^2 & 0 \\ 0 & 0 \end{bmatrix}$$

and

$$C = \begin{bmatrix} 0 & 0 \\ 0 & 2\alpha_2 \end{bmatrix}$$

for

$$S = \sqrt{\alpha_4^2 + 6\,\alpha_4\,\alpha_5\,f_r}\ .$$

First we prove that the subsystem

$$\Delta\dot{x}(t) = A\Delta x(t) - B\Delta p(t) = (A - BP)\Delta x(t) = \mathcal{A}\Delta x(t) \qquad (2.34)$$

is locally asymptotically stable. Observe, (2.34) is the result of (2.23) using the fact that

$$\Delta p(t) = P\Delta x(t)$$

as given on page 12.

Let G be a matrix having the same rank as B and such that $B = GG'$, and Q_1 a matrix having the same rank as C and such that $C = Q_1'Q_1$. Checking, therefore, $[A, G]$ for completely controllableness (c.c.) and $[A, Q_1]$ for completely observableness (c.o.) should suffice to establish that the closed loop system matrix $\mathcal{A} = A - BP$ is asymptotically stable - see Appendix C for details -.

G turns out to be

$$G = \begin{bmatrix} \mu/V_h & \nu/V_z \\ -\mu/V_z & 0 \end{bmatrix}\ .$$

for

$$\mu^2 = \frac{9q_z^2\alpha_5^2}{2k^2S(S - \alpha_4)^2}$$

and

$$\nu^2 = \frac{1}{2\alpha_3 k^2}\ ,$$

since

$$B = \mu^2 \begin{bmatrix} 1/V_h^2 & -1/(V_h V_z) \\ -1/(V_h V_z) & 1/V_z^2 \end{bmatrix} + \nu^2 \begin{bmatrix} 1/V_h^2 & 0 \\ 0 & 0 \end{bmatrix},$$

and Q_1 turns out to be

$$Q_1 = \begin{bmatrix} 0 & \sqrt{2\alpha_2} \end{bmatrix}.$$

$[A, G]$ is c.c. because [G, AG] has rank 2, and $[A, Q_1]$ is c.o. because $[Q_1', (Q_1 A)']'$ has rank 2. Therefore $\mathcal{A}$ is asymptotically stable, i.e. $x(t) \to x^*$ as $t \to \infty$. Since P is a finite matrix it follows that $p(t) \to p^*$ as $t \to \infty$ [3]. We, therefore, have established that the linearized HVAC system of (2.23) is locally asymptotically stable.

2.4   Conclusion

This Chapter presented a feedback scheme for the Optimal Control of an HVAC System with the goal to reduce the cost of system operation while retaining acceptable conditions of thermal and environmental comfort. The scheme presented here has assumed perfect knowledge of the system parameters . First we have presented the HVAC system, the cost function to be optimized, and some other preliminary information in Section 2.1. Then the promised Optimal Control scheme was derived in Section 2.2 with its local stability proven at Section 2.3.

CHAPTER 3

ADAPTIVE CONTROLLER SCHEME 1: GRADIENT DESCENT

The nonlinear optimal controller presented in the previous chapter assumes perfect knowledge of the parameters and assumes all to be constant. Unfortunately, in practice, over a course of a day operation, parameters vary and some of them in particular may be difficult to measure. Thus we are presenting an adaptive version of the controller given in Chapter 2. The parameters object to being identified are the effective volume of the heat exchanger (V_h), the temperature of the outside air (T_a), $k = \rho C_p$ where ρ is the air density and C_p is the constant pressure specific heat of air, the effective thermal space volume (V_z) and the thermal load (q_z).

In essence the overall scheme is as depicted in Figure 3.1, where $u(t)$ is the input vector comprising the heat input to the heat exchanger $q_h(t)$, and the volumetric air flow rate $f(t)$, i.e.

$$u(t) = [q_h(t) \ \ f(t)]'; \tag{3.1}$$

and $x(t)$ is the state vector

$$x(t) = [T_2(t) \ \ T_3(t)]' \tag{3.2}$$

$T_2(t)$ being the temperature of the air immediately after the heat exchanger and $T_3(t)$ the temperature of the thermal zone. The major difference between the scheme of Chapter 2 and the adaptive scheme presented here is the inclusion of the identifier. Using the input and state vector measurements, the identifier provides estimate $\hat{\theta}$ of parameters, estimate that is continuously updated. The controller in
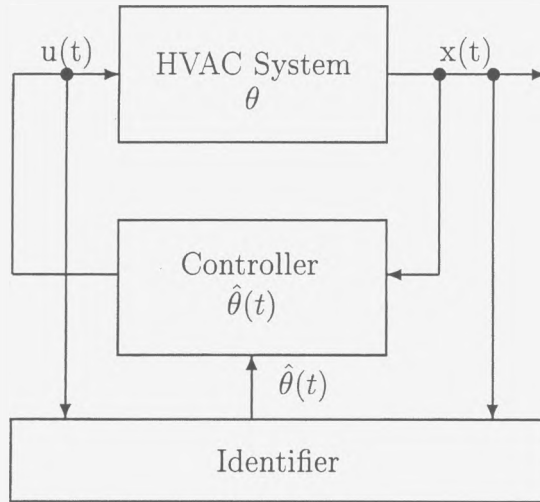
Figure 3.1: An Adaptive Control Scheme

its turn is exactly as in Chapter 2 with the estimates of the parameters replacing the parameters in the controller equations of Chapter 2.

For the estimation of the parameters, first gradient descent approach will be used. The current chapter, therefore, will give theoretical background to gradient descent and then apply it to the nonlinear optimal controller of Chapter 2. After applications of Nonlinear Adaptive Optimal HVAC algorithm using gradient descent to different combinations of the five aforementioned system parameters in the present chapter, and simulations (Chapter 4), Recursive Least Squares approach to the parameter estimation will be undertaken in Chapter 5.

The outline of this chapter is as follows. Section 3.1 presents the theory behind the gradient descent theory and its application to the nonlinear optimal HVAC system in general. Section 3.2 shows the application of the gradient descent scheme into the specific cases for the nonlinear optimal HVAC system. Section 3.3 gives the

conclusion for this chapter.

3.1 Adaptive Identifier 1: Gradient Descent

The model-reference adaptive system (MRAS) is one of the main approaches to adaptive control [8]. A reference model expresses the desired performance and gives the desired response to a command signal. The system also has an ordinary feedback loop composed of the process and the controller. The error e is the difference between the output of the system and the reference model. The controller has parameters that are changed based on the error. The inner loop, which is an ordinary control feedback, is assumed to be faster than the outer loop which adjusts the parameters in the inner loop.

The gradient descent approach is one of the three approaches to the analysis and design of a MRAS, the other two being Lyapunov functions and passivity theory [8], and is indeed a fundemantel idea in the MRAS approach. The gradient descent approach is based on the assumption that the parameters change more slowly than the other variables in the system [8]. This assumption, which admits a quasi-stationary treatment, is essential for the computation of the sensitivity derivatives that are needed in the adaptation mechanism. In general the gradient descent approach does not result in a stable closed loop system. Lyapunov stability theory has been used to modify the adaptation mechanism.

3.1.1 Application of the Gradient Descent

For the system equations of the HVAC plant

$$\dot{x}_1(t) = \frac{1}{V_h} \left[u_1(t)\left(x_2(t) - x_1(t)\right) + f_a\left(T_a - x_2(t)\right) + \frac{u_1(t)}{k} \right]$$

$$\dot{x}_2(t) = \frac{u_1(t)}{V_z}\left(x_1(t) - x_2(t)\right) + \frac{q_z}{kV_z}, \tag{3.3}$$

there is a need to filter the signals to avoid explicit differentiation. For this purpose we introduce

$$W(s) \triangleq \frac{1}{s+1}X(s) \tag{3.4}$$

and

$$\overline{X}(s) \triangleq \frac{s}{s+1}X(s) = sW(s), \tag{3.5}$$

where $X(s)$ is the Laplace transform of the state vector $x(t)$, i.e. $X(s) = \mathcal{L}[x(t)]$, and likewise, $W(s) = \mathcal{L}[w(t)]$, and $\overline{X}(s) = \mathcal{L}[\overline{x}(t)]$. The definitions (3.4) and (3.5) would translate into the time domain as

$$\overline{x}(t) = \dot{w}(t) = -w(t) + x(t). \tag{3.6}$$

The new set of system equations are therefore

$$\overline{x}(t) = V'(t)\,\theta \tag{3.7}$$

where θ is a vector of parameters to be estimated and V is a matrix whose elements represent state variable filter outputs that permit adaptive identification without having to explicitly differentiate any signal. Observe that elements of V are known or measurable. The adaptive identifier to be presented here assumes that the parameters, though unknown, are constant.

Define, with $\hat{\theta}$ being the vector of identified parameters,

$$\hat{\overline{x}}(t) = V'(t)\,\hat{\theta}, \tag{3.8}$$

Again, $V(t)$ and $\bar{x}(t)$ can be directly measured. The gradient descent would be to minimize $E^2(t)$ where

$$E(t) = \hat{\bar{x}}(t) - \bar{x}(t).$$

(3.9)

Then the parameter estimate law is given by

$$
\begin{aligned}
\dot{\hat{\theta}}(t) &= -\frac{1}{2}\Lambda\frac{\partial E^2}{\partial \theta} \\
&= -\Lambda V(t) E(t) \\
&= -\Lambda V(t) [\hat{\bar{x}}(t) - \bar{x}(t)]
\end{aligned}
$$

(3.10)

where Λ is an $n \times n$ diagonal matrix whose diagonal elements are positive real numbers and used as selected update gains, with n being the number of the parameters to be estimated.

3.1.2 Adaptive Controller Using Gradient Descent

As noted at the outset of this chapter, the overall adaptive control algorithm is a combination of the identifier given in section 3.1.1 and the controller as given in Chapter 2, with θ replaced by $\hat{\theta}$.

Thus the overall adaptive control algorithm is as follows:

$$u_1(t) = \frac{-p_1(t)}{2\alpha_3 k V_h}$$

and

$$u_2(t) = \max\left\{ f_{am}, \frac{-\alpha_4 + \sqrt{\alpha_4^2 + 3\alpha_5\left[2\alpha_4 f_r - \left(x_2(t) - x_1(t)\right)\left(\frac{p_1(t)}{V_h} - \frac{p_2(t)}{V_z}\right)\right]}}{3\alpha_5} \right\}$$

with $p(t) = [p_1(t), p_2(t)]'$ computed by

$$p(t) = P(t)[x(t) - x^*(t)] + p^*(t),$$

$$x_1^*(t) = \frac{3\,\alpha_5\,q_z}{k\,(\alpha_4 - S)} + x_2^*(t)\,,$$

$$x_2^*(t) = \frac{T_r\,\alpha_2 + k\,f_a\,(q_z + k\,f_a\,T_a)\,\alpha_3}{\alpha_2 + k^2\,f_a^2\,\alpha_3}\,,$$

$$p_1^*(t) = \frac{2\,k\,(q_z + k\,f_a\,(T_a - T_r))\,V_h\,\alpha_2\,\alpha_3}{\alpha_2 + k^2\,f_a^2\,\alpha_3}\,,$$

$$p_2^*(t) = \frac{V_z}{V_h}p_1^*(t)\,,$$

and $P(t)$ being the unique positive definite symmetric solution of the Algebraic Riccati Equation

$$A'P(t) + P(t)A - P(t)B(t)P(t) + C = 0 \qquad (3.11)$$

with A, B and C as

$$A = \frac{\alpha_4 - S}{3\alpha_5}\begin{bmatrix} 1/V_h & -1/V_h \\ -1/V_z & 1/V_z \end{bmatrix} - f_a\begin{bmatrix} 0 & 1/V_h \\ 0 & 0 \end{bmatrix}\,,$$

$$B = \frac{9q_z^2\alpha_5^2}{2k^2S(S-\alpha_4)^2}\begin{bmatrix} 1/V_h^2 & -1/(V_hV_z) \\ -1/(V_hV_z) & 1/V_z^2 \end{bmatrix} + \frac{1}{2\alpha_3k^2}\begin{bmatrix} 1/V_h^2 & 0 \\ 0 & 0 \end{bmatrix}\,,$$

$$C = \begin{bmatrix} 0 & 0 \\ 0 & 2\alpha_2 \end{bmatrix}$$

for

$$S = \sqrt{\alpha_4^2 + 6\,\alpha_4\,\alpha_5\,f_r}$$

together with the identifier. Observe there are fast and accurate algorithms for solving the Algebraic Riccati Equation in (3.11).

3.2 Applications: Gradient Descent

In this section the identifier of Section 3.1 will be used to estimate different combinations of five system parameters, namely,

- the effective volume of the heat exchanger V_h,

- the temperature of the outside air T_a,

- $k = \rho C_p$ where ρ is the air density and C_p is the constant pressure specific heat of air,

- the effective thermal space volume V_z, and

- the thermal load q_z.

When five or four of the system parameters form the θ to be identified, the gradient descent algorithm does not converge. Combinations of some two or three parameters can, on the other hand, be identified using gradient descent. There will be six subsections subsequently in the present chapter, each one presenting the adaptive identifier for the specific combination. The simulations for these combinations will be given in Chapter 4 with the corresponding case numbers.

3.2.1 Case(1): T_a and q_z unknown

The adaptive identifier to be presented here assumes that the temperature of the outside air T_a and the thermal load q_z are constant but unknown, i.e. $\hat{\theta} = [\hat{T}_a, \hat{q}_z]'$.

Define the signals $w_1(t), w_2(t), z_1(t), ..., z_4(t)$ as follows

$$
\begin{aligned}
\dot{w}_1(t) &= -w_1(t) + T_2(t), \\
\dot{w}_2(t) &= -w_2(t) + T_3(t)
\end{aligned}
\tag{3.12}
$$

and

$$
\begin{aligned}
\dot{z}_1(t) &= -z_1(t) + \frac{1}{V_h}\left[f(t)[T_3(t) - T_2(t)] - f_a T_3(t) + \frac{q_h(t)}{k} \right], \\
\dot{z}_2(t) &= -z_2(t) + \frac{f_a}{V_h}, \\
\dot{z}_3(t) &= -z_3(t) + \frac{f}{V_z}[T_2(t) - T_3(t)], \\
\dot{z}_4(t) &= -z_4(t) + \frac{1}{kV_z}
\end{aligned}
\tag{3.13}
$$

where f_a is the flow rate at which the outdoors air enters the system; V_h and V_z are the effective volumes of the heat exchanger and the thermal zone respectively, and k equals to ρC_p with ρ the air density and C_p the constant pressure specific heat of the air. Observe, (3.12) and (3.13) represent state variable filters that permit adaptive identification without having to explicitly differentiate any signal. All quantities in (3.12) and (3.13) are known or measurable. Define

$$
V(t) = \begin{bmatrix} z_2(t) & 0 \\ 0 & z_4(t) \end{bmatrix}
\tag{3.14}
$$

and, for $\hat{\theta}(t) = [\hat{T}_a(t), \hat{q}_z(t)]'$,

$$
\hat{\bar{x}}(t) = V'(t)\hat{\theta}(t)
\tag{3.15}
$$

and

$$
\bar{x}(t) = \begin{bmatrix} T_2(t) \\ T_3(t) \end{bmatrix} - \begin{bmatrix} w_1(t) \\ w_2(t) \end{bmatrix} - \begin{bmatrix} z_1(t) \\ z_3(t) \end{bmatrix}.
\tag{3.16}
$$

Again (3.14)-(3.16) can be directly measured. Then the parameter estimate law is given by

$$
\dot{\hat{\theta}}(t) = -\Lambda V(t)[\hat{\bar{x}}(t) - \bar{x}(t)].
\tag{3.17}
$$

3.2.2 Case(2): V_h and q_z unknown

The adaptive identifier to be presented here assumes that the effective volume of the heat exchanger V_h and the thermal load q_z constant unknowns, i.e. $\hat{\theta} = [1/\hat{V}_h, \hat{q}_z]'$.

Define the signals $z_1(t), z_2(t)$ and $z_3(t)$ as follows

$$\begin{aligned}
\dot{z}_1(t) &= -z_1(t) + f(t)[T_3(t) - T_2(t)] - f_a[T_a - T_3(t)] + \frac{q_h(t)}{k}, \\
\dot{z}_2(t) &= -z_2(t) + \frac{f}{V_z}[T_2(t) - T_3(t)], \\
\dot{z}_3(t) &= -z_3(t) + \frac{1}{kV_z}.
\end{aligned} \tag{3.18}$$

All quantities in (3.18) are known or measurable. Define

$$V(t) = \begin{bmatrix} z_1(t) & 0 \\ 0 & z_3(t) \end{bmatrix} \tag{3.19}$$

and, with $\hat{\theta}(t) = [1/\hat{V}_h(t), \hat{q}_z(t)]'$,

$$\hat{\bar{x}}(t) = V'(t)\hat{\theta}(t) \tag{3.20}$$

and

$$\bar{x}(t) = \begin{bmatrix} T_2(t) \\ T_3(t) \end{bmatrix} - \begin{bmatrix} w_1(t) \\ w_2(t) \end{bmatrix} - \begin{bmatrix} 0 \\ z_2(t) \end{bmatrix}. \tag{3.21}$$

The signals $w_1(t)$ and $w_2(t)$ are as given by (3.12) at Section 3.2.1. Again (3.19)-(3.21) can be directly measured. Then the parameter estimate law is given by

$$\dot{\hat{\theta}}(t) = -\Lambda V(t)[\hat{\bar{x}}(t) - \bar{x}(t)]. \tag{3.22}$$

3.2.3 Case(3): T_a and V_z unknown

The adaptive identifier to be presented here assumes that the temperature of the outside air, T_a and the effective thermal space volume, V_z are constant unknowns, i.e. $\hat{\theta} = [\hat{T}_a, 1/\hat{V}_z]'$.

Define the signals $z_1(t), z_2(t)$ and $z_3(t)$ as follows

$$
\begin{aligned}
\dot{z}_1(t) &= -z_1(t) + \frac{1}{V_h}\left[f(t)[T_3(t) - T_2(t)] - f_a T_3(t) + \frac{q_h(t)}{k}\right], \\
\dot{z}_2(t) &= -z_2(t) + \frac{f_a}{V_h}, \\
\dot{z}_3(t) &= -z_3(t) + f(t)[T_2(t) - T_3(t)] + \frac{q_z}{k}
\end{aligned}
\tag{3.23}
$$

Observe, (3.23) represent state variable filters that permit adaptive identification without having to explicitly differentiate any signal. All quantities in (3.23) are known or measurable. Define

$$
V(t) = \begin{bmatrix} z_2(t) & 0 \\ 0 & z_3(t) \end{bmatrix}
\tag{3.24}
$$

and, with $\hat{\theta}(t) = [\hat{T}_a(t), 1/\hat{V}_z(t)]'$,

$$
\hat{\bar{x}}(t) = V'(t)\hat{\theta}(t)
\tag{3.25}
$$

and

$$
\bar{x}(t) = \begin{bmatrix} T_2(t) \\ T_3(t) \end{bmatrix} - \begin{bmatrix} w_1(t) \\ w_2(t) \end{bmatrix} - \begin{bmatrix} z_1(t) \\ 0 \end{bmatrix}.
\tag{3.26}
$$

The signals $w_1(t)$ and $w_2(t)$ are as given by (3.12) at Section 3.2.1. Again (3.24)-(3.26) can be directly measured. Then the parameter estimate law is given by

$$
\dot{\hat{\theta}}(t) = -\Lambda V(t)[\hat{\bar{x}}(t) - \bar{x}(t)].
\tag{3.27}
$$

3.2.4 Case(4): k and q_z unknown

The adaptive identifier to be presented here assumes that both $k = \rho C_p$, with ρ the air density and C_p the constant pressure specific heat of air, and the thermal load q_z are unknown constants, i.e. $\hat{\theta} = [1/\hat{k}, \hat{q}_z/\hat{k}]'$.

Define the signals $z_1(t), z_2(t), z_3(t)$ and $z_4(t)$ as follows

$$
\begin{aligned}
\dot{z}_1(t) &= -z_1(t) + \frac{1}{V_h}\left[f(t)[T_3(t) - T_2(t)] - f_a[T_a - T_3(t)]\right], \\
\dot{z}_2(t) &= -z_2(t) + \frac{q_h}{V_h}, \\
\dot{z}_3(t) &= -z_3(t) + \frac{f}{V_z}[T_2(t) - T_3(t)], \\
\dot{z}_4(t) &= -z_4(t) + \frac{1}{V_z}
\end{aligned}
\tag{3.28}
$$

Define

$$
V(t) = \begin{bmatrix} z_2(t) & 0 \\ 0 & z_4(t) \end{bmatrix}
\tag{3.29}
$$

and, with $\hat{\theta}(t) = [1/\hat{k}(t), \hat{q}_z(t)/\hat{k}(t)]'$,

$$
\hat{\bar{x}}(t) = V'(t)\hat{\theta}(t)
\tag{3.30}
$$

and

$$
\bar{x}(t) = \begin{bmatrix} T_2(t) \\ T_3(t) \end{bmatrix} - \begin{bmatrix} w_1(t) \\ w_2(t) \end{bmatrix} - \begin{bmatrix} z_1(t) \\ z_3(t) \end{bmatrix}.
\tag{3.31}
$$

The signals $w_1(t)$ and $w_2(t)$ are as given by (3.12) at Section 3.2.1. Again (3.29)-(3.31) can be directly measured. Then the parameter estimate law is

$$
\dot{\hat{\theta}}(t) = -\Lambda V(t)[\hat{\bar{x}}(t) - \bar{x}(t)].
\tag{3.32}
$$

3.2.5 Case(5): V_h, T_a and V_z unknown

The adaptive identifier to be presented here assumes that V_h, T_a and V_z are unknown constants, i.e. $\hat{\theta} = [1/\hat{V}_h, \hat{T}_a/\hat{V}_h, 1/\hat{V}_z]'$.

Define the signals $z_1(t)$, $z_2(t)$ and $z_3(t)$ as follows

$$
\begin{aligned}
\dot{z}_1(t) &= -z_1(t) + f(t)[T_3(t) - T_2(t)] - f_a T_3(t) + \frac{q_h(t)}{k}, \\
\dot{z}_2(t) &= -z_2(t) + f_a, \\
\dot{z}_3(t) &= -z_3(t) + f(t)[T_2(t) - T_3(t)] + \frac{q_z}{k}
\end{aligned}
\tag{3.33}
$$

Observe, (3.33) represent state variable filters that permit adaptive identification without having to explicitly differentiate any signal. All quantities in (3.33) are known or measurable. Define

$$
V(t) = \begin{bmatrix} z_1(t) & 0 \\ z_2(t) & 0 \\ 0 & z_3(t) \end{bmatrix}
\tag{3.34}
$$

and, with $\hat{\theta}(t) = [1/\hat{V}_h(t), \hat{T}_a(t)/\hat{V}_h(t), 1/\hat{V}_z(t)]'$,

$$
\hat{\bar{x}}(t) = V'(t)\hat{\theta}(t),
\tag{3.35}
$$

$$
\bar{x}(t) = \begin{bmatrix} T_2(t) \\ T_3(t) \end{bmatrix} - \begin{bmatrix} w_1(t) \\ w_2(t) \end{bmatrix}
\tag{3.36}
$$

The signals $w_1(t)$ and $w_2(t)$ are as given by (3.12) at Section 3.2.1. Again (3.34)-(3.36) can be directly measured. Then the parameter estimate law is given by

$$
\dot{\hat{\theta}}(t) = -\Lambda\, V(t)[\hat{\bar{x}}(t) - \bar{x}(t)].
\tag{3.37}
$$

3.2.6 Case(6): T_a, V_z and q_z unknown

The adaptive identifier to be presented here assumes that T_a, V_z and q_z are unknown constants, and $\hat{\theta} = [\hat{T}_a, 1/\hat{V}_z, \hat{q}_z/\hat{V}_z]'$.

Define the signals $z_1(t), z_2(t), z_3(t)$ and $z_4(t)$ as follows

$$\dot{z}_1(t) = -z_1(t) + \frac{1}{V_h}\left[f(t)[T_3(t) - T_2(t)] - f_a T_3(t) + \frac{q_h(t)}{k}\right],$$

$$\dot{z}_2(t) = -z_2(t) + \frac{f_a}{V_h},$$

$$\dot{z}_3(t) = -z_3(t) + f(t)[T_2(t) - T_3(t)]$$

$$\dot{z}_4(t) = -z_4(t) + \frac{1}{k} \tag{3.38}$$

Observe, (3.38) represent state variable filters that permit adaptive identification without having to explicitly differentiate any signal. All quantities in (3.38) are known or measurable. Define

$$V(t) = \begin{bmatrix} z_2(t) & 0 \\ 0 & z_3(t) \\ 0 & z_4(t) \end{bmatrix} \tag{3.39}$$

and, with $\hat{\theta}(t) = [\hat{T}_a(t), 1/\hat{V}_z(t), \hat{q}_z(t)/\hat{V}_z(t)]'$,

$$\hat{\bar{x}}(t) = V'(t)\hat{\theta}(t) \tag{3.40}$$

and

$$\bar{x}(t) = \begin{bmatrix} T_2(t) \\ T_3(t) \end{bmatrix} - \begin{bmatrix} w_1(t) \\ w_2(t) \end{bmatrix} - \begin{bmatrix} z_1(t) \\ 0 \end{bmatrix}. \tag{3.41}$$

The signals $w_1(t)$ and $w_2(t)$ are as given by (3.12) at Section 3.2.1. Again (3.39)-(3.41) can be directly measured. Then the parameter estimate law is given by

$$\dot{\hat{\theta}}(t) = -\Lambda\, V(t)[\hat{\bar{x}}(t) - \bar{x}(t)]. \tag{3.42}$$

3.3   Conclusion

This chapter has presented an adaptive version of the controller of the Chapter 2 by using the gradient descent approach. After the theoretical information about the gradient descent, we have applied it to the nonlinear optimal controller. Then in the Section 3.2 the applications of Nonlinear Adaptive Optimal HVAC algorithm using gradient descent to identify different combinations of the five aforementioned system parameters have taken place.

The adaptive identifier presented has assumed that the parameters, though unknown, are constant. Note that during the process of applying the gradient descent to the HVAC system there is a need to filter the signals to avoid explicit differentiation. The overall adaptive control algorithm turned out to be a combination of the identifier given in Section 3.1.1 and the controller as given in Chapter 2, with θ replaced by $\hat{\theta}$.

CHAPTER 4

SIMULATIONS FOR THE GRADIENT DESCENT

This chapter documents simulations conducted on the Adaptive Control Algorithm formulated in Section 3.2 of Chapter 3. The principle purpose of the simulations reported in this chapter is to compare the Adaptive Control Algorithm of Chapter 3 with its nonadaptive counterpart in Chapter 2. For this purpose, two types of simulation results for six different combinations are reported. The first set, given in Sections 4.1 through 4.4, considers the cases where just the two out of the five parameters -see Section 3.2- are constant but unknown. The second set, given in Sections 4.5 and 4.6, considers the cases where three out of the five parameters are constant but unknown. Section 4.7 differs from the rest in having varying parameters to be identified. Specifically, the following setting from Table 1 is considered throughout this chapter:

$$\alpha_2 = 4.86 \times 10^{-3} \text{ \$/min-}^{\circ}\text{C}^2,$$

$$\alpha_3 = 5.39 \times 10^{-10} \text{ \$/min-W}^2,$$

$$\alpha_4 = 5.20 \times 10^{-5} \text{ \$-min/m}^6,$$

$$\alpha_5 = 1.22 \times 10^{-6} \text{ \$-min}^2/\text{m}^9$$

and

$$f_{am} = 0.05 \text{ m}^3/\text{s}.$$

The set points T_{ref} and f_{ref} are 24 °C and 0.142 m^3/s, respectively, and the initial value for the state vector is

$$\begin{cases} T_2(0) = 16^oC \\ T_3(0) = 28^oC \end{cases}$$

for all of the simulations.

For each of the following seven sections, two simulations are conducted. In the first simulation of each case, all the parameters are assumed known and the nonadaptive control law of Chapter 2 is implemented. In the second simulation of each case, corresponding combinations of two or three parameters are assumed as being unknown but constant and the adaptive algorithm of Chapter 3 is implemented with specified initial estimates. Following is the actual values of the parameters used throughout the simulations;

$$k = \rho C_p = 1.19 \text{ kg/m}^3 \times 1005 \text{ J/kg-}^oC = 1195.95 \text{ J/m}^3\text{-}^oC,$$

$$V_h = 25.5 \text{ m}^3,$$

$$V_z = 255 \text{ m}^3,$$

$$T_a = 30^oC \quad \text{and}$$

$$q_z = 1900 \text{ W}.$$

4.1   Case(1): T_a and q_z unknown

This section documents the simulations conducted on the Adaptive Control Algorithm formulated in Subsection 3.2.1 of Chapter 3. The actual values of the parameters to be identified are $\theta = [T_a, q_z]' = [30, 1900]'$. For the adaptive control law implementation of this case, T_a and q_z are assumed as being unknown constants
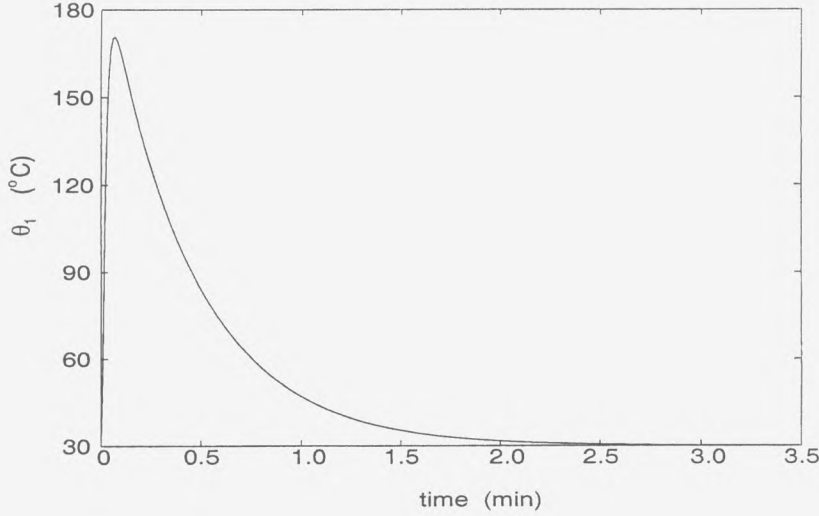
Figure 4.1: Case(1): Ambient Temperature Estimation

and the adaptive algorithm of Chapter 3 is implemented with the initial estimates of T_a and q_z respectively given by

$$
\begin{cases}
\hat{\theta}_1(0) = \hat{T}_a(0) = 31\,{}^o\mathrm{C}\,, \\[2mm]
\hat{\theta}_2(0) = \hat{q}_z(0) = 2000\,\mathrm{W}\,.
\end{cases}
$$

Figures 4.1 and 4.2 depict the estimation ability of the adaptive identifier with respect to the estimates of T_a and q_z. It is evident from these figures that the estimated ambient temperature converges to the actual T_a of 30 °C in about 3 minutes while the estimated thermal load converges to the true q_z, value of 1900 W, in less than 10 minutes. The selected adaptation gains for this specific case is

$$
\begin{cases}
\lambda_1 = 10^4 \\[2mm]
\lambda_2 = 10^9\,.
\end{cases}
\tag{4.1}
$$

Observe in Figures 4.3 to 4.8 the relative performance of the adaptive and
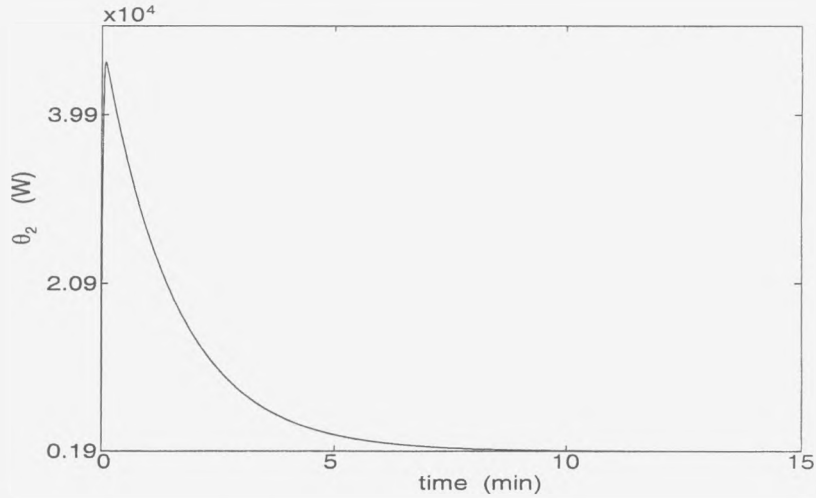
Figure 4.2: Case(1): Thermal Load Estimation

nonadaptive laws with respect to a variety of performance measures. Now consider the details of this performance. The theoretical values of T_2 and T_3 that minimize the integrand in (2.4) are

$$T_2^* = 10.125\,{}^o\text{C}$$

and

$$T_3^* = 24.015\,{}^o\text{C}$$

Indeed in Figure 4.3 one sees on the left that the actual T_2 attains this value T_2^* in around 20 minutes for both the adaptive and nonadaptive controller. Likewise T_3 also achieves its optimizing value T_3^* in about 20 minutes as seen on the right of Figure 4.3.

Figure 4.4 depicts the total cost over the attainable steady state minimum on the left side and the total cost itself over period of 72 minutes on the right. Recall that the total cost over the attainable steady state minimum is calculated as $J_e(t_f)$ given
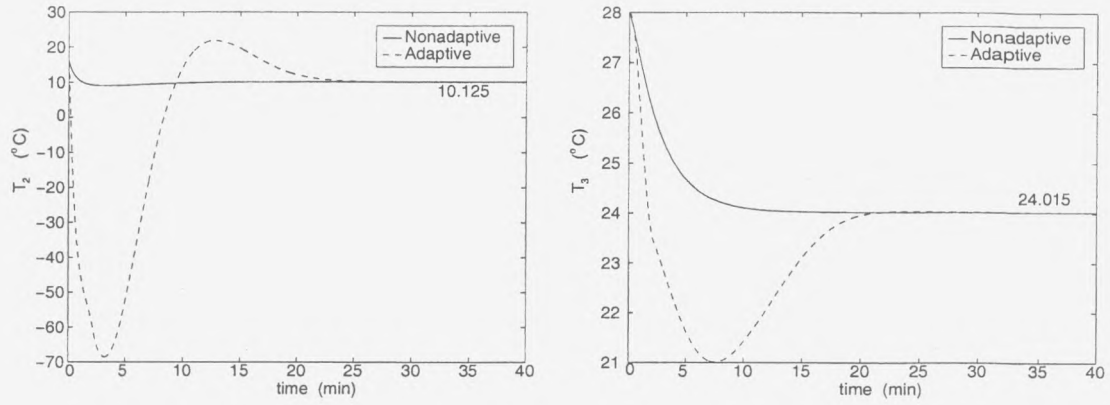
Figure 4.3: Case(1): Temperature Regulation

by (2.11) on page 10

$$J_e(t_f) = \int\limits_0^t \left[\alpha_2\Big(T_3(\tau) - T_r\Big)^2 + \alpha_3 q_h^2(\tau) + \alpha_4\Big(f(\tau) - f_r\Big)^2 + \alpha_5 f^3(\tau) - J_e \right] d\tau \quad (4.2)$$

for

$$J_e = \min\Big(\alpha_2(T_3(t) - T_r)^2 + \alpha_3 q_h^2(t) + \alpha_4(f(t) - f_r)^2 - \alpha_5 f^3(t)\Big) \quad (4.3)$$

subject to

$$\dot{T}_2(t) = 0, \qquad \dot{T}_3(t) = 0 \quad (4.4)$$
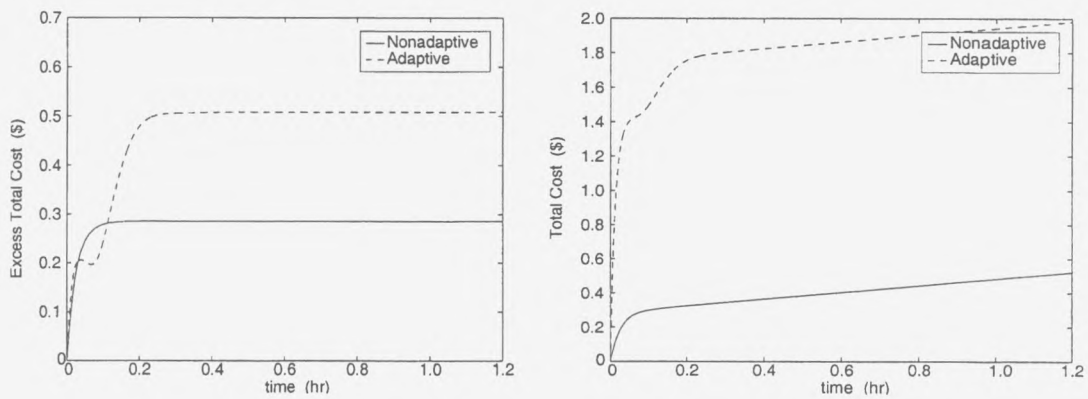
Figure 4.4: Case(1): Total Cost
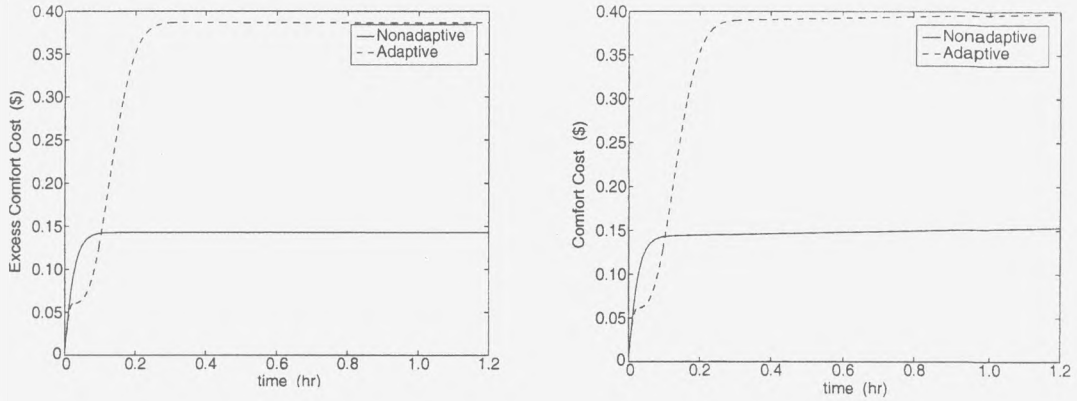
Figure 4.5: Case(1): Comfort Cost

and

$$f(t) \geq f_{am} \,, \tag{4.5}$$

and the total cost itself is

$$J(t_f) = \int\limits_0^t \left[\alpha_2 \big(T_3(\tau) - T_r\big)^2 + \alpha_3 q_h^2(\tau) + \alpha_4 \big(f(\tau) - f_r\big)^2 + \alpha_5 f^3(\tau) \right] \mathrm{d}\tau \,. \tag{4.6}$$

Observe in Figure 4.4, in less than 15 minutes J_e settles down to a constant value i.e. the integrand in (4.2) becomes zero. Similarly Figure 4.5 depicts the portions of
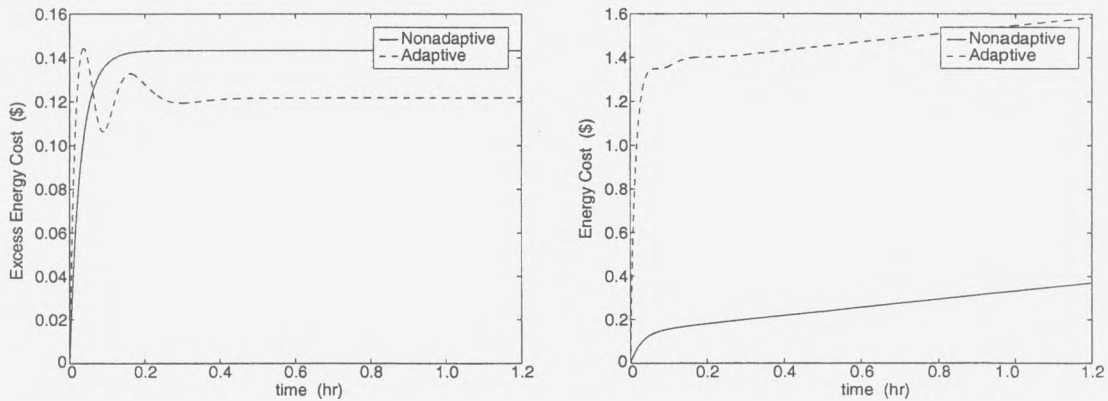
Figure 4.6: Case(1): Energy Cost
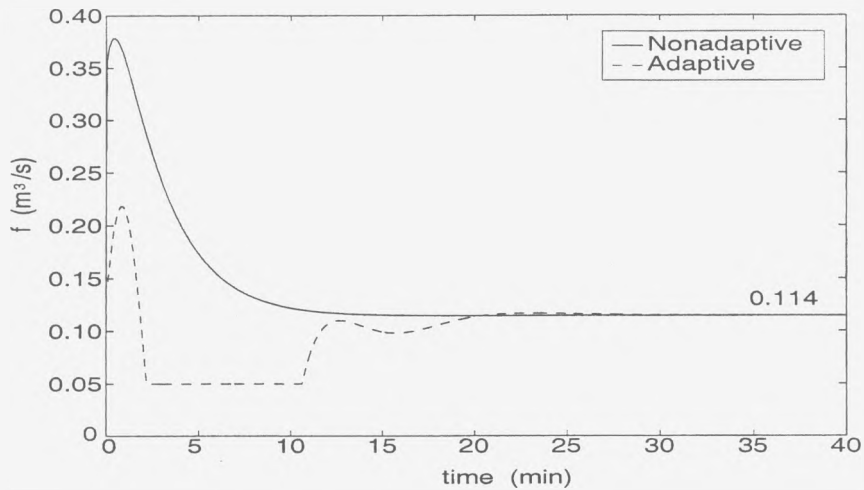
Figure 4.7: Case(1): Airflow Rate

J_e and J attributable to the comfort cost, just as Figure 4.6 depicts the energy components of J_e and J. Again, two plots on the left of Figures 4.5 and 4.6 indicate that costs stop rising after 15 minutes which reflects to the plots on the right of these figures as cost and energy costs rising at constant rates after 15 minutes. To
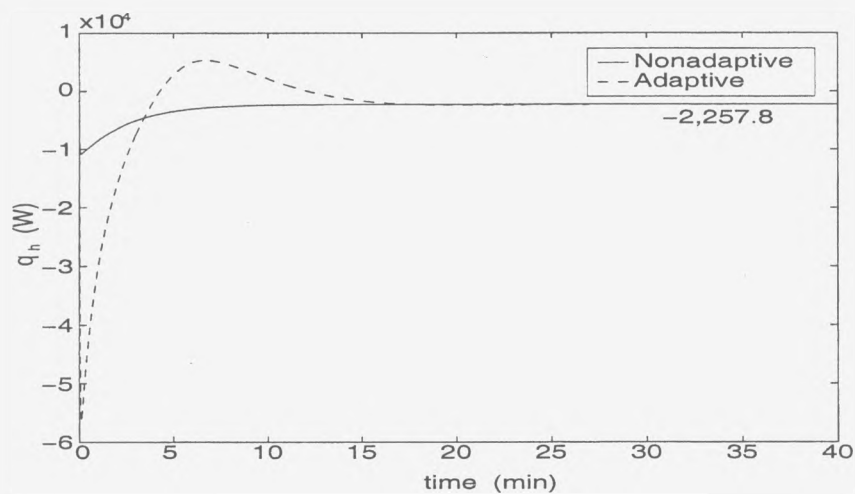
Figure 4.8: Case(1): Heat Input

be more precise, after about 12 minutes total cost rises linearly at the rate of about 25 cents per hour.

Figures 4.7 and 4.8 give the corresponding plots for the air flow rate and heat input respectively. After some initial transients, in about 20 minutes these settle down to values of $0.114 \text{ m}^3/\text{s}$ and $-2,257.8$ W, respectively. Observe f is always larger than f_{am}. Note again that each of these performance curves applies to both adaptive control with unknown T_a and q_z and non-adaptive control with known T_a and q_z.

4.2   Case(2): V_h and q_z unknown

As the title of the section suggests, the effective volume of the heat exchanger V_h and the thermal load q_z are assumed unknown for the simulations of the adaptive algorithm. The actual effective volume of the heat exchanger V_h is 25.5 m^3 and the actual thermal load q_z is 1900 Watts, therefore $\theta = [1/V_h, q_z]' = [1/25.5, 1900]'$ $= [0.039, 1900]'$. For the simulation where V_h and q_z are assumed as being unknown and the adaptive algorithm of Chapter 3 is implemented, the initial estimate of θ is chosen as

$$\begin{cases} \hat{\theta}_1(0) = \frac{1}{\hat{V}_h(0)} = \frac{1}{20} = 0.05 \,, \\ \hat{\theta}_2(0) = \hat{q}_z(0) = 2000 \,. \end{cases}$$

Figure 4.9 and 4.10 depict the estimation ability of the adaptive identifier with respect to the estimates of $1/V_h$ and q_z. It is evident from these figures that $\hat{\theta}_1 = 1/\hat{V}_h$ converges to the actual $1/V_h$ of 0.039 in less than 10 seconds while the estimated thermal load converges to the true q_z value of 1900 W in less than 10
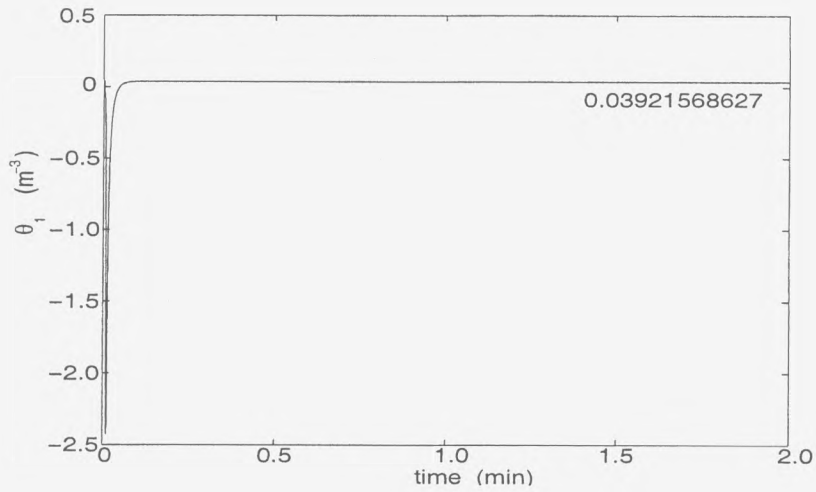
Figure 4.9: Case(2): Estimation of $\frac{1}{V_h}$

minutes. The selected adaptation gains are

$$\begin{cases} \lambda_1 = 1\,, \\ \lambda_2 = 10^9\,. \end{cases}$$
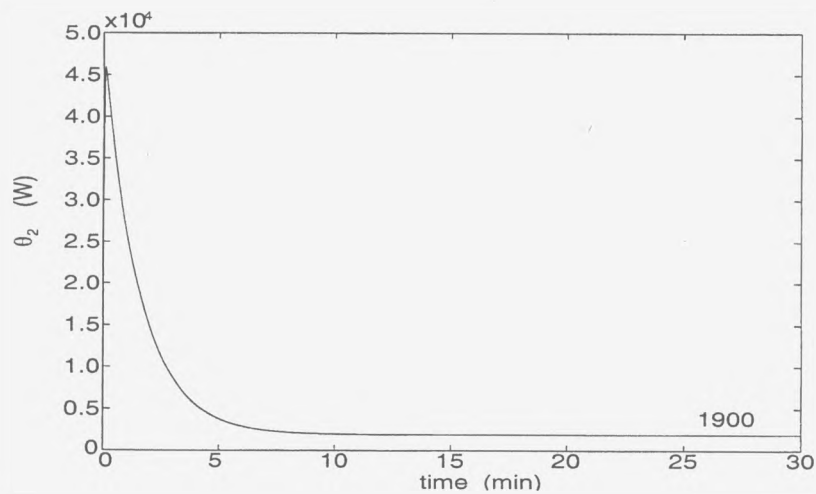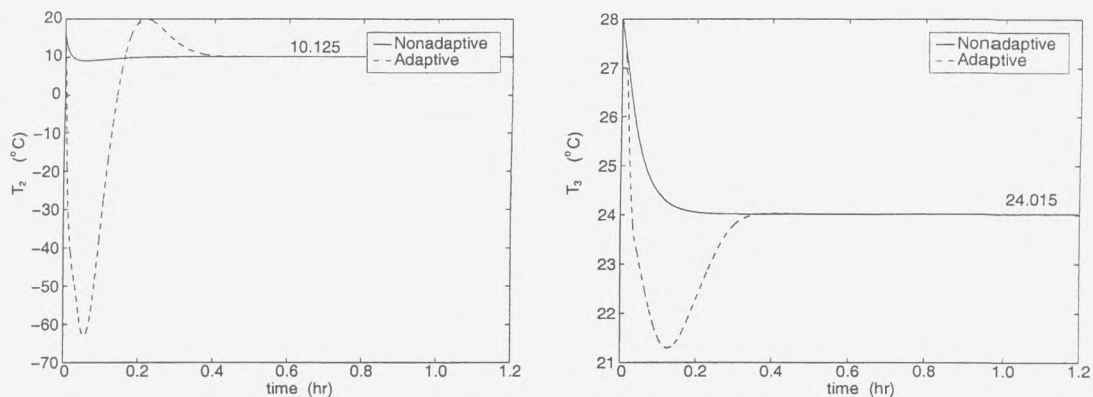

Figure 4.10: Case(2): Thermal Load Estimation

Figure 4.11: Case(2): Temperature Regulation

Observe in Figures 4.11 to 4.16 the relative performance of the adaptive and non-adaptive laws with respect to a variety of performance measures. Now consider the details of this performance. The theoretical values of T_2 and T_3 that minimize the integrand in (2.4) are

$$T_2^* = 10.125\,{}^{o}\mathrm{C}$$

and

$$T_3^* = 24.015\,{}^{o}\mathrm{C}$$
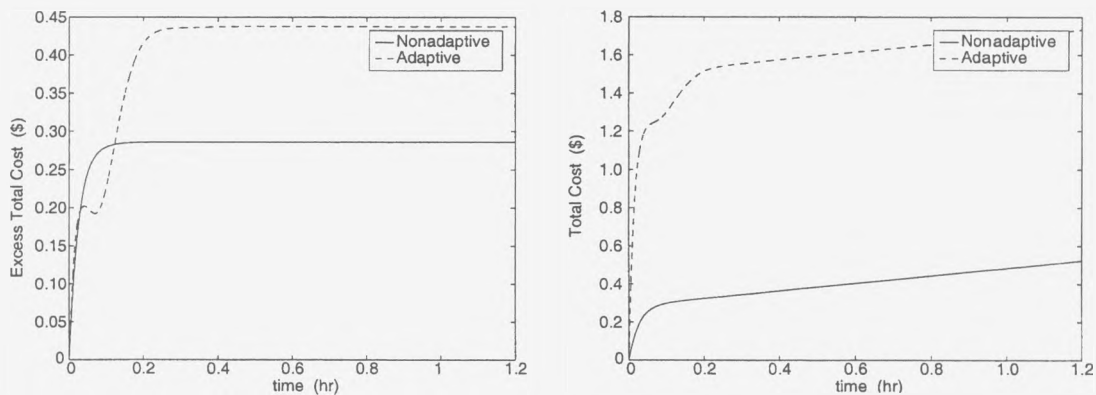
Figure 4.12: Case(2): Total Cost
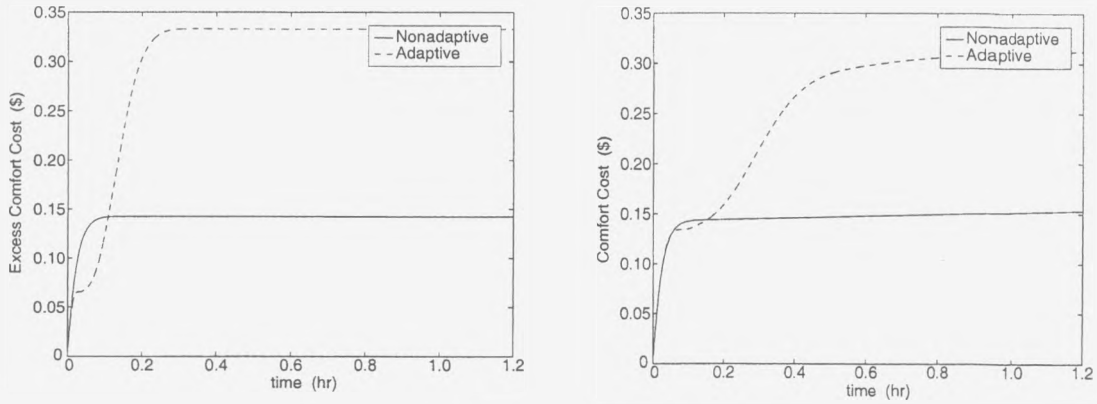
Figure 4.13: Case(2): Comfort Cost

Indeed in Figure 4.11 one sees that the actual T_2 attains this value T_2^* in around 20 minutes for both the adaptive and non-adaptive controller. Likewise T_3 also achieves its optimizing value in about 20 minutes.

The left plot of Figure 4.12 depicts the total cost over the attainable steady state minimum, i.e $J_e(t)$ given by (4.2), and the right plot depicts the total cost $J(t)$ given by (4.6). Observe in Figure 4.12, in less than half an hour J_e settles down to a constant value i.e. the integrand in (4.2) becomes zero. Similarly Figure 4.13
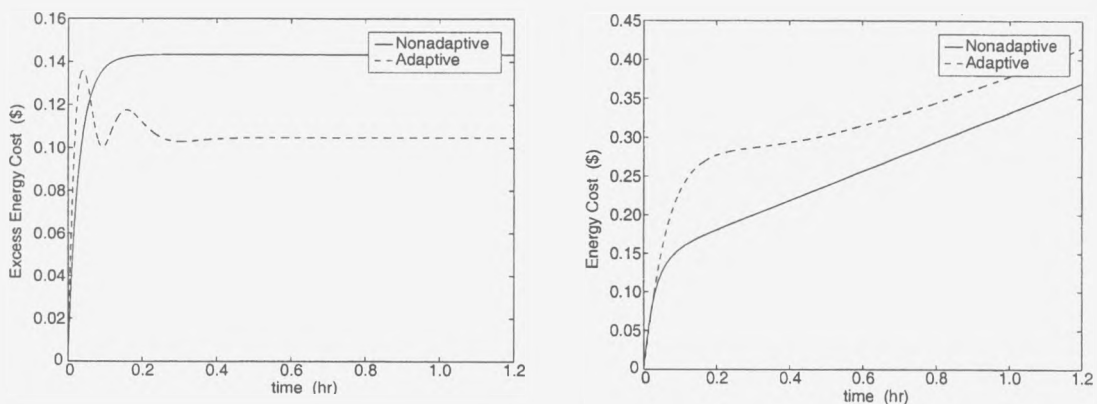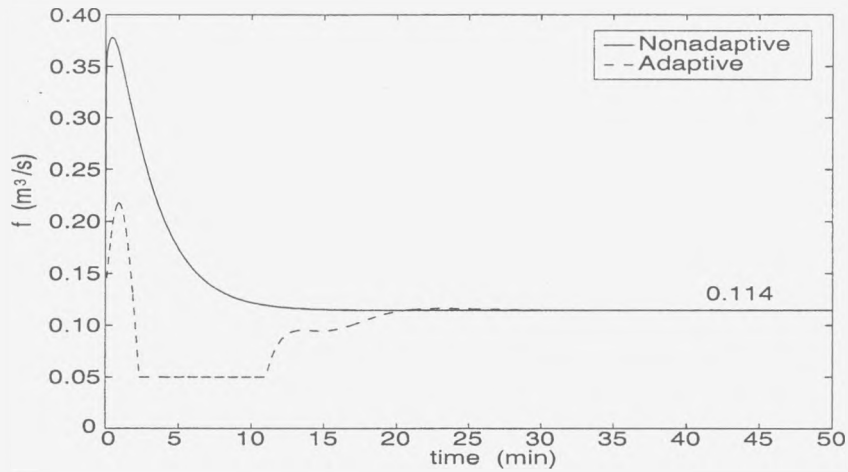

Figure 4.14: Case(2): Energy Cost

Figure 4.15: Case(2): Airflow Rate

depicts the portion of J_e and J attributable to the comfort cost, just as Figure 4.14 depicts the energy component of J_e and J. The two plots on the left of Figures 4.13 and 4.14 indicate that costs stop rising after half an hour. In about 25 minutes, total cost rises linearly at the rate of about 18 cents per hour.
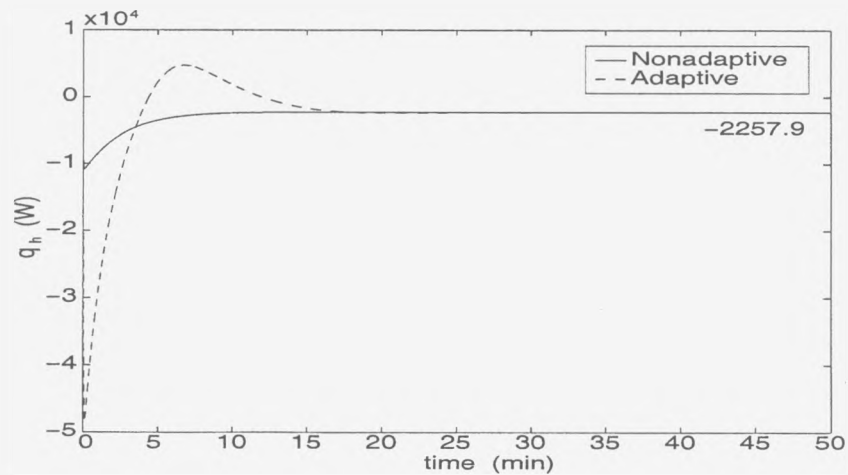

Figure 4.16: Case(2): Heat Input

Figures 4.15 and 4.16 give the corresponding plots for the air flow rate and the heat input respectively. After some initial transients, in about 20 minutes these settle down to values of 0.114 m^3/s and $-2,257.9$ W, respectively. Observe f is always larger than f_{am}. Note again that each of these performance curves applies to both adaptive control with unknown V_h and q_z and non-adaptive control with known V_h and q_z.

4.3 Case(3): T_a and V_z unknown

As the title of the section suggests, the ambient temperature T_a and the effective thermal space volume V_z are assumed unknown for the simulations of the adaptive algorithm. The actual ambient temperature T_a is 30 °C and the actual effective thermal space volume V_z is 255 m^3, therefore the actual value for θ is $\theta = [T_a, \frac{1}{V_z}]' = [30, \frac{1}{255}]' = [30, 3.9 \times 10^{-3}]'$. The initial estimate of θ is chosen to be

$$\begin{cases} \hat{\theta}_1(0) = \hat{T}_a(0) = 31\,, \\ \hat{\theta}_2(0) = 1/\hat{V}_z(0) = \frac{1}{255} = 5 \times 10^{-3}\,. \end{cases}$$

Figures 4.17 and 4.18 depict the estimation ability of the adaptive identifier with respect to the estimates of θ_1 and θ_2. It is evident from these figures that the estimated ambient temperature converges to the actual T_a of 30 °C in about 6 seconds while θ_2 converges to the true $\frac{1}{V_z}$, value of 3.9×10^{-3}, in 3 minutes. The selected adaptation gains are

$$\begin{cases} \lambda_1 = 10^7\,, \\ \lambda_2 = 1\,. \end{cases}$$

Observe in Figures 4.19 to 4.24 the relative performance of the adaptive and nonadaptive laws with respect to a variety of performance measures. Now consider the details of this performance. On the left plot of Figure 4.19 the actual T_2 attains the value T_2^* in around 20 minutes for both the adaptive and nonadaptive controller.
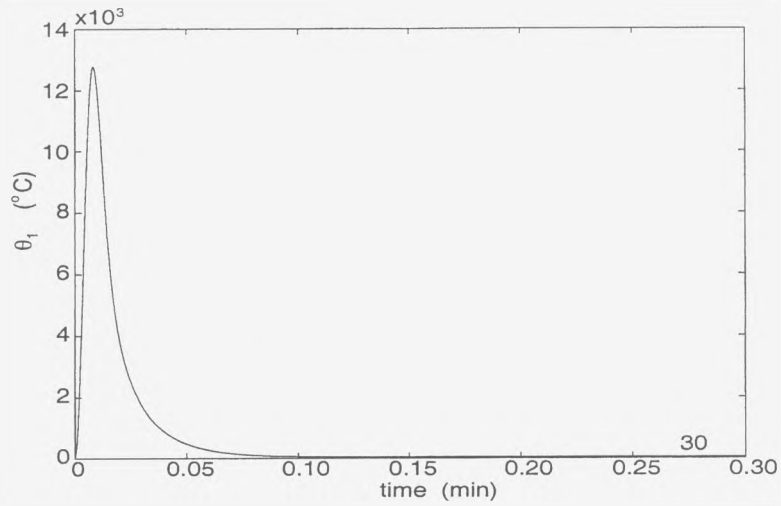
Figure 4.17: Case(3): Ambient Temperature Estimation

Likewise T_3 on the right also achieves its optimizing value in about 20 minutes.

The left plot of Figure 4.20 depicts the total cost over the attainable steady state minimum, i.e $J_e(t)$ given by (4.2), and the right plot depicts the total cost $J(t)$
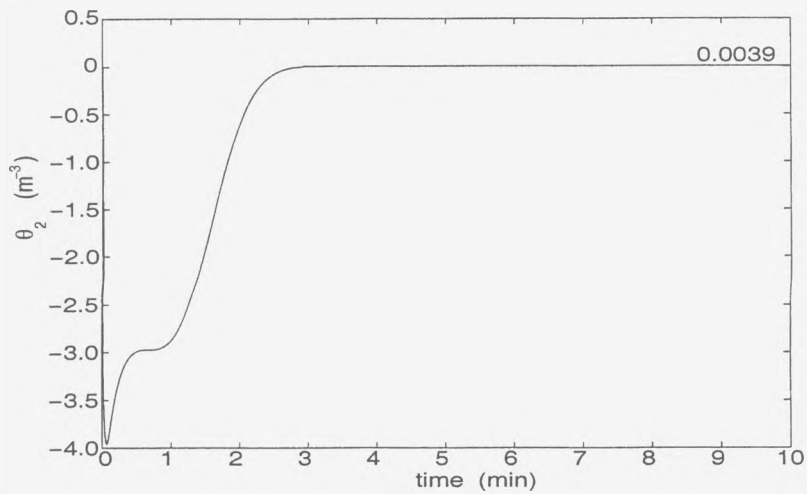

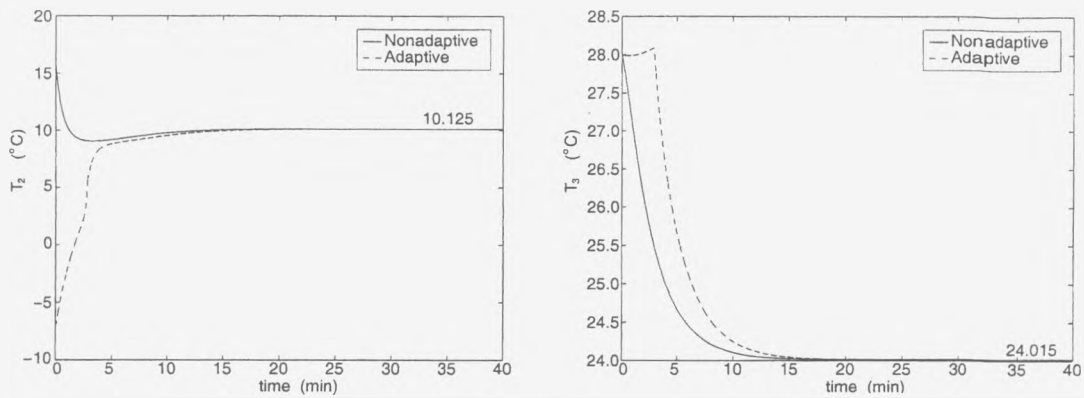Figure 4.18: Case(3): Estimation of $\frac{1}{V_z}$

Figure 4.19: Case(3): Temperature Regulation

given by (4.6). Observe, in around 10 minutes J_e settles down to a constant value i.e. the integrand in (4.2) becomes zero. Similarly Figure 4.21 depicts the portion of J_e and J attributable to the comfort cost, just as Figure 4.22 depicts the energy component of J_e and J. Again, two plots on the left of Figures 4.21 and 4.22 indicate that costs stop rising after 10 minutes. After about 12 minutes total cost rises linearly at the rate of about 10 cents per hour.

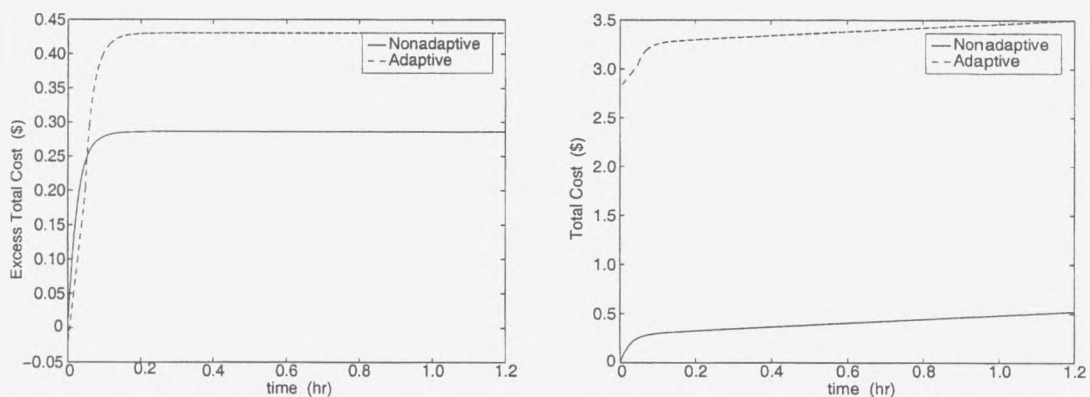Figures 4.23 and 4.24 give the corresponding plots for the air flow rate and the
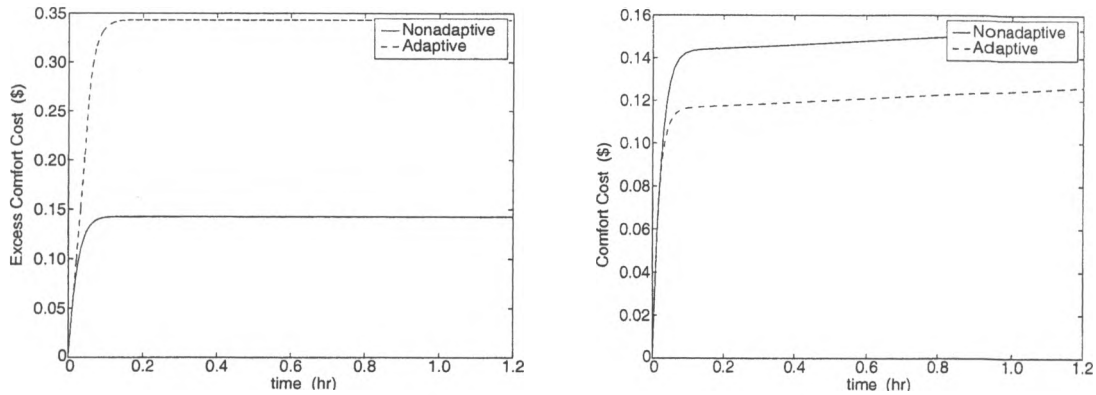

Figure 4.20: Case(3): Total Cost

Figure 4.21: Case(3): Comfort Cost

heat input respectively. After some initial transients, in about 15 minutes the air flow rate settles down to 0.114 m^3/s and the heat input to -2258 W. Observe f is always larger than f_{am}. Note again that each of these performance curves applies to both adaptive control with unknown T_a and V_z and non-adaptive control with known T_a and V_z.
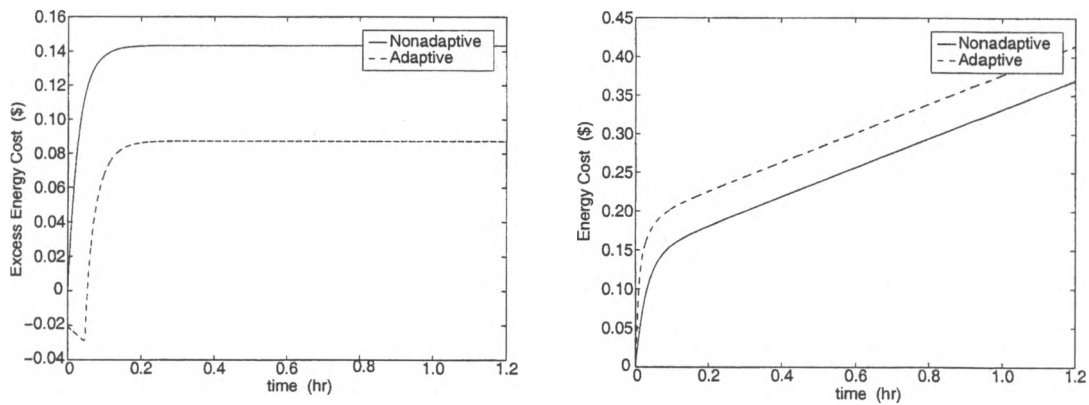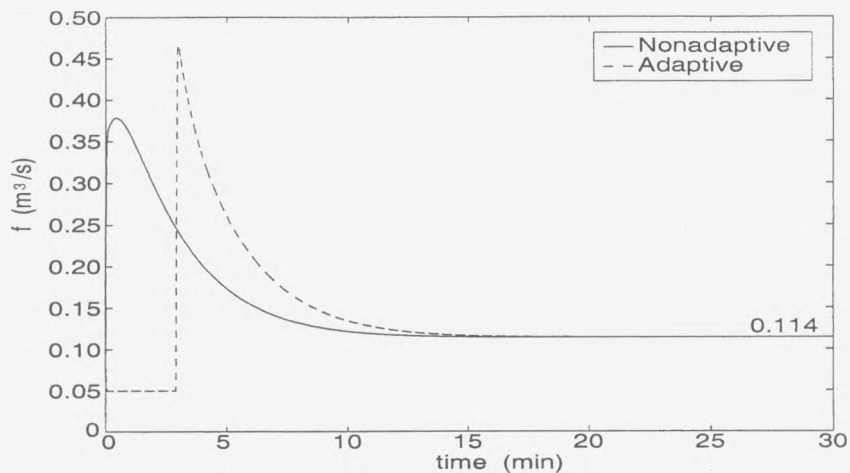

Figure 4.22: Case(3): Energy Cost
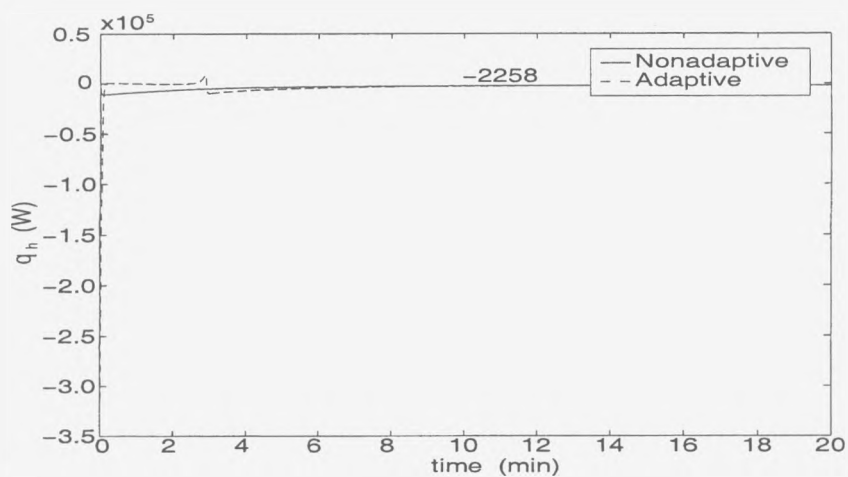
Figure 4.23: Case(3): Airflow Rate

Figure 4.24: Case(3): Heat Input

4.4   Case(4): k and q_z unknown

In this section, the parameter k, (ρC_p), and the thermal load q_z are assumed unknown for the simulations of the adaptive algorithm. The actual value for the parameter k is 1195.95 and the actual thermal load q_z is 1900 W, therefore the
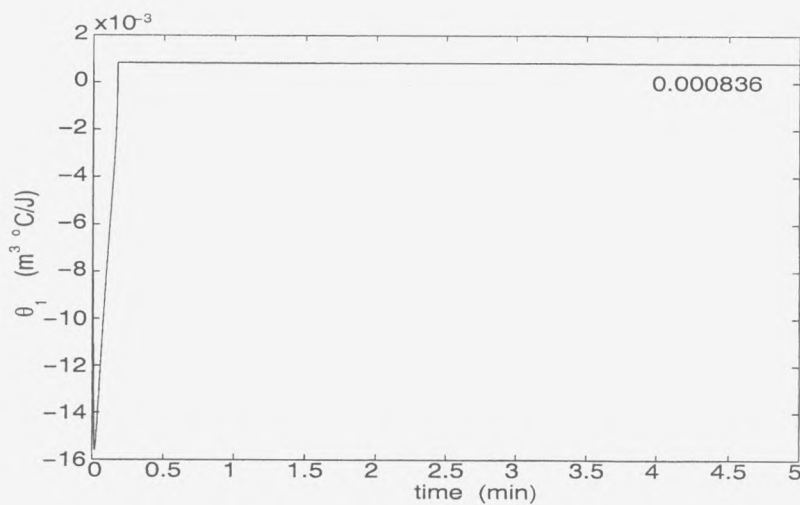
Figure 4.25: Case(4): Estimation of $\frac{1}{k}$

actual value for θ is $\theta = [\frac{1}{k}, \frac{q_z}{k}]' = [\frac{1}{1195.95}, \frac{1900}{1195.95}] = [8.36 \times 10^{-4}, 1.589]'$. The initial
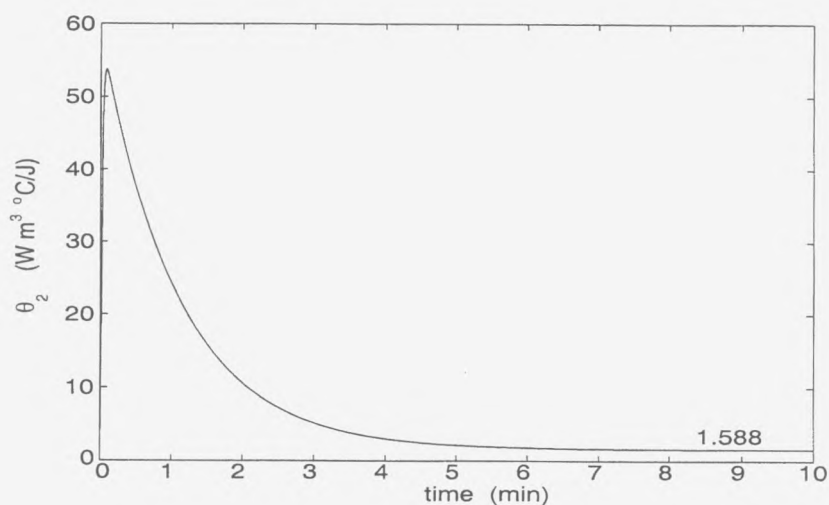

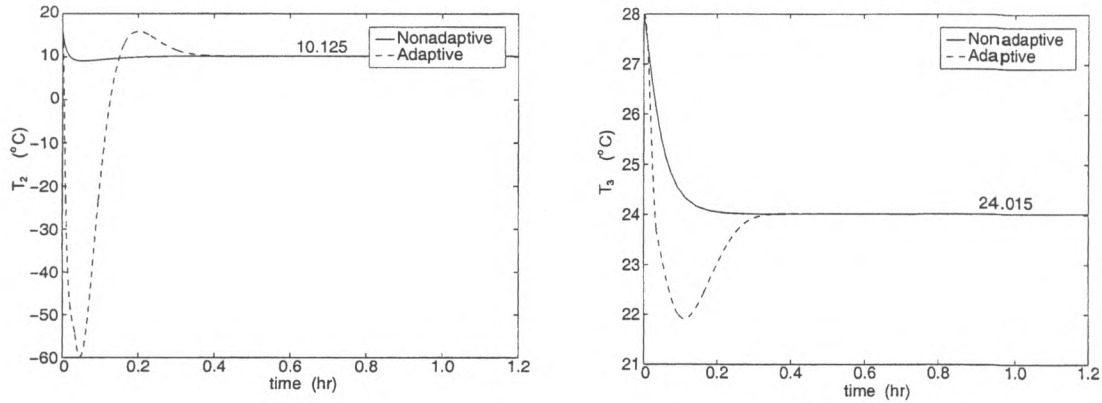Figure 4.26: Case(4): Estimation of $\frac{q_z}{k}$

Figure 4.27: Case(4): Temperature Regulation

estimate of θ is chosen as

$$
\begin{cases}
\hat{\theta}_1(0) = \frac{1}{\hat{k}(0)} = \frac{1}{1000} = 10^{-3}\,, \\[2mm]
\hat{\theta}_2(0) = \frac{\hat{q}_z(0)}{\hat{k}(0)} = \frac{2000}{1000} = 2\,.
\end{cases}
$$

Figures 4.25 and 4.26 depict the estimation ability of the adaptive identifier with respect to the estimates of θ_1 and θ_2. It is evident from these figures that the estimated parameter $\hat{k}$ converges to the actual k of 1195.95 in less than half minutes while the estimated thermal load converges to the true q_z value of 1900 W in around
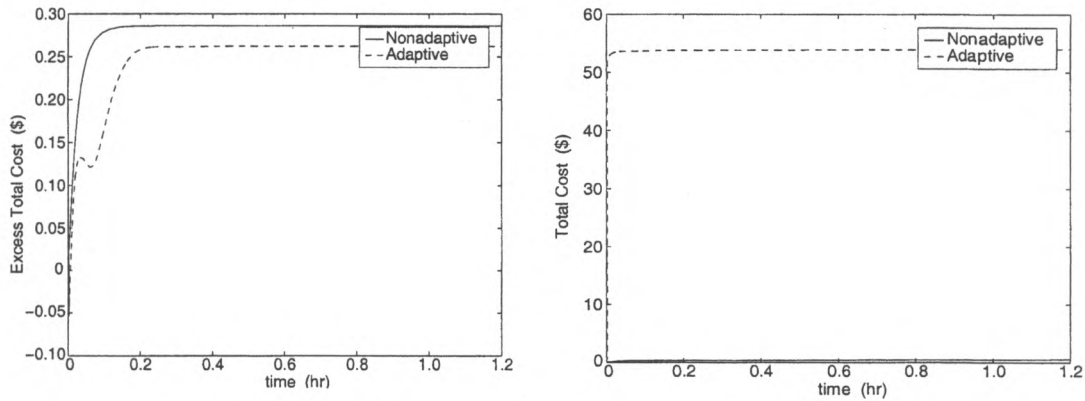

Figure 4.28: Case(4): Total Cost
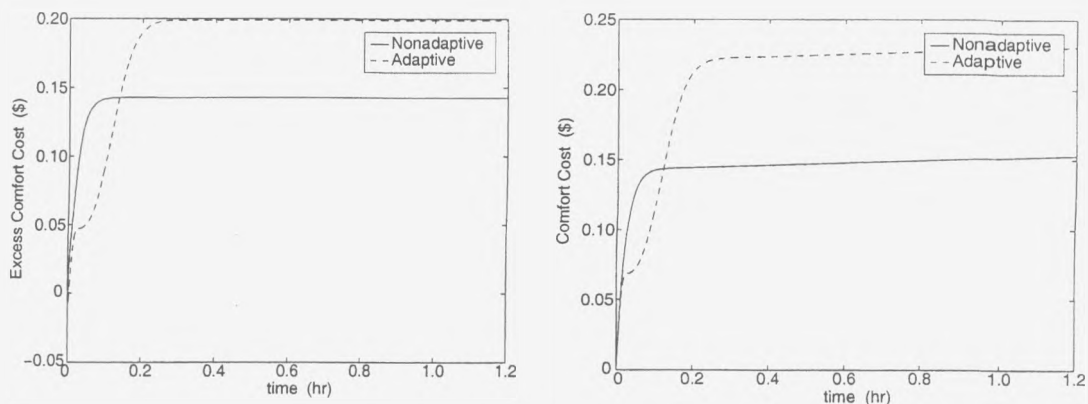
Figure 4.29: Case(4): Comfort Cost

10 minutes. The selected adaptation gains are

$$\begin{cases} \lambda_1 = 10^{-5}, \\ \lambda_2 = 10^3. \end{cases}$$

Observe in Figures 4.27 to 4.32 the relative performance of the adaptive and non-adaptive laws with respect to a variety of performance measures. Now consider the details of this performance. On the left plot of Figure 4.27 one sees that the actual T_2 attains the value T_2^* in around 20 minutes for both the adaptive and non-adaptive controller. Likewise T_3 also achieves its optimizing value in about 20

Figure 4.30: Case(4): Energy Cost

Figure 4.31: Case(4): Airflow Rate

minutes.

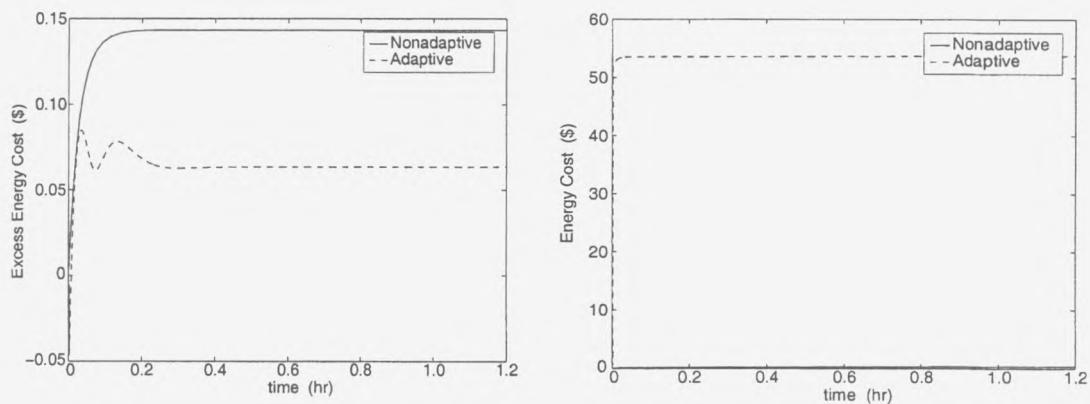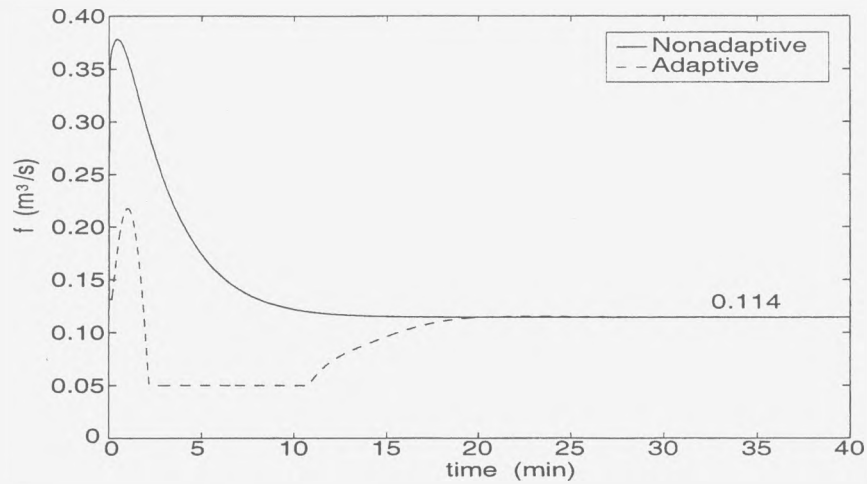Figure 4.28 depicts the total cost over the attainable steady state minimum, i.e $J_e(t)$ given by (4.2) on the left plot, and the total cost $J(t)$ given by (4.6) on the right plot. Observe, in less than 15 minutes J_e settles down to a constant value i.e.
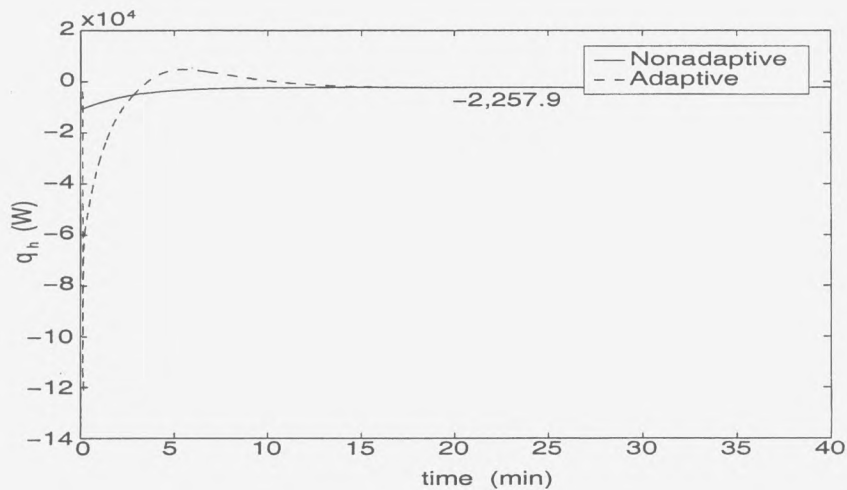

Figure 4.32: Case(4): Heat Input

the integrand in (4.2) becomes zero. Similarly Figure 4.29 depicts the portion of J_e and J attributable to the comfort cost, just as Figure 4.30 depicts the energy component of J_e and J. Again, two plots on the left of Figures 4.29 and 4.30 indicate that costs stop rising after 15 minutes. After about 15 minutes total cost rises linearly at the rate of about 75 cents per hour.

Figures 4.31 and 4.32 give the corresponding plots for the air flow rate and heat input respectively. After some initial transients, in about 20 minutes these settle down to values of 0.114 m³/s and $-2,257.9$ W, respectively. Observe f is always larger than f_{am}. Note again that each of these performance curves applies to both adaptive control with unknown k and q_z and non-adaptive control with known k and q_z.

4.5   Case(5): V_h, T_a and V_z unknown

This section documents simulations conducted on the Adaptive Control Algorithm formulated in Subsection 3.2.5 of Chapter 3. The actual value of θ is $\theta = [\frac{1}{V_h}, \frac{T_a}{V_h}, \frac{1}{V_z}]' = [\frac{1}{25.5}, \frac{30}{25.5}, \frac{1}{255}]' = [0.039, 1.176, 3.9 \times 10^{-3}]'$. The initial estimate of θ is given by

$$\begin{cases} \hat{\theta}_1(0) = \frac{1}{\hat{V}_h(0)} = \frac{1}{20} = 0.05, \\ \hat{\theta}_2(0) = \frac{\hat{T}_a(0)}{\hat{V}_h(0)} = \frac{31}{20} = 1.55 \\ \hat{\theta}_3(0) = 1/\hat{V}_z(0) = 1/200 = 5 \times 10^{-3}. \end{cases}$$

The selected adaptation gains are

$$\begin{cases} \lambda_1 = 0.5 \times 10^{-2}, \\ \lambda_2 = 1, \\ \lambda_3 = 10^{-2}. \end{cases}$$

Figures 4.33, 4.34, and 4.35 depict the estimation ability of the adaptive identifier with respect to the estimates of $\frac{1}{V_h}$, $\frac{T_a}{V_h}$ and $\frac{1}{V_z}$. It is evident from Figure 4.33 that
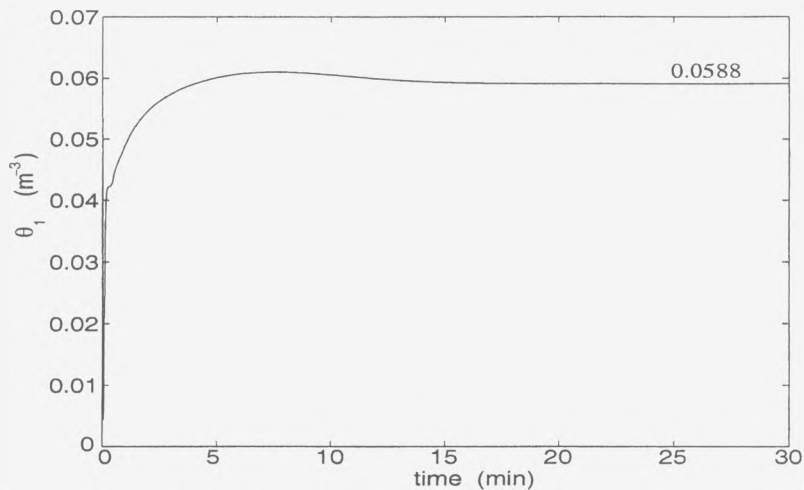
Figure 4.33: Case(5): Estimation of $\frac{1}{V_h}$

$\hat{V}_h$ does not converge to the actual V_h of 25.5 m^3, however it converges to 17 m^3 in about 15 minutes. Having more than two parameters to estimate causes the gradient descent based adaptive controller algorithm to fail to estimate the third
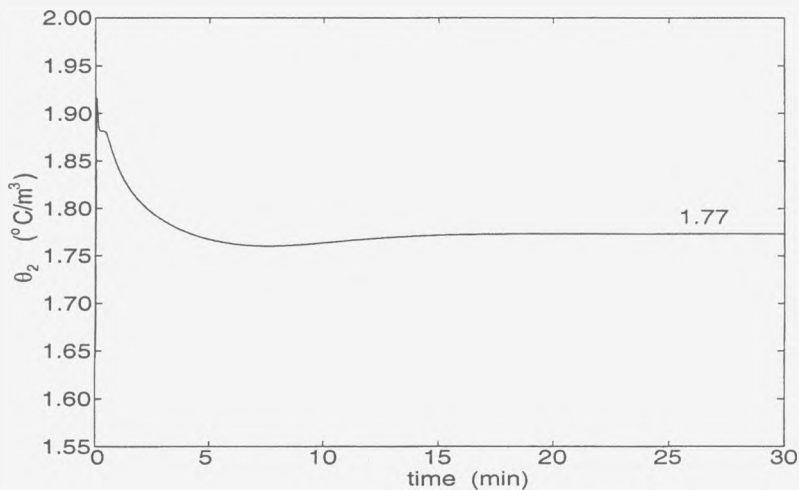
Figure 4.34: Case(5): Estimation of $\frac{T_a}{V_h}$
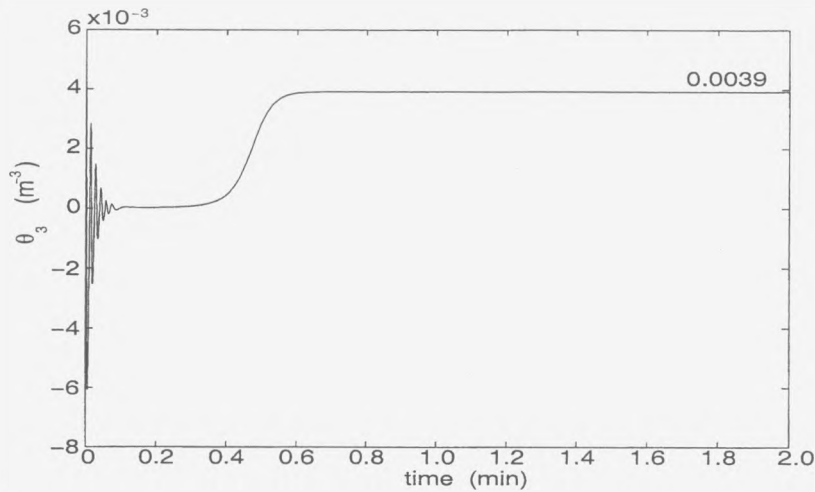
Figure 4.35: Case(5): Estimation of $\frac{1}{V_z}$

parameter. The estimated ambient temperature, on the other hand, converges to the actual T_a of 30 ^{o}C in about 17 minutes while the estimated thermal load converges to the true V_z value of 1900 W in less than 1 minute.

Observe in Figures 4.36 to 4.41 the relative performance of the adaptive and nonadaptive laws with respect to a variety of performance measures. Now consider
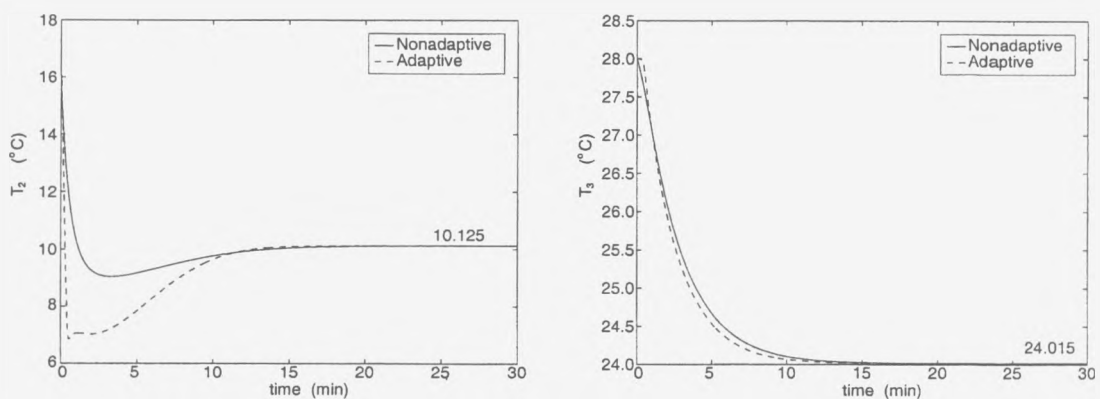
Figure 4.36: Case(5): Temperature Regulation
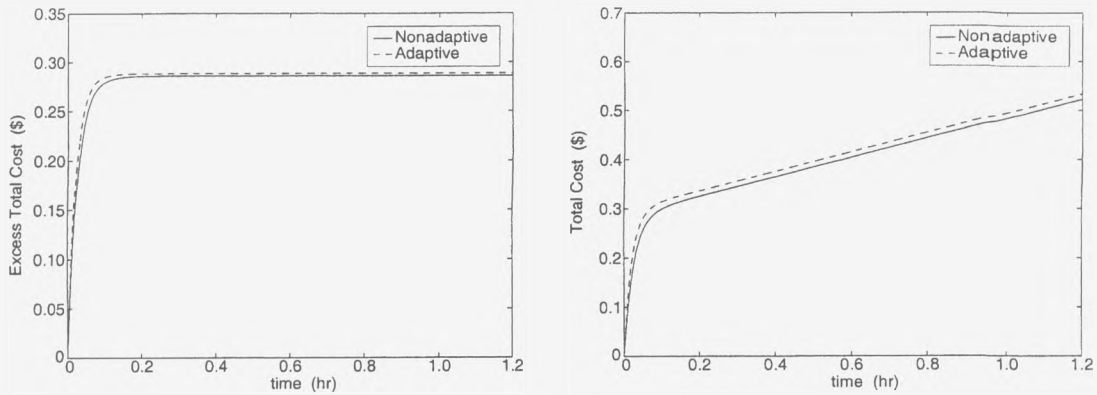
Figure 4.37: Case(5): Total Cost

the details of this performance. On the left plot of Figure 4.36 one sees that the actual T_2 attains the value $T_2{}^*$ in around 20 minutes for both the adaptive and non-adaptive controller. Likewise T_3 also achieves its optimizing value in about 20 minutes.

Figure 4.37 depicts the total cost over the attainable steady state minimum, i.e $J_e(t)$ given by (4.2) on the left plot, and the total cost $J(t)$ given by (4.6) on the right plot. Observe, in less than 10 minutes J_e settles down to a constant value i.e.
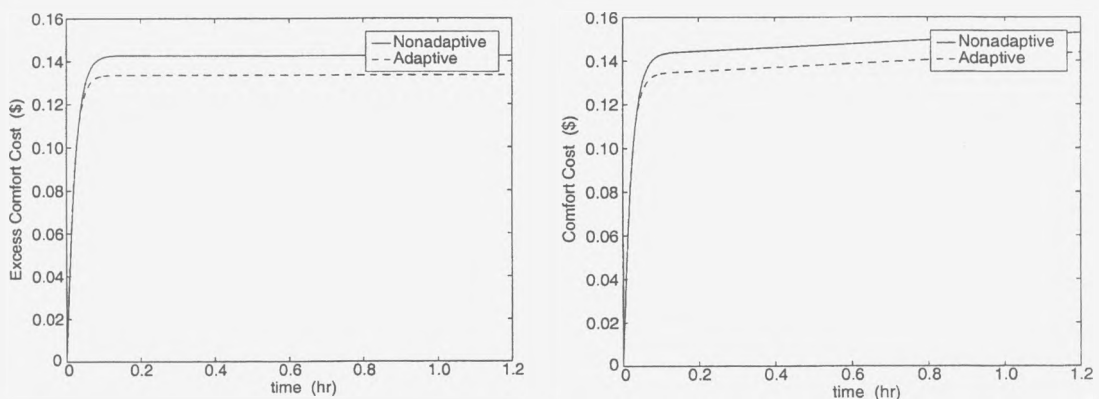
Figure 4.38: Case(5): Comfort Cost
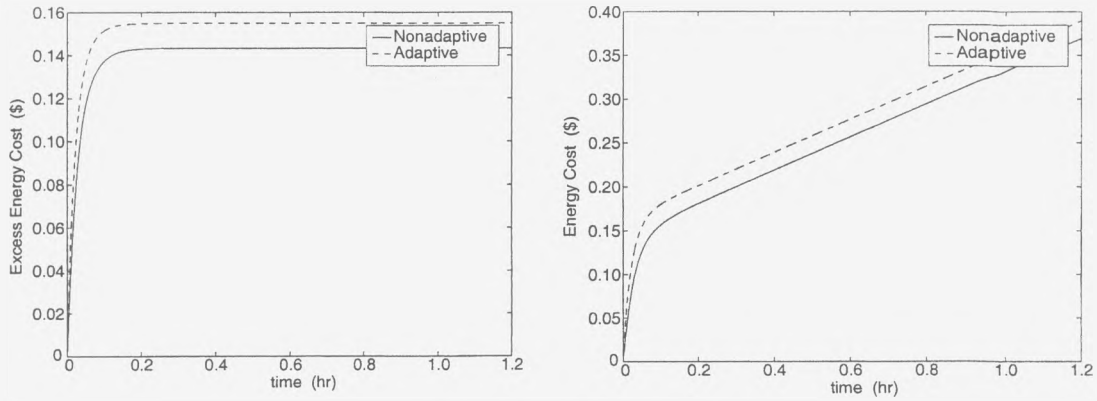
Figure 4.39: Case(5): Energy Cost

the integrand in (4.2) becomes zero. Similarly Figure 4.38 depicts the portion of J_e and J attributable to the comfort cost, just as Figure 4.39 depicts the energy component of J_e and J. Again, two plots on the left of Figures 4.38 and 4.39 indicate that costs stop rising after 10 minutes. After about 12 minutes total cost rises linearly at the rate of about 20 cents per hour.

Figures 4.40 and 4.41 give the corresponding plots for the air flow rate and heat
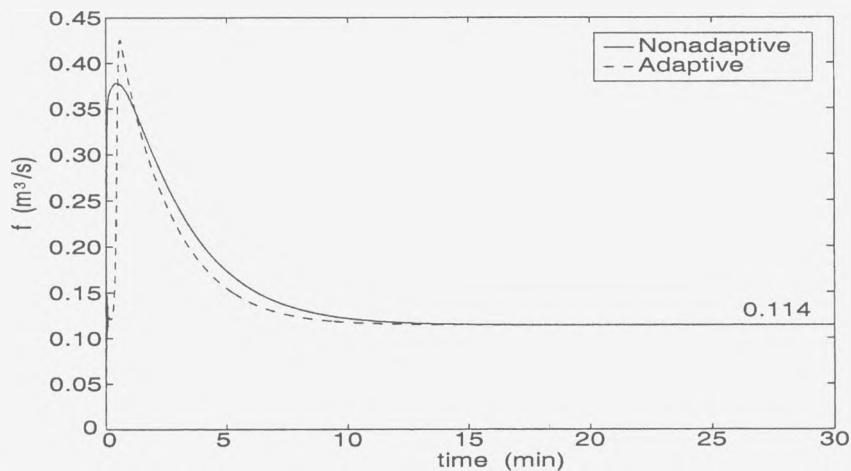
Figure 4.40: Case(5): Airflow Rate
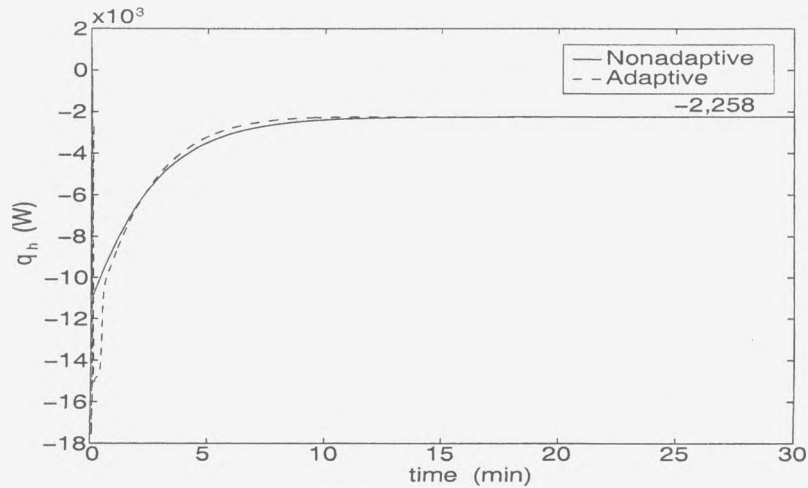
Figure 4.41: Case(5): Heat Input

input respectively. After some initial transients, in about 15 minutes these settle down to values of 0.114 m^3/s and $-2,258$ W, respectively. Observe f is always larger than f_{am} . Note again that each of these performance curves applies to both adaptive control with unknown V_h, T_a and V_z, and non-adaptive control with known V_h, T_a and V_z.

4.6 Case(6): T_a, V_z and q_z unknown

This section documents simulations conducted on the Adaptive Control Algorithm formulated in Subsection 3.2.6 of Chapter 3. The actual value of θ is $\theta = [T_a, \frac{1}{V_z}, \frac{q_z}{V_z}]' = [30, \frac{1}{255}, \frac{1900}{255}]' = [30, 3.9 \times 10^{-3}, 7.45]'$. For this section, like the others, two simulations are conducted. In the first, T_a, V_z and q_z are assumed to be known and the nonadaptive control law of Chapter 2 is implemented. In the second, T_a, V_z and q_z are assumed as being unknown and the adaptive algorithm of

Chapter 3 is implemented with the initial estimate of θ given by

$$\begin{cases} \hat{\theta}_1(0) = \hat{T}_a(0) = 31\,, \\ \hat{\theta}_2(0) = 1/\hat{V}_z(0) = 1/200 = 5 \times 10^{-3}\,, \\ \hat{\theta}_3(0) = \hat{q}_z(0)/\hat{V}_z(0) = 2000/200 = 10\,. \end{cases}$$

The selected adaptation gains are

$$\begin{cases} \lambda_1 = 10^4\,, \\ \lambda_2 = 10^{-4}\,, \\ \lambda_3 = 10^5\,. \end{cases}$$

Figure 4.42, 4.43 and 4.44 depict the estimation ability of the adaptive identifier with respect to the estimates of T_a, V_z and q_z. It is evident from Figure 4.42 that the estimated ambient temperature converges to the actual T_a of 30 °C in about 3 minutes. The estimated effective thermal space volume, on the other hand, converges to the value of $1/0.0176 = 56.818$ m^3 in 25 minutes as can be seen from Figure 4.43. Recall that the true value of V_z is 255 m^3. Estimating three parameters by using gradient descent method has resulted in failure to estimate one of them
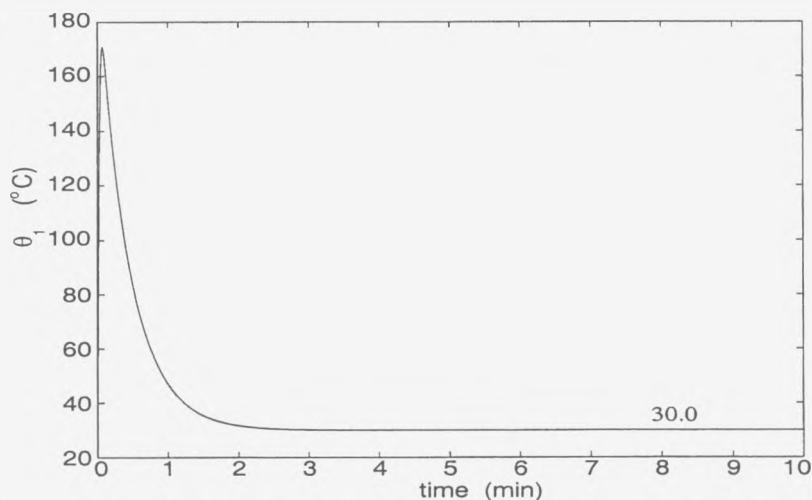
Figure 4.42: Case(6): Ambient Temperature Estimation
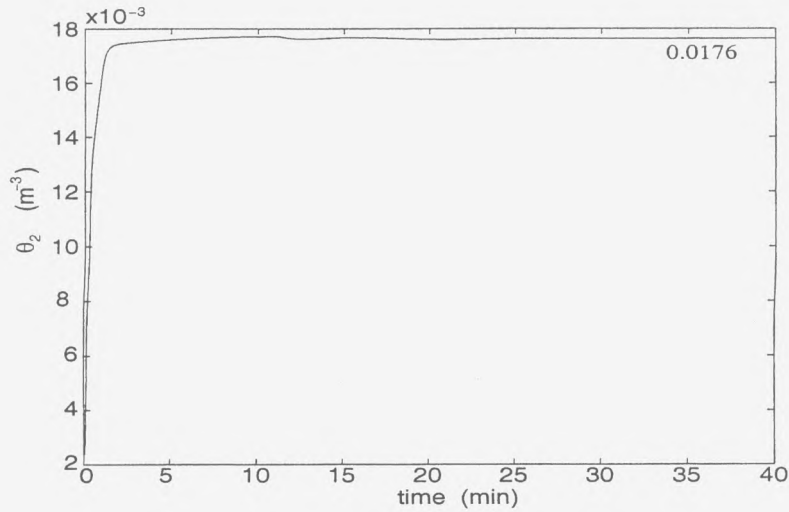
Figure 4.43: Case(6): Estimation of $\frac{1}{V_z}$

correctly as was the case with the Case(5) in previous subsection. The estimated thermal load also converges to the value of $33.5051/0.0176 = 1,903.7$ W, which is quite close to the true value of 1900 W, in 25 minutes as can be seen from
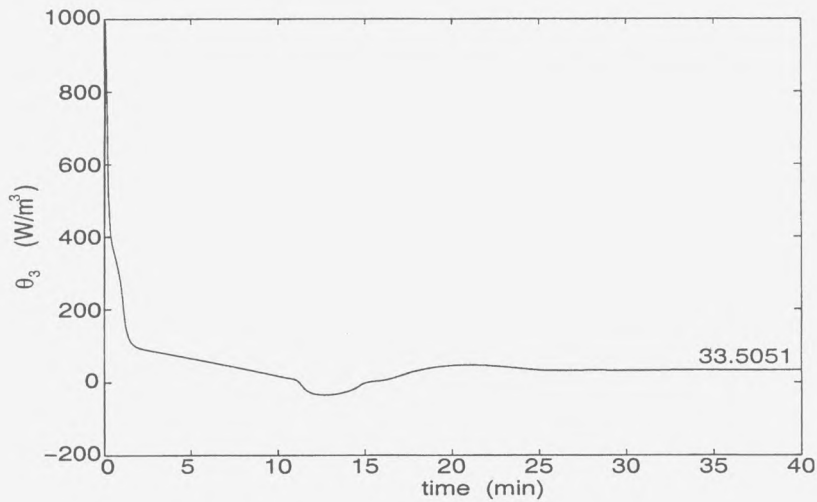
Figure 4.44: Case(6): Estimation of $\frac{q_z}{V_z}$
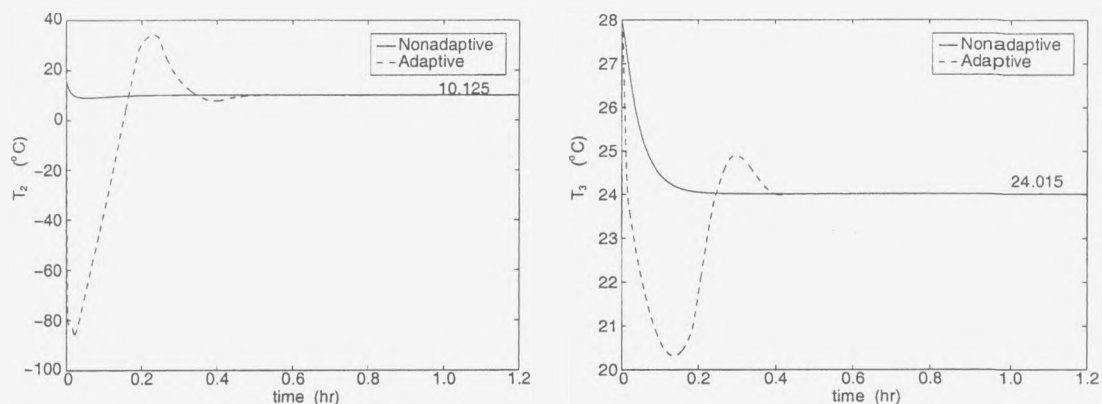
Figure 4.45: Case(6): Temperature Regulation

Figure 4.44.

Observe in Figures 4.45 to 4.50 the relative performance of the adaptive and nonadaptive laws with respect to a variety of performance measures. Now consider the details of this performance. On the left plot of Figure 4.45 one sees that the actual T_2 attains the value T_2^* in around 30 minutes for both the adaptive and nonadaptive controller. Likewise T_2 also achieves its optimizing value in about 30 minutes.
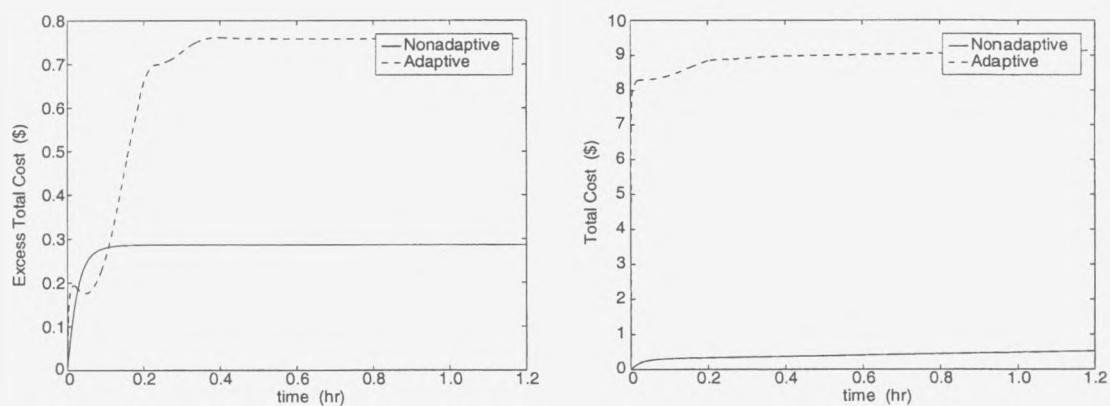
Figure 4.46: Case(6): Total Cost
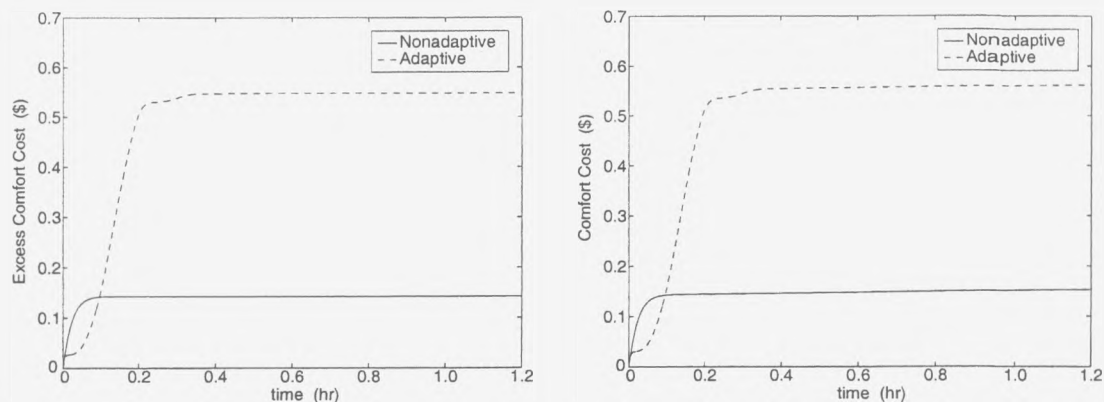
Figure 4.47: Case(6): Comfort Cost

Figure 4.46 depicts the total cost over the attainable steady state minimum, i.e $J_e(t)$ given by (4.2) on the left plot, and the total cost $J(t)$ given by (4.6) on the right plot. Observe, in around 25 minutes J_e settles down to a constant value i.e. the integrand in (4.2) becomes zero. Similarly Figure 4.47 depicts the portion of J_e and J attributable to the comfort cost, just as Figure 4.48 depicts the energy component of J_e and J. Again these two plots on the left of Figures 4.47 and 4.48 indicate that indicate that costs stop rising after 25 minutes. After about 25
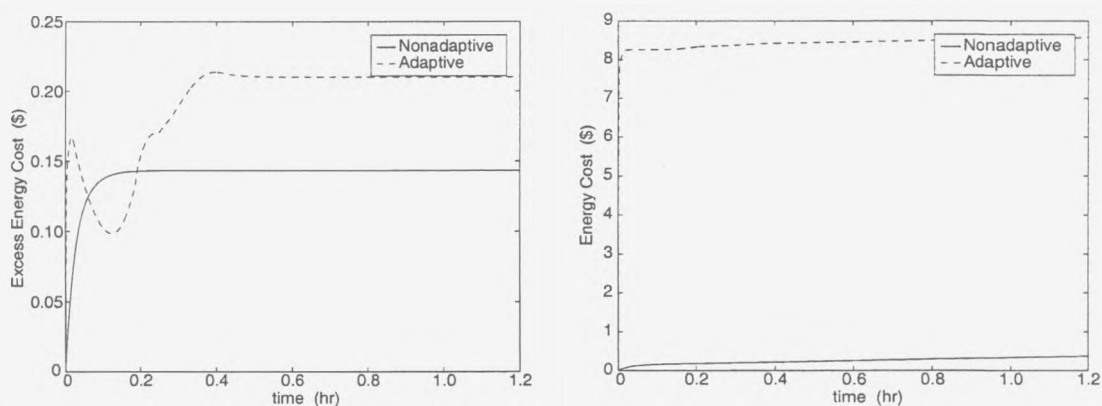
Figure 4.48: Case(6): Energy Cost
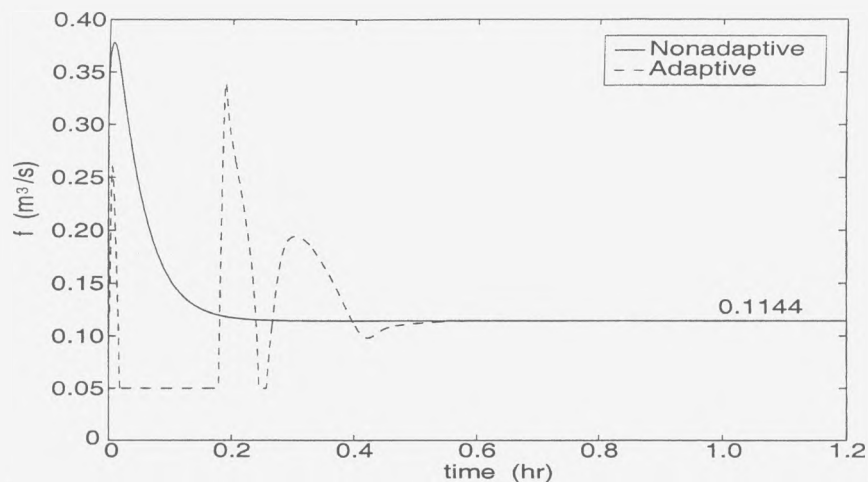
Figure 4.49: Case(6): Airflow Rate

minutes total cost rises linearly at the rate of about 10 cents per hour.

Figures 4.49 and 4.50 give the corresponding plots for the air flow rate and heat input respectively. After some initial transients, in about 20 minutes these settle down to values of 0.114 m^3/s and -2258 W, respectively. Observe f is always larger
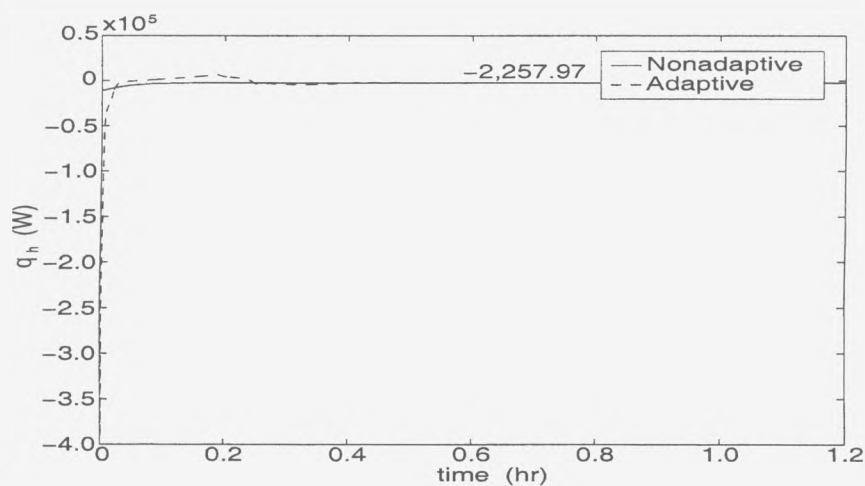
Figure 4.50: Case(6): Heat Input

than f_{am} . Note again that each of these performance curves applies to both adaptive control with unknown T_a, V_z and q_z, and non-adaptive control with known T_a, V_z and q_z.

4.7   Case(7): T_a and q_z time varying

This section documents the performance of the adaptive controller over half a day under a realistic time varying ambient temperature and thermal load profile. The profile itself has been borrowed from Roth et al [6].

While all the other parameters are as in Table 1, the rest are as follows. The flow rate set point is fixed throughout at $f_r = 0.142$ m^3/s. The simulation begins at $t = 0$ hours, with all the variables at their steady state optimum. A change occurs in the set point temperature T_r from 27°C to 24°C at the one hour mark. The
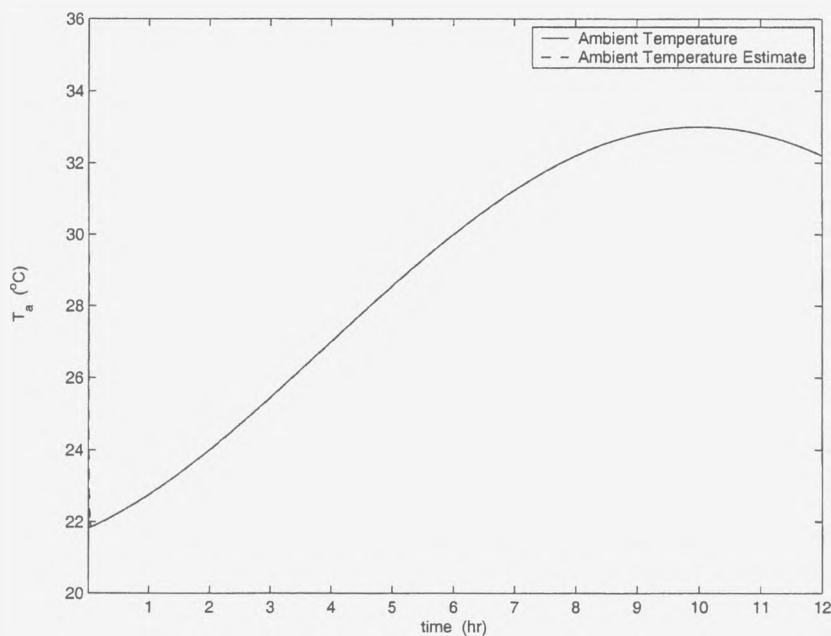
Figure 4.51: Case(7): Ambient Temperature and its Estimate
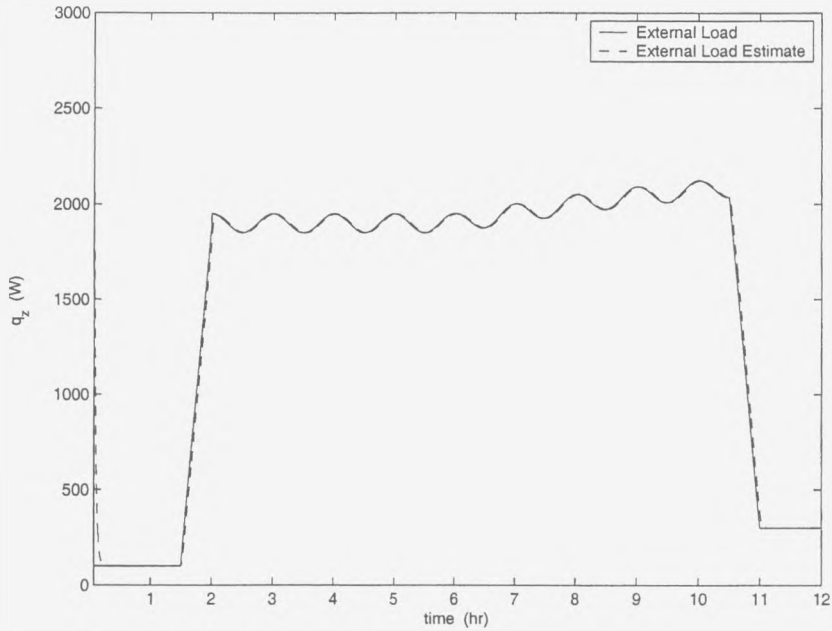
Figure 4.52: Case(7): External Load and its Estimate

ambient temperature $T_a(t)$ is sinusoidal, with a time period of 24 hours, mean of 27°C, amplitude of 6°C and a peak at the 10 hour mark. The thermal load begins at a constant value of 100 W, ramps up to 1900 W between the 1.5 and 2 hour marks and oscillates sinusoidally with an amplitude of 50 W and period of 1 hour, around a mean of 1900 W, until about the 6 hour mark. This rise in load and oscillation is due to lighting, equipment and varying occupancy. At about the 6 hour mark, an additional load due to solar intensity takes effect. This load is zero mean, sinusoidal with 200 W amplitude and 24 hour time period. At the 10.5 hour mark, the thermal load due to occupancy and lighting begins to be removed linearly until at the 11 hour mark it is reduced to its constant 100 W level plus a residual solar load. This simulates the beginning of the unoccupied period of the building.

The adaptive algorithm is implemented with λ_1 and λ_2 as in (4.1). Figures 4.51
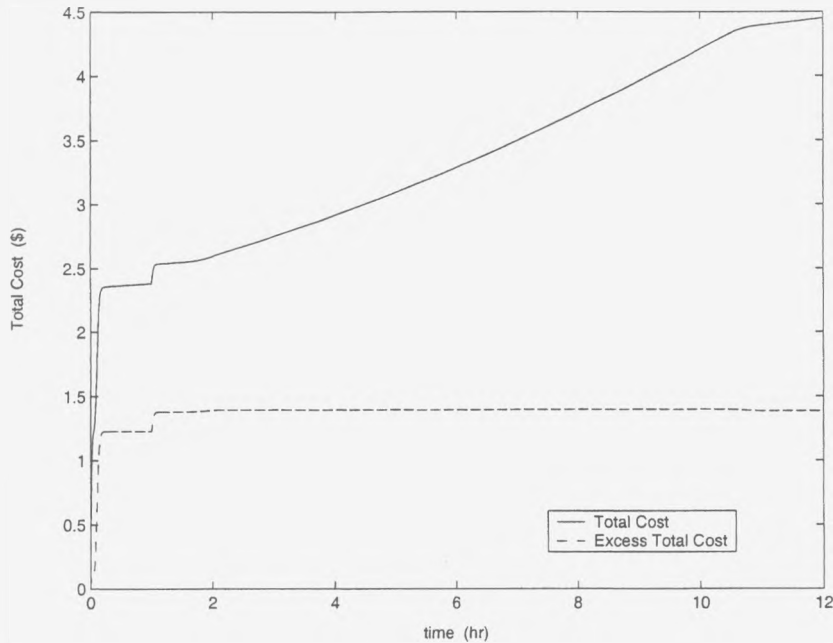
Figure 4.53: Case(7): Total Cost and Excess Total Cost

and 4.52 respectively display the ability of $\hat{T}_a(t)$ and $\hat{q}_z(t)$ to track T_a and q_z.
Observe that the tracking is almost perfect.

Figure 4.53 displays the total cost incurred and the so called minimum steady
state total cost. The latter is computed with the integrand in (2.4) obtained at time
t as the minimum value it can attain for the current values of $T_a(t)$ and $q_z(t)$, with
the right hand sides of (2.2) and (2.3) equated to zero.

Since under the time varying $T_a(t)$ and $q_z(t)$, steady state is in general
unattainable, the actual cost could theoretically be below the so called steady state
minimum. This is indeed the case in Figure 4.53, where once the variable load and
ambient temperature effects get in, the unattainability of steady state forces the
controller to seek a lower value of the cost function than what would have been
possible under steady state condition.
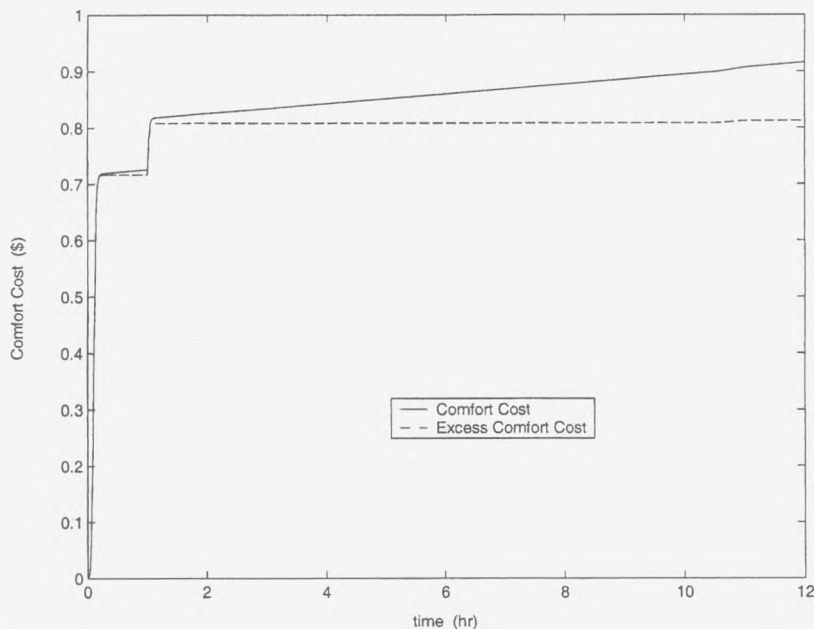
Figure 4.54: Case(7): Comfort Cost and Excess Comfort Cost

As expected, the gradient of the total cost is highest in the period of greatest occupancy. Overall, over the 12 hour period under consideration, (observe, this includes the period of maximum occupancy), the total cost incurred is less that $4.50. Figures 4.54 and 4.55 display the cost component attributable to comfort and energy respectively.

Figure 4.56 depicts the actual room temperature $T_3(t)$ and the desired reference $T_r(t)$. Observe T_3 tracks T_r quite closely, with slight glitces at points that mark the onset of substantial changes in the $q_z(t)$ profile. Figures 4.57 and 4.58 give the flow rate f and heat input q_h respectively. Except at points of sudden changes in $q_z(t)$ profile, these more or less follow a steady course. Observe, q_h is reduced in magnitude in periods of low $q_z(t)$. Moreover, the actual flow rate exceeds the allowed minimum f_{am}.
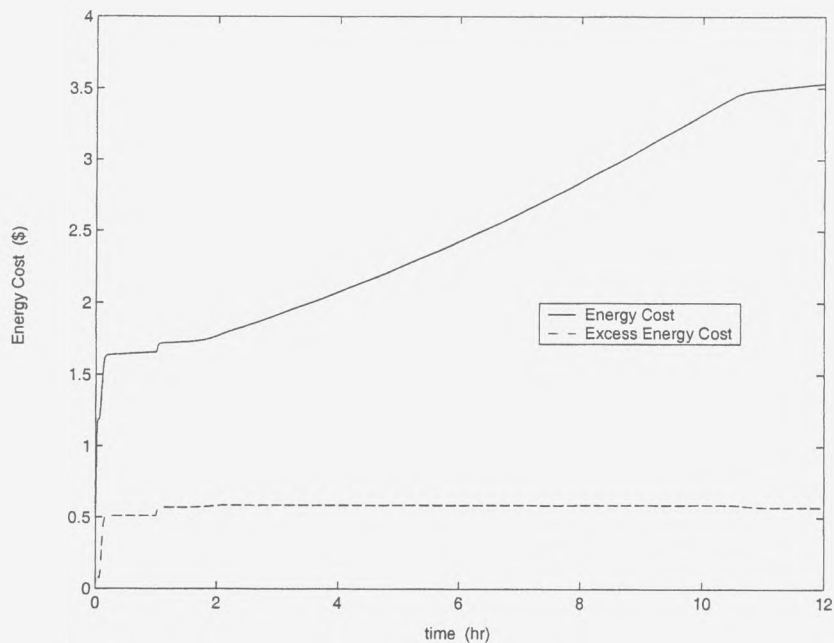
Figure 4.55: Case(7): Energy Cost and Excess Energy Cost
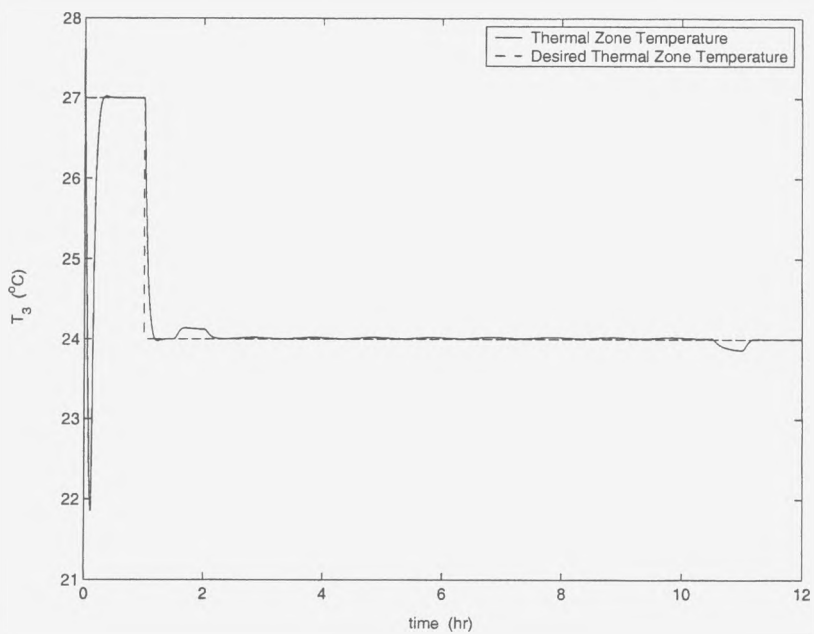
Figure 4.56: Case(7): Room Temperature and Desired Room Temperature
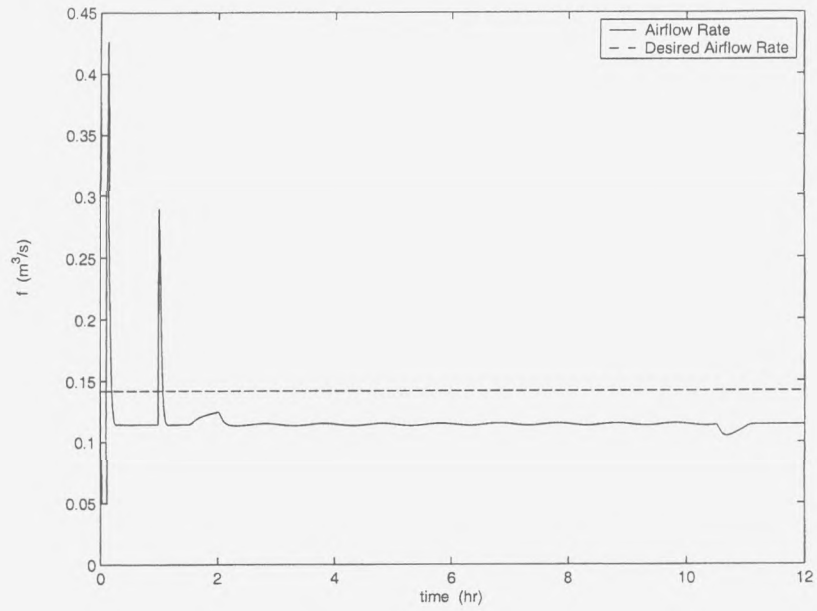
Figure 4.57: Case(7): Airflow Rate and Desired Airflow Rate
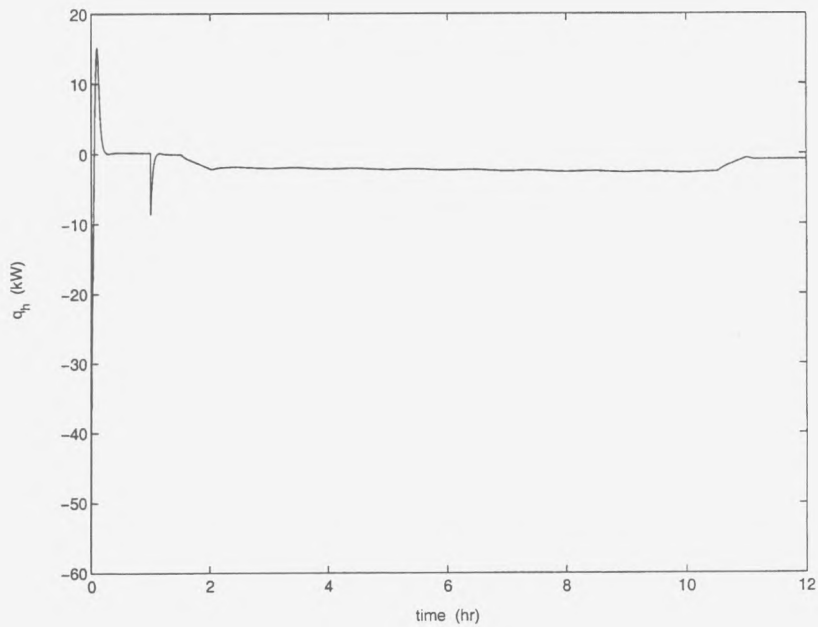
Figure 4.58: Case(7): Heat Input

4.8 Conclusion

This chapter has documented simulations conducted on the Adaptive Control Algorithm formulated in Section 3.2 of Chapter 3. The principle purpose of the simulations reported in this chapter has been to compare the Adaptive Control Algorithm of Chapter 3 with its nonadaptive counterpart in Chapter 2. For this purpose, two types of simulation results for first six different combinations have been reported. The first set, cases (1) through (4), has considered the situations where just the two out of the five parameters are constant but unknown. There are actually $C_2^5 = 10$ possible combinations of two parameters out of five parameters possible. The second set, cases (5) and (6), considers the situations where three out of the five parameters are constant but unknown. Again, there are actually $C_3^5 = 10$ possible combinations of three parameters out of five parameters possible. For these six cases, the identifier actually works fine. In a quarter of an hour most of the identifications were done. In some cases identification took only a few seconds. For the cases (5) and (6), the identifier failed to identify one out of three parameters correctly, though. Still, in 15 minutes $\hat{\theta}$ settled down at a value close to θ.

For the first six cases, the actual state variables T_2 and T_3 attain the theoretical values that minimize the integrand in (2.4) in less than 20 minutes for both the adaptive and nonadaptive controller. The total cost over the attainable steady state minimum, $J_e(t)$, settles down to a constant value, i.e. the integrand in (4.2) becomes zero. This constant value, however, is higher for the adaptive case than the nonadaptive case as expected. Still, it is clear from the simulations that after about a quarter of an hour, total cost rises linearly at a constant rate.

For each adaptive case identifying constant and unknown parameters, the air flow rate and the heat input plots have been compared with their nonadaptive counterparts. After some initial transients, before half an hour finishes these settle down to values of $0.114 \text{ m}^3/\text{s}$ and -2258 W respectively.

The last case, case (7), by identifying time varying parameters, differs from the first six cases. It documents the performance of the adaptive controller over half a day under a realistic time varying ambient temperature and thermal load profile. The tracking observed to be almost perfect. Since under the time varying parameters steady state is in general unattainable, the actual cost is below the so called steady state minimum. The gradient of the total cost is highest in the period of greatest occupancy.

CHAPTER 5

ADAPTIVE CONTROLLER SCHEME 2: RECURSIVE LEAST SQUARES

While the Adaptive Controller Scheme 1 presented in Chapter 3 works fine for some of the double and triple unknown parameters, it simply does not identify the parameters once the number of them that are unknown becomes four or five. As observed in the last two cases of the Gradient Descent Algorithm simulations of Chapter 4, even for three parameter identification, the algorithm has problems identifying one of the parameters. The present chapter, therefore, focuses on a different scheme for an identifier, using the recursive least squares (RLS). The outline of this chapter is as follows. Section 5.1 presents the RLS theory, Section 5.2 presents the application of RLS to the HVAC system, Section 5.3 presents the simulations, and Section 5.4 is the conclusion.

5.1 Recursive Least Squares

The principle of least squares is formulated by Gauss at the end of the eighteenth century to determine the orbits of planets [8]. According to this principle, the unknown parameters of a mathematical model should be chosen in such a way that

> the sum of the squares of the differences between the actually observed
> and the computed values, multiplied by numbers that measure the
> degree of precision, is a minimum.

Recursive least squares can be applied to the HVAC system model which is written in the following *linear_in_parameters* form for the convenience

$$
\begin{cases}
\overline{x}_1(t) = V_1'(t)\theta_1(t) \\
\overline{x}_2(t) = V_2'(t)\theta_2(t)
\end{cases}
\tag{5.1}
$$

where the elements of θ_i's, $i = 1, 2$, are unknown parameters and the elements of V_i's, $i = 1, 2$, are known functions that depend on other known variables. These elements of V are called regression variables, or the regressors [8], because the model in (5.1) is itself a regression model. The vector $\theta' = [\theta_1\ \theta_2]$ and the block diagonal matrix $V(t)$ whose diagonal blocks are simply $V_1(t)$ and $V_2(t)$ are the same θ and V which have been introduced in Section 3.1.1.

Pairs of observations and regressors are obtained online. The problem is to determine the parameters in such a way that the outputs computed from the HVAC system model (5.1) agree as closely as possible with the measured variables $\overline{x}(t)$ in the sense of least squares. Since measured variable $\overline{x}(t)$'s are linear in parameters θ and the least squares criterion is quadratic, the problem admits an analytical solution [8].

Introduce the notation

$$
\overline{x}(t) = [\ \overline{x}_1(t)\quad \overline{x}_2(t)\ ]'
\tag{5.2}
$$

and the least squares error

$$
\epsilon(t) = V'(t)\hat{\theta}(t) - \overline{x}(t)
\tag{5.3}
$$

where

$$
V'(t) = \begin{bmatrix} V_1'(t) & 0 \\ 0 & V_2'(t) \end{bmatrix}
\tag{5.4}
$$

have also been introduced. The least squares algorithm then minimizes the *integral_squared_error* (ISE) [9]

$$ISE = \int\limits_0^t \epsilon^2(\tau)\mathrm{d}\tau.$$ (5.5)

Owing to the linearity of the error equation, the estimate may be obtained directly from the condition

$$\frac{\partial}{\partial\theta}\left[\int\limits_0^t \epsilon^2(\tau)\mathrm{d}\tau\right] = 2\int\limits_0^t V(\tau)\left[V'(\tau)\hat{\theta}(\tau)\bar{x}(\tau)\right]\mathrm{d}\tau = 0$$ (5.6)

so that the *least-squares estimate* is given by

$$\hat{\theta}(t) = \left[\int\limits_0^t V(\tau)V'(\tau)\mathrm{d}\tau\right]^{-1}\left[\int\limits_0^t V(\tau)\bar{x}(\tau)\mathrm{d}\tau\right].$$ (5.7)

5.2 Application _ Recursive Least Squares

The overall adaptive control algorithm is a combination of the identifier given in Section 5.1 and the controller as given in Chapter 2, with θ replaced by $\hat{\theta}$ as was the case in Section 3.1.2 for the adaptive controller using gradient descent. The rest of this section presents the adaptive identifier using RLS for the HVAC system. The simulations for this case are given in Section 5.3.

In this section the identifier of Section 5.1 is used to estimate five system parameters, namely,

- the effective volume of the heat exchanger V_h,

- the temperature of the outside air T_a,

- $k = \rho C_p$ where ρ is the air density and C_p is the constant pressure specific heat of air,

- the effective thermal space volume V_z and

- the thermal load q_z.

The HVAC system

$$T_1(t) = T_3(t) + \left(T_a - T_3(t)\right)\frac{f_a}{f(t)}$$

$$\rho C_p V_h \dot{T}_2(t) = f(t)\rho C_p\left(T_1(t) - T_2(t)\right) + q_h(t)$$

$$\rho C_p V_z \dot{T}_3(t) = f(t)\rho C_p\left(T_2(t) - T_3(t)\right) + q_z$$

is written first as

$$\dot{x}_1(t) = \frac{1}{V_h}\left[u_2(t)\left(x_2(t) - x_1(t)\right) + f_a\left(T_a - x_2(t)\right) + \frac{u_1(t)}{k}\right]$$

$$\dot{x}_2(t) = \frac{u_2(t)}{V_z}\left(x_1(t) - x_2(t)\right) + \frac{q_z}{kV_z}$$

where

$$u(t) = [u_1(t) \ u_2(t)]' = [q_h(t) \ f(t)]'$$

and

$$x(t) = [x_1(t) \ x_2(t)]' = [T_2(t) \ T_3(t)]',$$

and then in *linear_in_parameters* form as

$$\overline{x}(t) = V'(t)\theta \tag{5.8}$$

where

$$V(t) = \begin{bmatrix} z_1(t) & 0 \\ z_2(t) & 0 \\ z_3(t) & 0 \\ 0 & z_4(t) \\ 0 & z_5(t) \end{bmatrix} \tag{5.9}$$

for the state variable filters

$$\dot{z}_1(t) = -z_1(t) + [f(t)[T_3(t) - T_2(t)] - f_a T_3(t)]$$

$$\dot{z}_2(t) = -z_2(t) + f_a$$

$$\dot{z}_3(t) = -z_3(t) + q_h$$

$$\dot{z}_4(t) = -z_4(t) + f(t)[T_2(t) - T_3(t)]$$

$$\dot{z}_5(t) = -z_5(t) + 1$$

and

$$\theta' = \left[\frac{1}{V_h}, \frac{T_a}{V_h}, \frac{1}{V_h k}, \frac{1}{V_z}, \frac{q_z}{V_z k} \right].$$

The *least-squares estimate* is therefore by (5.7)

$$\hat{\theta}(t) = \left[\frac{1}{\hat{V}_h(t)}, \frac{\hat{T}_a(t)}{\hat{V}_h(t)}, \frac{1}{\hat{V}_h(t)\hat{k}(t)}, \frac{1}{\hat{V}_z(t)}, \frac{\hat{q}_z(t)}{\hat{V}_z(t)\hat{k}(t)} \right]$$

$$= \left[\int_0^t V(\tau)V'(\tau)d\tau \right]^{-1} \left[\int_0^t V(\tau)\overline{x}(\tau)d\tau \right] \tag{5.10}$$

for $V(t)$ and $\overline{x}(t)$ given above by (5.9) and (5.8) respectively.

5.3 RLS Simulations

This section documents simulations conducted on the Adaptive Control Algorithm formulated in Section 5.1 of the present chapter. The principle purpose

of the simulations reported in this chapter is to compare the Adaptive Control Algorithm of Chapter 5 with its nonadaptive counterpart in Chapter 2. For this purpose, two types of simulation results are reported. In the first simulation, all of the parameters are assumed known and the nonadaptive control law of Chapter 2 is implemented. In the second simulation, five parameters are assumed as being unknown but constant and the adaptive algorithm of Chapter 5 is implemented with specified initial estimates.

5.3.1 Specifics of the Simulation

Specifically, the following setting from Table 1 is considered throughout the simulations:

$$\alpha_2 = 4.86 \times 10^{-3} \; \$/\text{min-}^\circ\text{C}^2,$$

$$\alpha_3 = 5.39 \times 10^{-10} \; \$/\text{min-W}^2,$$

$$\alpha_4 = 5.20 \times 10^{-5} \; \$\text{-min}/\text{m}^6,$$

$$\alpha_5 = 1.22 \times 10^{-6} \; \$\text{-min}^2/\text{m}^9 \;\; \text{and}$$

$$f_{am} = 0.05 \; \text{m}^3/\text{s}.$$

The set points T_r and f_r are $24\,^\circ\text{C}$ and $0.142 \; \text{m}^3/\text{s}$ respectively, and the initial value for the state vector is

$$\begin{cases} T_2(0) = 16\,^\circ\text{C} \\ T_3(0) = 28\,^\circ\text{C} \end{cases}$$

for all of the simulations.

The actual values of the parameters used throughout the simulations are;

$$k = \rho C_p = 1.19 \; \text{kg}/\text{m}^3 \times 1005 \; \text{J/kg-}^\circ\text{C} = 1195.95 \; \text{J/m}^3\text{-}^\circ\text{C},$$

$$V_h = 25.5 \text{ m}^3,$$

$$V_z = 255 \text{ m}^3,$$

$$T_a = 30^o\text{C} \quad \text{and}$$

$$q_z = 1900 \text{ W}.$$

The initial estimate of θ is given by

$$\begin{cases} \hat{\theta}_1(0) = 1/\hat{V}_h(0) = 1/20, \\ \hat{\theta}_2(0) = \hat{T}_a/\hat{V}_z(0) = 31/20, \\ \hat{\theta}_3(0) = 1/\hat{V}_h(0)/\hat{k}(0) = 1/20/1190, \\ \hat{\theta}_2(0) = 1/\hat{V}_z(0) = 1/200, \\ \hat{\theta}_3(0) = \hat{q}_z(0)/\hat{V}_z(0)/\hat{k}(0) = 2000/200/1190. \end{cases}$$

For the identification process using RLS, there is no identification for the first 5 minutes so that $\int_0^t V(\tau)V'(\tau)\mathrm{d}\tau$ becomes well conditioned. After that, we apply the identifier between $t = 5$ and $t = 6.5$ minutes. The estimated parameters are then applied to the control algorithm.

5.3.2 Plots

Observe Figures 5.1 to 5.6 which depict the relative performance of the adaptive and nonadaptive laws with respect to a variety of performance measures. Now consider the details of this performance. On the right plot of Figure 5.1 one sees that the actual T_3 attains the value $T_3^* = 24.015^oC$ in around 20 minutes for both the adaptive and non-adaptive controller. On the left plot of the same figure, however, it is observed that even though the actual T_2 attains a constant value for both the adaptive and non-adaptive controller, the constant values differ by 0.804^oC with the adaptive controller value T_2 being lower than its non-adaptive counterpart.
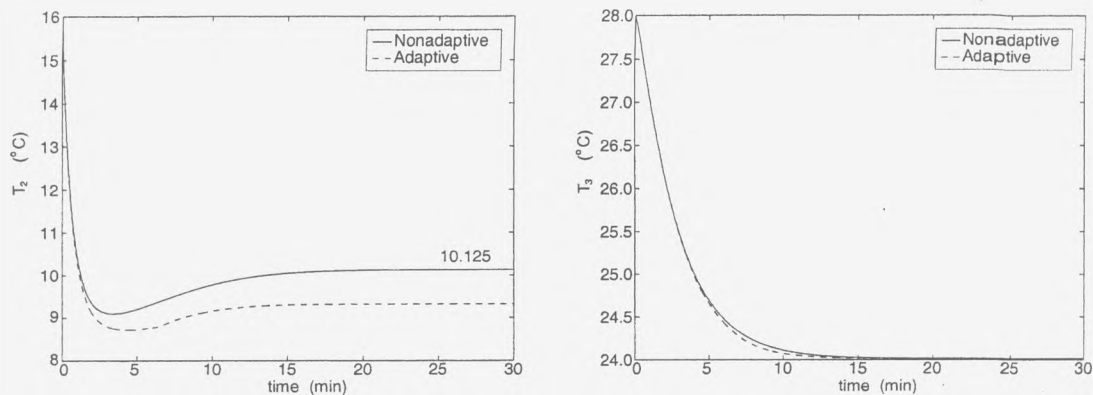
Figure 5.1: RLS: Temperature Regulation

Figure 5.2 depicts the total cost J incurred and the so called minimum steady state total cost J_e. The latter is computed with the integrand in (2.4) obtained at time t as the minimum value it can attain subject to (2.9) and (2.10). Observe, in less than 15 minutes J_e settles down to a constant value i.e. the integrand in (4.2) becomes zero. After about 15 minutes total cost rises linearly at the rate of about 18 cents per hour for the non-adaptive case and 21 cents per hour for the adaptive case. Similarly Figure 5.3 depicts the portion of J_e and J attributable to the comfort cost, just as Figure 5.4 depicts the energy component of J_e and J. Again, two plots
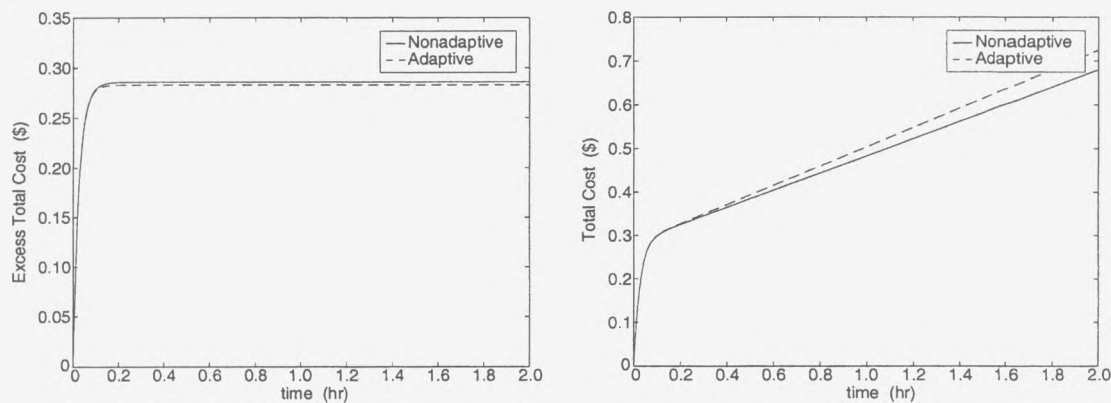
Figure 5.2: RLS: Total Cost
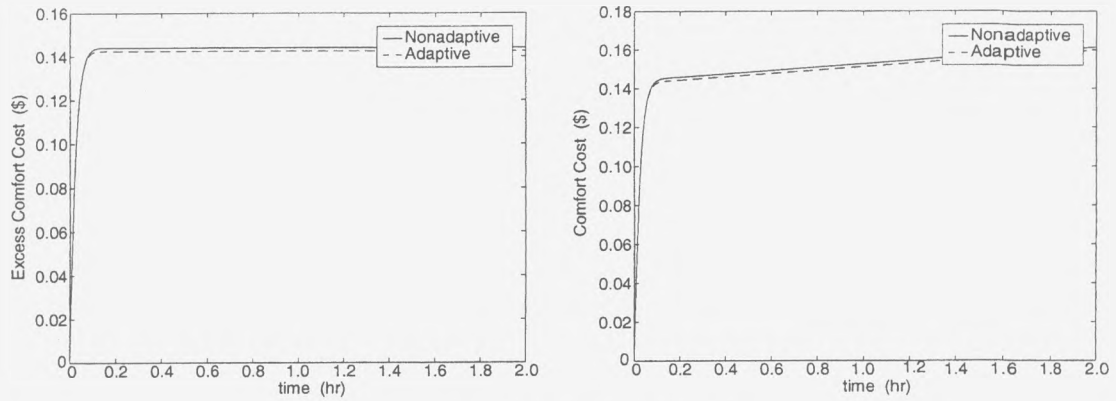
Figure 5.3: RLS: Comfort Cost

on the left of Figures 5.3 and 5.4 indicate that costs stop rising after 10 minutes.

Figures 5.5 and 5.6 give the corresponding plots for the air flow rate and heat input respectively. After some initial transients, in about 15 minutes, the air flow rate settles down to 0.114 m^3/s and the heat input for the adaptive case becomes $-2,424.8$ W compared to $-2,257.5$ W for the non-adaptive case. Observe the actual flow rate always exceeds the allowed minimum f_{am} .
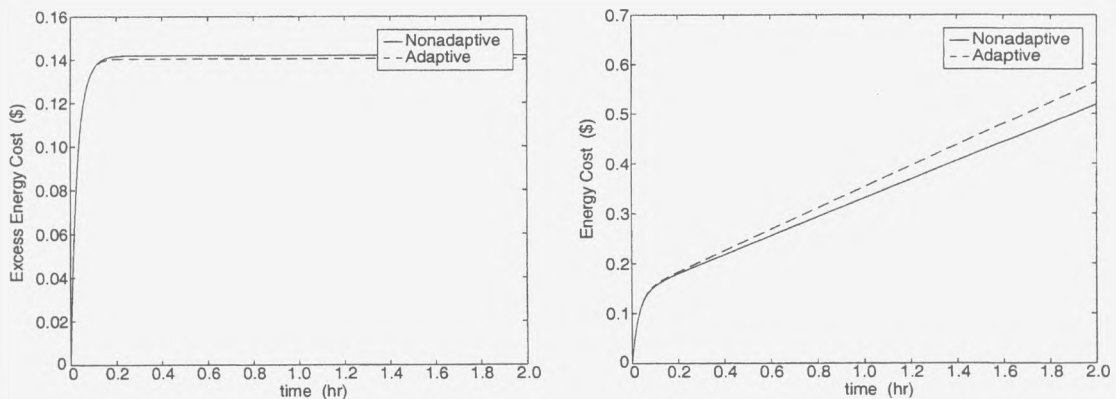
Figure 5.4: RLS: Energy Cost
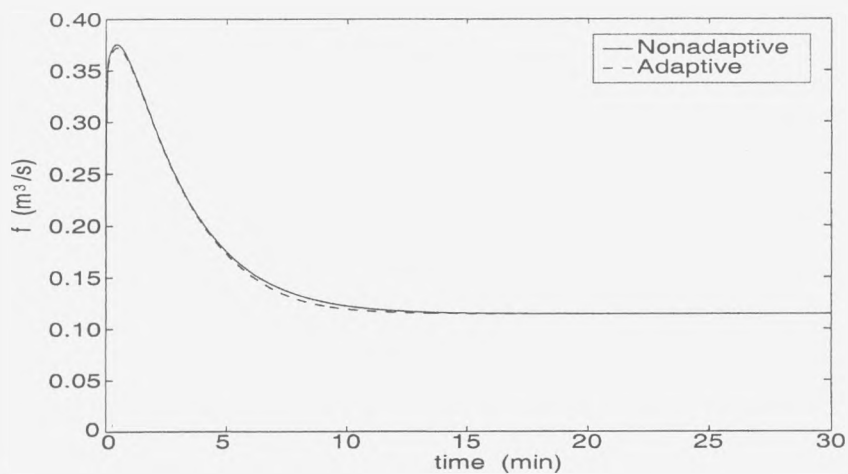
Figure 5.5: RLS: Airflow Rate
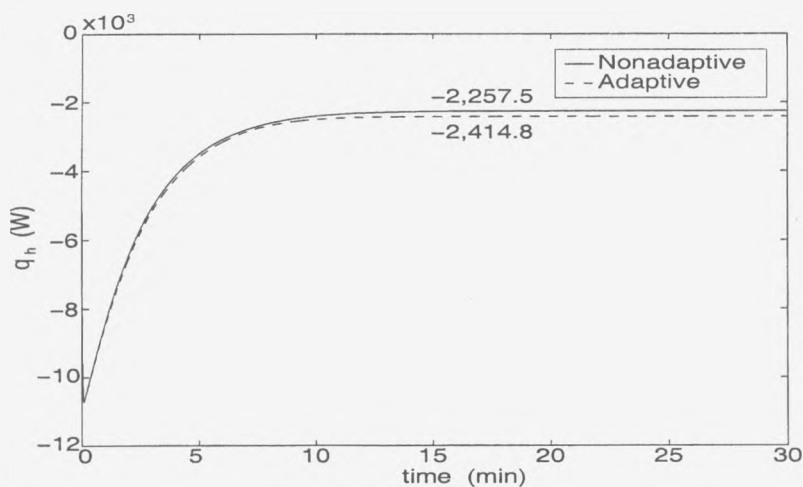
Figure 5.6: RLS: Heat Input

5.4 Conclusion

This chapter has presented an adaptive version of the controller described in the Chapter 2 by using the recursive least square approach. After the theoretical information about RLS in Section 5.1, the identifier is applied to the nonlinear

optimal controller in Section 5.2. Section 5.3 has documented simulations conducted on the RLS Algorithm. The principle purpose of the simulations reported in this chapter has been to compare the Adaptive Control Algorithm of Chapter 5 with its nonadaptive counterpart in Chapter 2.

The actual state variable T_3 attains the theoretical value that minimizes the integrand in (2.4) in less than 20 minutes for both the adaptive and nonadaptive controller. The actual state variable T_2, on the other hand, attains a value slightly lower than the theoretical value that minimizes the integrand in (2.4) for the adaptive controller. The total cost over the attainable steady state minimum, $J_e(t)$ settles down to a constant value, i.e. the integrand in (4.2) becomes zero.

CHAPTER 6

CONCLUSION

This study presents a new nonlinear optimal control algorithm for HVAC systems. Adaptive implementation when the defining parameters are unknown is also given. A key feature of the adaptive identification algorithm imbedded within the overall scheme is its ability to track estimated system parameters. This algorithm differs from its predecessors in that it does not suffer from some of their major limitations. Thus it can be implemented on line. Further, it eschews the traditional LQR framework, and thus does not have to discard a non-quadratic term from the underlying cost function to be optimized. This term measures a crucial component contributed by the cost of operating the fan within the HVAC system.

Although the non-adaptive control law itself does not require implementation of any differential equations, the adaptive law does. Since differential equations can be computationally onerous, it is recommended that a sampled data version of this law can be considered. Such a sampled data controller will be amenable to current microprocessor based implementations and naturally defines a direction of future work.

The actual optimal controller, even in its non-adaptive form, involves a linearization in its derivation. As such, unless one starts "close" to the state values that optimize the integrand in (2.5), subject to the right hand sides of (2.2, 2.3) being zero, the law itself is suboptimal. Such a linearization can be avoided if one

obtains a closed form solution to the boundary value problem that defines the optimal controller. Exploring the existence of such a solution is recommended.

APPENDIX A

MINIMIZING THE COST FUNCTION

We will determine the control law that minimizes the cost function

$$J(u) = \int_{t_0}^{t_1} F(x, u, t) \mathrm{d}t \qquad (A.1)$$

subject to the system equations which are a general set of n nonlinear differential equations

$$\dot{x}(t) = g(x, u, t) \qquad (A.2)$$

and subject to the initial conditions

$$x(t_0) = x_0 , \qquad (A.3)$$

where x is the column n-vector of state variables, u is the column m-vector of input or control variables and t denotes time [3]. We shall assume that the components $g_i(x, u, t)$, $i = 1, 2, \ldots, n$, of vector g are continuous and satisfy standard conditions, such as having continuous first partial derivatives so that the unique solution for (A.1) exists for given initial conditions [10].

Introduce a vector of Lagrange multipliers $p = [p_1, \ldots, p_n]'$, where prime denotes the transpose, so as to form an augmented functional incorporating the constraints:

$$J_a = \int_{t_0}^{t_1} [F(x, u, t) + p'(g - \dot{x})] \mathrm{d}t . \qquad (A.4)$$

Integrating the second term of the integrand of (A.4) by parts gives

$$J_a = \int_{t_0}^{t_1} [F + p'g + (\dot{p})'x]\mathrm{d}t - [p'x]_{t_0}^{t_1}$$

$$= \int_{t_0}^{t_1} [H + (\dot{p})'x]\mathrm{d}t - [p'x]_{t_0}^{t_1}$$

where the *Hamiltonian* function is defined by

$$H(x, u, t) = F(x, u, t) + p'g. \qquad (A.5)$$

For continuous and differentiable u on $t_0 \leq t \leq t_1$ and for fixed t_0 and t_1, the variation in J_a corresponding to a variation δu in u is

$$\delta J_a = (-p'\delta x)_{t=t_1} + \int_{t_0}^{t_1} \left[\frac{\partial H}{\partial x}\delta x + \frac{\partial H}{\partial u}\delta u + (\dot{p})'\delta x \right] \mathrm{d}t, \qquad (A.6)$$

where δx is the variation in x in the differential equations (A.2) due to δu. Since $x(t_0)$ is specified, $(\delta x)_{t=t_0} = 0$. We can simply remove the term involving δx in (A.6) by suitably choosing p, i.e. by taking

$$\dot{p}_i = -\frac{\partial H}{\partial x_i}, \quad i = 1, 2, \ldots, n, \qquad (A.7)$$

and

$$p_i(t_1) = 0. \qquad (A.8)$$

Equation (A.6) then reduces to

$$\delta J_a = \int_{t_0}^{t_1} \left(\frac{\partial H}{\partial u}\delta u \right) \mathrm{d}t$$

which results in the condition

$$\left(\frac{\partial H}{\partial u_i} \right)_{u=u^*} = 0, \quad t_0 \leq t \leq t_1, \quad i = 1, \ldots, m. \qquad (A.9)$$

Therefore necessary conditions for u^* to minimize (A.1) subject to (A.2) and (A.3) are that (A.7), (A.8) and (A.9) hold.

APPENDIX B

LINEARIZATION

First we will describe a linearization process that expands the nonlinear state equation into a Taylor series about a nominal operating point, then we will apply it to the HVAC system to get a linearized set of system equations in Section B.1. For the linearization process, all the terms of the Taylor series which have a higher order than the first order are discarded, and linear approximation of the nonlinear state equation at the nominal point results [11].

We will represent a nonlinear system by the following vector-matrix state equations:

$$\dot{x}(t) = h\big(x(t), u(t)\big) \tag{B.1}$$

where $x(t)$ represents the $n \times 1$ state vector, $u(t)$ the $m \times 1$ input vector, and denotes an $n \times 1$ function vector. The nominal operating trajectory will be denoted by x^*, corresponding to the nominal input u^* and some fixed initial states. Expanding the nonlinear state equation of (B.1) into a Taylor series about $x(t) = x^*(t)$ and neglecting all the higher-order terms yields

$$\dot{x}_i(t) = h_i(x^*, u^*) + \sum_{j=1}^{n} \left. \frac{\partial h_i(x, u)}{\partial x_j} \right|_{(x^*, u^*)} (x_j - x_j^*)$$

$$+ \sum_{j=1}^{m} \left. \frac{\partial h_i(x, u)}{\partial u_j} \right|_{(x^*, u^*)} (u_j - u_j^*) \tag{B.2}$$

where $i = 1, 2, \ldots, n$. Let

$$\Delta x_i = x_i - x_i^*$$

and

$$\Delta u_j = u_j - u_j^*.$$

Then

$$\Delta \dot{x}_i = \dot{x}_i - \dot{x}_i^*$$

since

$$\dot{x}_i^* = h_i(x^*, u^*).$$

Equation (B.2) can therefore be written as

$$\Delta \dot{x}_i = \sum_{j=1}^{n} \left. \frac{\partial h_i(x, u)}{\partial x_j} \right|_{x^*, u^*} \Delta x_j + \sum_{j=1}^{m} \left. \frac{\partial h_i(x, u)}{\partial u_j} \right|_{x^*, u^*} \Delta u_j. \tag{B.3}$$

We can write equation (B.3) in vector-matrix form:

$$\Delta \dot{x} = A \Delta x + B \Delta u$$

where, with

$$A(x, u) = \begin{bmatrix} \frac{\partial h_1}{\partial x_1} & \frac{\partial h_1}{\partial x_2} & \cdots & \frac{\partial h_1}{\partial x_n} \\ \frac{\partial h_2}{\partial x_1} & \frac{\partial h_2}{\partial x_2} & \cdots & \frac{\partial h_2}{\partial x_n} \\ \vdots & \vdots & \ddots & \vdots \\ \frac{\partial h_n}{\partial x_1} & \frac{\partial h_n}{\partial x_2} & \cdots & \frac{\partial h_n}{\partial x_n} \end{bmatrix} \tag{B.4}$$

and

$$B(x, u) = \begin{bmatrix} \frac{\partial h_1}{\partial u_1} & \frac{\partial h_1}{\partial u_2} & \cdots & \frac{\partial h_1}{\partial u_n} \\ \frac{\partial h_2}{\partial u_1} & \frac{\partial h_2}{\partial u_2} & \cdots & \frac{\partial h_2}{\partial u_n} \\ \vdots & \vdots & \ddots & \vdots \\ \frac{\partial h_n}{\partial u_1} & \frac{\partial h_n}{\partial u_2} & \cdots & \frac{\partial h_n}{\partial u_n} \end{bmatrix}, \tag{B.5}$$

$$A = A(x^*, u^*), \tag{B.6}$$

and

$$B = B(x^*, u^*). \tag{B.7}$$

Thus, we have linearized the nonlinear system of (B.1) at a nominal operating point (x^*, u^*).

B.1   Linearization of the HVAC System

Using the process described above, we linearize the HVAC system

$$\begin{bmatrix} \dot{x}_1(t) \\ \dot{x}_2(t) \\ \dot{p}_1(t) \\ \dot{p}_2(t) \end{bmatrix} = \begin{bmatrix} h_1(x, p, t) \\ h_2(x, p, t) \\ h_3(x, p, t) \\ h_4(x, p, t) \end{bmatrix}. \tag{B.8}$$

where $h_i(x, p, t)$'s are given by (2.16), (2.17), (2.18) and (2.19) in Section 2.2 as

$$h_1(x, p, t) = \frac{u_2(t)}{V_h}\Big(x_2(t) - x_1(t)\Big) + \frac{f_a}{V_h}\Big(T_a - x_2(t)\Big) + \frac{u_1(t)}{kV_h} ,$$

$$h_2(x, p, t) = \frac{u_2(t)}{V_z}\Big(x_1(t) - x_2(t)\Big) + \frac{q_z}{kV_z} ,$$

$$h_3(x, p, t) = u_2(t)\Big(\frac{p_1(t)}{V_h} - \frac{p_2(t)}{V_z}\Big) ,$$

$$h_4(x, p, t) = -2\alpha_2\Big(x_2(t) - T_r\Big) + u_2(t)\Big(\frac{p_2(t)}{V_z} - \frac{p_1(t)}{V_h}\Big) + f_a\frac{p_1(t)}{V_h} .$$

First the nominal trajectory about which the nonlinear state equation of (B.8) is linearized, i.e. x^* and p^*, corresponding to the nominal input u^*, is obtained by

setting the $h_j(x, p, t)$'s to zero for $j = 1, 2, 3$ and 4 subject to

$$\left(\frac{\partial H}{\partial u_i} \right)_{u=u^*} = 0 \ , \ i = 1, 2 \ ,$$

i.e.

$$\dot{x}_1 |_* = \frac{u_2^*}{V_h} \left(x_2^* - x_1^* \right) + \frac{f_a}{V_h} \left(T_a - x_2^* \right) + \frac{u_1^*}{kV_h} = 0 \ , \tag{a}$$

$$\dot{x}_2 |_* = \frac{u_2^*}{V_z} \left(x_1^* - x_2^* \right) + \frac{q_z}{kV_z} = 0 \ , \tag{b}$$

$$\dot{p}_1 |_* = u_2^* \left(\frac{p_1^*}{V_h} - \frac{p_2^*}{V_z} \right) = 0 \ , \tag{c}$$

$$\dot{p}_2 |_* = -2\alpha_2 \left(x_2^* - T_r \right) + u_2^* \left(\frac{p_2^*}{V_z} - \frac{p_1^*}{V_h} \right) + f_a \frac{p_1^*}{V_h} = 0 \tag{d}$$

$$\tag{B.9}$$

subject to

$$\left. \frac{\partial H}{\partial u_1} \right|_* = 2\alpha_3 u_1^* + \frac{p_1^*}{kV_h} = 0 \ , \tag{a}$$

$$\left. \frac{\partial H}{\partial u_2} \right|_* = 2\alpha_4 \left(u_2^* - f_r \right) + 3\alpha_5 u_2^{*2} + \left(x_2^* - x_1^* \right) \left(\frac{p_1^*}{V_h} - \frac{p_2^*}{V_z} \right) = 0 \ , \tag{b}$$

$$\tag{B.10}$$

where

$$H = \alpha_2 (x_2(t) - T_{3,ref})^2 + \alpha_3 u_1^2(t) + \alpha_4 (u_2(t) - f_r)^2 + \alpha_5 u_2^3(t) - J_e +$$

$$p_1(t)\dot{x}_1(t) + p_2(t)\dot{x}_2(t) \ , \ J_e \text{ constant} \ .$$

Observe, (B.9)(c) and (B.10)(b) together result in

$$p_2^* = \frac{V_z}{V_h} p_1^* \tag{B.11}$$

and

$$u_2^* = \frac{-\alpha_4 \pm \sqrt{\alpha_4^2 + 6\alpha_4\alpha_5 f_r}}{3\alpha_5}.$$

(B.12)

Because the condition (2.10)

$$f(t) \geq f_{am}$$

should always hold, (B.12) becomes

$$f(t^*) = f^* = u_2^* = \max\left\{f_{am}, \frac{-\alpha_4 \pm \sqrt{\alpha_4^2 + 6\alpha_4\alpha_5 f_r}}{3\alpha_5}\right\}$$

$$= \frac{-\alpha_4 + \sqrt{\alpha_4^2 + 6\alpha_4\alpha_5 f_r}}{3\alpha_5}.$$

(B.13)

Eliminating the common denominators for each of (B.9)(a) and (b), and simplifying (B.9)(d) using (B.9)(c) we get

$$u_2^*\left(x_2^* - x_1^*\right) + f_a\left(T_a - x_2^*\right) + \frac{u_1^*}{k} = 0,$$
(a)

$$u_2^*\left(x_1^* - x_2^*\right) + \frac{q_z}{k} = 0,$$
(b)

$$-2\alpha_2\left(x_2^* - T_r\right) + f_a\frac{p_1^*}{V_h} = 0.$$
(c)

(B.14)

(B.14) and (B.10)(a) can be expressed as follows

$$\begin{bmatrix} -u_2^* & u_2^*-f_a & 0 & 1/k \\ u_2^* & -u_2^* & 0 & 0 \\ 0 & -2\alpha_2 & f_a/V_h & 0 \\ 0 & 0 & 1/kV_h & 2\alpha_3 \end{bmatrix}\begin{bmatrix} x_1^* \\ x_2^* \\ p_1^* \\ u_1^* \end{bmatrix} + \begin{bmatrix} f_aT_a \\ q_z/k \\ 2\alpha_2T_r \\ 0 \end{bmatrix} = \begin{bmatrix} 0 \\ 0 \\ 0 \\ 0 \end{bmatrix}.$$

(B.15)

(B.15) can be solved as

$$\begin{bmatrix} x_1^* \\ x_2^* \\ p_1^* \\ u_1^* \end{bmatrix} = \begin{bmatrix} -u_2^* & u_2^*-f_a & 0 & 1/k \\ u_2^* & -u_2^* & 0 & 0 \\ 0 & -2\alpha_2 & f_a/V_h & 0 \\ 0 & 0 & 1/kV_h & 2\alpha_3 \end{bmatrix}^{-1} \begin{bmatrix} -f_a T_a \\ -q_z/k \\ -2\alpha_2 T_r \\ 0 \end{bmatrix}. \tag{B.16}$$

(B.11), (B.13) and (B.16) yield the nominal trajectory as

$$x_1^* = \frac{-q_z\left(\alpha_2 + k^2 f_a(f_a - f^*)\,\alpha_3\right) + k\,f^*\left(T_r\,\alpha_2 + k^2\,f_a^2\,T_a\,\alpha_3\right)}{k\,f^*\left(\alpha_2 + k^2\,f_a^2\,\alpha_3\right)}$$

$$= \frac{3\,\alpha_5\,q_z}{k\,(\alpha_4 - S)} + x_2^*,$$

$$x_2^* = \frac{T_r\,\alpha_2 + k\,f_a\,(q_z + k\,f_a\,T_a)\,\alpha_3}{\alpha_2 + k^2\,f_a^2\,\alpha_3},$$

$$p_1^* = \frac{2\,k\,(q_z + k\,f_a\,(T_a - T_r))\,V_h\,\alpha_2\,\alpha_3}{\alpha_2 + k^2\,f_a^2\,\alpha_3},$$

$$p_2^* = \frac{2\,k\,(q_z + k\,f_a\,(T_a - T_r))\,V_z\,\alpha_2\,\alpha_3}{\alpha_2 + k^2\,f_a^2\,\alpha_3} \tag{B.17}$$

corresponding to the nominal input

$$u_1^* = q_h^* = -\frac{(q_z + k\,f_a\,(T_a - T_r))\,\alpha_2}{\alpha_2 + k^2\,f_a^2\,\alpha_3} = -\frac{p_1^*}{2\,\alpha_3\,k\,V_h},$$

$$u_2^* = f^* = \frac{-\alpha_4 + S}{3\alpha_5} \tag{B.18}$$

for

$$S = \sqrt{\alpha_4^2 + 6\,\alpha_4\,\alpha_5\,f_r}. \tag{B.19}$$

Now that the nominal trajectory about which the nonlinear state equation of (B.8) is linearized is obtained, we can continue with the linear approximation described previously at the beginning of the present Appendix. Namely, we rewrite the system equation (B.8) in vector-matrix form as

$$
\begin{bmatrix} \Delta\dot{x}(t) \\ \Delta\dot{p}(t) \end{bmatrix} = \begin{bmatrix} A & -B \\ -C & -A' \end{bmatrix} \begin{bmatrix} \Delta x(t) \\ \Delta p(t) \end{bmatrix}
$$

where, from (B.4)-(B.7),

$$
A = A(x^*, p^*, u^*) = \begin{bmatrix} \frac{\partial h_1}{\partial x_1} & \frac{\partial h_1}{\partial x_2} \\ \frac{\partial h_2}{\partial x_1} & \frac{\partial h_2}{\partial x_2} \end{bmatrix}_{(x^*, p^*, u^*)}, \tag{B.20}
$$

$$
B = B(x^*, p^*, u^*) = -\begin{bmatrix} \frac{\partial h_1}{\partial p_1} & \frac{\partial h_1}{\partial p_2} \\ \frac{\partial h_2}{\partial p_1} & \frac{\partial h_2}{\partial p_2} \end{bmatrix}_{(x^*, p^*, u^*)}, \tag{B.21}
$$

$$
C = C(x^*, p^*, u^*) = -\begin{bmatrix} \frac{\partial h_3}{\partial x_1} & \frac{\partial h_3}{\partial x_2} \\ \frac{\partial h_4}{\partial x_1} & \frac{\partial h_4}{\partial x_2} \end{bmatrix}_{(x^*, p^*, u^*)}. \tag{B.22}
$$

Using the information obtained until now in the present Section we get

$$
\left.\frac{\partial h_1}{\partial x_1}\right|_* = \left.-\frac{u_2}{V_h}\right|_* = -\frac{u_2^*}{V_h} = \frac{\alpha_4 - S}{3\alpha_5 V_h},
$$

$$
\left.\frac{\partial h_1}{\partial x_2}\right|_* = \left.\left(\frac{u_2}{V_h} - \frac{f_a}{V_h}\right)\right|_* = \left(\frac{u_2^*}{V_h} - \frac{f_a}{V_h}\right) = \frac{-\alpha_4 + S - 3\alpha_5 f_a}{3\alpha_5 V_h},
$$

$$
\left.\frac{\partial h_2}{\partial x_1}\right|_* = \left.\frac{u_2}{V_z}\right|_* = \frac{u_2^*}{V_z} = \frac{-\alpha_4 + S}{3\alpha_5 V_z},
$$

$$
\left.\frac{\partial h_2}{\partial x_2}\right|_* = \left.-\frac{u_2}{V_z}\right|_* = -\frac{u_2^*}{V_z} = \frac{\alpha_4 - S}{3\alpha_5 V_z},
$$

which result in by (B.20)

$$A = \begin{bmatrix} \frac{\alpha_4 - S}{3\alpha_5 V_h} & \frac{-\alpha_4 + S - 3\alpha_5 f_a}{3\alpha_5 V_h} \\ \frac{-\alpha_4 + S}{3\alpha_5 V_z} & \frac{\alpha_4 - S}{3\alpha_5 V_z} \end{bmatrix}$$

$$= \frac{\alpha_4 - S}{3\alpha_5} \begin{bmatrix} 1/V_h & -1/V_h \\ -1/V_z & 1/V_z \end{bmatrix} - f_a \begin{bmatrix} 0 & 1/V_h \\ 0 & 0 \end{bmatrix}, \tag{B.23}$$

and

$$\left. \frac{\partial h_1}{\partial p_1} \right|_* = -\frac{1}{2\alpha_3 k^2 V_h^2} - \frac{9\alpha_5^2 q_z^2}{2V_h^2 k^2 S(\alpha_4 - S)^2},$$

$$\left. \frac{\partial h_1}{\partial p_2} \right|_* = \frac{9\alpha_5^2 q_z^2}{2V_h V_z k^2 S(\alpha_4 - S)^2},$$

$$\left. \frac{\partial h_2}{\partial p_1} \right|_* = \frac{9\alpha_5^2 q_z^2}{2V_h V_z k^2 S(\alpha_4 - S)^2},$$

$$\left. \frac{\partial h_2}{\partial p_2} \right|_* = -\frac{9\alpha_5^2 q_z^2}{2V_z^2 k^2 S(\alpha_4 - S)^2},$$

which result in by (B.21)

$$B = \frac{9\alpha_5^2 q_z^2}{2k^2 S(S - \alpha_4)^2} \begin{bmatrix} 1/V_h^2 & -1/(V_h V_z) \\ -1/(V_h V_z) & 1/V_z^2 \end{bmatrix} + \frac{1}{2\alpha_3 k^2} \begin{bmatrix} 1/V_h^2 & 0 \\ 0 & 0 \end{bmatrix},$$
$$\tag{B.24}$$

and

$$\left. \frac{\partial h_3}{\partial x_1} \right|_* = 0,$$

$$\left. \frac{\partial h_3}{\partial x_2} \right|_* = 0,$$

$$\frac{\partial h_4}{\partial x_1}\bigg|_* = 0,$$

$$\frac{\partial h_4}{\partial x_2}\bigg|_* = -2\alpha_2,$$

which result in by (B.22)

$$C = \begin{bmatrix} 0 & 0 \\ 0 & 2\alpha_2 \end{bmatrix} \tag{B.25}$$

where S is given by (B.19).

APPENDIX C

STABILITY OF THE LINEAR REGULATOR

A general closed form solution of the optimal control problem is possible for a linear regulator with quadratic performance index [3]. Specifically, we will consider the time invariant system

$$\dot{x}(t) = Ax(t) + Bu(t) \tag{C.1}$$

with a criterion

$$\int_0^{t_1} [x'Qx + u'Ru]\, dt \tag{C.2}$$

with R real symmetric positive definite (r.s.p.d.) and Q real symmetric positive semidefinite (r.s.p.s.d.) for $t \geq 0$. The Hamiltonian (A.5) is

$$H = x'Qx + u'Ru + p'(Ax + Bu), \tag{C.3}$$

and the necessary condition (A.9) for optimality gives

$$\frac{\partial}{\partial u}\left[(u^*)'Ru^* + (p^*)'Bu^*\right] = Ru^* + B'p^* = 0, \tag{C.4}$$

so that

$$u^* = -R^{-1}B'p^*, \tag{C.5}$$

R being nonsingular since it is positive definite. The adjoint equations (A.7) are

$$\dot{p}^* = -Qx^* - A'p^*. \tag{C.6}$$

Substituting (C.5) into (C.1) gives

$$\dot{x}^* = Ax^* - BR^{-1}B'p^* \tag{C.7}$$

and combining this equation with (C.6) produces the system of linear equations

$$\frac{\mathrm{d}}{\mathrm{d}t} \begin{bmatrix} x^*(t) \\ p^*(t) \end{bmatrix} = \begin{bmatrix} A & -BR^{-1}B' \\ -Q & -A' \end{bmatrix} \begin{bmatrix} x^*(t) \\ p^*(t) \end{bmatrix}. \tag{C.8}$$

The boundary condition (A.8) is

$$p^*(t_1) = 0. \tag{C.9}$$

The solution of (C.8) in terms of the conditions at time t_1 is

$$\begin{bmatrix} x^*(t) \\ p^*(t) \end{bmatrix} = \Phi(t, t_1) \begin{bmatrix} x^*(t_1) \\ p^*(t_1) \end{bmatrix} = \begin{bmatrix} \phi_1 \\ \phi_2 \end{bmatrix} x^*(t_1), \tag{C.10}$$

where Φ is the transition matrix for (C.8), using (C.9). Hence

$$x^*(t) = \phi_1 x^*(t_1) \tag{C.11}$$

and

$$p^*(t) = \phi_2 x^*(t_1) = \phi_2 \phi_1^{-1} x^*(t) = P(t)x^*(t) \tag{C.12}$$

using (C.11). It now follows from (C.5) and (C.12) that the optimal control is of linear feedback form

$$u^*(t) = -R^{-1}B'Px^*(t). \tag{C.13}$$

To determine the matrix P, differentiating (C.12) gives

$$\dot{P}x^* + P\dot{x}^* - \dot{p}^* = 0, \tag{C.14}$$

and substituting for $\dot{x}^*$, $\dot{p}^*$ from (C.8) and p^* from (C.12) produces

$$(\dot{P} + PA - PBR^{-1}B'P + Q + A'P)x^*(t) = 0. \tag{C.15}$$

Since this must hold throughout $0 \leq t \leq t_1$ it follows that $P(t)$ satisfies

$$\dot{P} = PBR^{-1}B'P - A'P - PA - Q \tag{C.16}$$

with boundary condition given by (C.9) and (C.12) as

$$P(t_1) = 0.$$
(C.17)

Equation (C.16) is *matrix Riccati differential* equation.

It should be noted that even tough the matrices A, B, Q and R are all time invariant the solution $P(t)$ of (C.16), and hence the feedback matrix in (C.13), are time varying. Of particular interest is the case when the final time t_1 in (C.2) tends to infinity. Let Q_1 be a matrix having the same rank as Q and such that $Q = Q_1' Q_1$. The solution $P(t)$ of (C.16) becomes a constant matrix P [12], and we have [3]

Theorem 1. *If the constant linear system (C.1) is c.c. and $[A, Q_1]$ is c.o. then the control which minimizes*

$$\int_0^\infty [x'Qx + u'Ru]\, dt$$
(C.18)

is given by

$$u^* = -R^{-1}B'Px^*.$$
(C.19)

where P is the unique r.s.p.d. matrix which satisfies the algebraic Riccati equation

$$PBR^{-1}B'P - A'P - PA - Q = 0.$$
(C.20)

The closed loop system obtained by substituting (C.19) into (C.1) is

$$\dot{x} = \mathcal{A}x$$
(C.21)

where $\mathcal{A} = A - BR^{-1}B'P$. It is easy to verify that

$$\begin{aligned}
\mathcal{A}'P + P\mathcal{A} &= A'P + PA - 2PBR^{-1}B'P \\
&= -PBR^{-1}B'P - Q,
\end{aligned}$$
(C.22)

using the fact that P is the solution of (C.20). Because of the assumption that $[A, Q_1]$ is c.o., $\mathcal{A}$ is asymptotically stable [13].

REFERENCES

[1] Metha, D. P.; Thumann, A. *Handbook of energy engineering*; Fairmont Press: Lilburn, Georgia, 1991.

[2] Kelley, M. "New directions for the buildings division"; *Solar Today* 1992, *6(1)*, 9-10.

[3] Barnett, S.; Cameron, R. G. *Introduction to mathematical control theory*, 2nd ed.; Clarendon Press: Oxford, 1985.

[4] Zaheeruddin, M.; Patel, R. V. *ASHRAE Transactions* 1993, *99(1)*, 554-564.

[5] House, J. M.; Smith, T. F.; and Arora J. S. "Optimal control of a thermal system"; *ASHRAE Transactions* 1991, *97(2)*, 991-1001.

[6] Roth, C. J.; Smith, T. F.; Yae, K. H. "Adaptive optimal control of an HVAC system"; Technical Report ME-TFS-94-002; Department of Mechanical Engineering, University of Iowa: August, 1994.

[7] Smith, T. F. "Energy efficient design and operation of HVAC systems for commercial and industrial buildings"; Interim Technical Report; Iowa Energy Center Grant No. 93-16-01: 1995.

[8] Åstrom, K. J.; Wittenmark, B. *Adaptive control*; Addison-Wesley Publishing Company: 1989.

[9] Sastry, S. *Adaptive control : stability, convergence, and robustness*; Prentice-Hall: Englewood Cliffs, New Jersey, 1989.

[10] Brauer, F.; Nohell, J. A. *The qualitative theory of ordinary differential equations: An introduction*; W. A. Benjamin: New York, 1969.

[11] Kuo, B. C. *Automatic control systems*, 6th ed.; Prentice Hall: Englewood Cliffs, New Jersey, 1991.

[12] Kwakernaak, H.; Sivan, R. *Linear optimal control systems*, 2nd ed.; Wiley-Interscience.: New York, 1972.

[13] Barnett, S. *Polynomials and linear control systems*, 2nd ed.; Marcel Dekker, Inc.: New York, 1983.